Department of Precision and Microsystems Engineering

A Predictive Energy Management Strategy for Plug-in Hybrid Electric Vehicles utilizing Route Preview

S. Boksebeld

Report no : 2018.002
Coach : Dr. ir. S. H. HosseinNia
Professor : Prof. dr. ir. J. L. Herder
Specialisation : Mechatronic System Design
Type of report : Master Thesis
Date : March 2, 2018

TU Delft Delft University of Technology

Challenge the future

A Predictive Energy Management Strategy for Plug-in Hybrid Electric Vehicles utilizing Route Preview

by

S. Boksebeld

in partial fulfillment of the requirements for the degree of

Master of Science

in Mechanical Engineering

at the Delft University of Technology,

to be defended publicly on March 2, 2018 at 11 AM.

Student number:	4157419	
Project duration:	April 1, 2017 – March 2, 2018	
Supervisor TU Delft:	Dr. ir. S. H. HosseinNia,	
Supervisor AVL:	Ir. A. Massoner,	
Thesis committee:	Prof. dr. ir. J. L. Herder,	TU Delft
	Dr. ir. S. H. HosseinNia,	TU Delft
	Dr. ir. S. Baldi,	TU Delft
	Dr. P. Mohajerin Esfahani,	TU Delft

This thesis is confidential and cannot be made public until March 2, 2023.

TU Delft Delft University of Technology

The work in this thesis was supported by AVL. Their cooperation is hereby gratefully acknowledged.

Abstract

Abstract – A Plug-in Hybrid Electric Vehicle (PHEV) can achieve a considerably higher overall fuel economy than conventional vehicles. The fuel economy of PHEVs however, strongly depends on the supervisory control strategy of the hybrid powertrain. Compared to conventional, non-predictive, supervisory control systems, predictive control methods can further improve the fuel economy by anticipating on future driving conditions. This thesis presents a predictive optimal control method for PHEVs that minimizes the fuel consumption in real-time operation, based on the preview of the future topographic profile and velocity profile. This strategy is realized by a global estimation method that determines the optimal battery depletion strategy on the global range, which is tracked by a novel adaptive heuristic control method that optimizes the driving mode and power distribution between the two power sources on the local range. Compared to state of the art predictive control methods, this control method makes it possible to include feasibility and drivability conditions (such as the number of engine starts and variation of the torque demand) in the control strategy, while allowing high update frequencies of the control actions.

The proposed control method is fine-tuned on a P2 parallel PHEV model based on a Volkswagen Jetta HEV, and its effectiveness is evaluated by implementation in a high fidelity simulation environment. It was found that route-preview based control strategies can obtain substantial improvements of up to 7.3% in fuel economy compared to a non-predictive heuristic control method. Simulation results also demonstrate that the application of optimization based control methods without any drivability considerations (such as A-ECMS) often leads to unacceptable control policies. The proposed control method on the other hand, was able to take feasibility limitations into account, which led to a reduction of the number of combustion engine starts of up to 52%.

Keywords: Plug-in Hybrid Electric Vehicle (PHEV), intelligent powertrain control, optimal control, predictive energy management, adaptive recalibration heuristic control.

Preface

First of all, I would like to thank my supervisor Dr. ir. S. H. HosseinNia for his guidance, critical feedback and general support during our real-life and Skype meetings. Special thanks goes as well to my supervisors at AVL, Alexander Massoner and Laurent Allouchery, for their assistance and the helpful discussions throughout this research.

Thank you as well to my AVL colleagues, Niklas, Alejandro and Pankit for their feedback and suggestions on the methodology, contents and presentation of this work. Additionally, I would like thank my fellow students, Andy, Bart and Chris for their fresh insights on some of the problems I faced.

Finally, I would like to thank AVL for providing the opportunity and facilities to work on this fascinating topic.

S. Boksebeld
Delft, March 2018

Contents

List of Figures

List of Tables

List of Acronyms

A-ECMS	Adaptive Equivalent Consumption Minimization Strategy
AC	alternating current
ACC	Adaptive Cruise Control
ADAS	advanced driver assistance system
APU	auxiliary power unit
BEV	battery electric vehicle
BSFC	brake specific fuel consumption
CDCS	charge depleting - charge sustaining
CO_2	carbon dioxide
DC	direct current
DOF	degree of freedom
DP	dynamic programming
eBoost	electric boost
ECMS	Equivalent Consumption Minimization Strategy
eDRV	electric driving
EM	electric machine
EMC	Energy Management Control
FCEV	fuel cell electric vehicle
GHG	greenhouse gases
GIS	Geographical Information System
GPS	Global Positioning System
HEV	hybrid electric vehicle
IC	internal combustion
ICE	internal combustion engine
LH	long horizon
LPM	load-point-moving
MINLP	mixed integer nonlinear programming
MPC	model predictive control
NEDC	New European Drive Cycle
NVH	noise-vibration-harshness
PHEV	plug-in hybrid electric vehicle
PI	proportional-integral
PMC	Power Management Control
PSO	particle swarm optimization
QP	quadratic programming
RDE	Real Driving Emissions
REEV	range extender electric vehicle
SH	Short horizon
SoC	State of Charge
V2X	vehicle-to-X
WLTC	Worldwide harmonized Light vehicles Test Cycles

1

Introduction

1.1 Environmental concerns and legislation

Environmental concerns, air pollution and the unsustainable exploitation of fossil fuels receive a lot of attention in today's society and especially in the automotive and transport industry. In the modern world there is a constant drive towards more energy efficient vehicles, more sustainable energy sources and more effective use of transportation. According to market predictions [3] however, the total number of vehicles worldwide will continue to increase in the near and long term future [4]. The biggest problem with this growing fleet of vehicles is their exhaust of harmful greenhouse gases (GHG), which has a large impact on the global and local environment [5]. A recent study from the European Environment Agency [6] demonstrates that the European transport section (which includes personal transportation) has a share of approximately 23% of the total European GHG emissions. Governments have introduced many forms of legislation with the intent to reduce the negative impacts of the continuously growing number of road vehicles. Most importantly, to reduce the global carbon dioxide (CO_2) emissions, governments have created legislation [7] that limits the maximum emissions of CO_2 per kilometer for all newly produced passenger cars and light-commercial vehicles and have set ambitious targets for the next 5-10 years, see Figure 1.1a. The exhaust emissions of a vehicle are determined in laboratory testing, during which the vehicle is operated on a chassis dynamometer and 'driven' over a certain drive cycle. The drive cycle is a route that consists of typical driving phases like city and extra-urban phases to obtain a representative analysis of the fuel consumption and emissions of the vehicle. The drive cycle is the same for all vehicles and manufacturers to enable direct comparison. For example, European legislation uses the New European Drive Cycle (NEDC) [7] cycle, where the upper limit for exhaust emissions by the end of the year 2020 is limited to 95 g/km of CO_2 , which roughly corresponds to 4.1L/100km for gasoline powered vehicles [8]. The intended result of the legislations is a lower fuel consumption of the average vehicle, which can only be achieved by the automotive manufacturers by increasing the efficiency of the overall vehicle and/or the introduction of more low- and zero-emission vehicles.

1.2 Hybrid electric vehicles

One way automotive manufacturers can achieve an increased overall system efficiency of their passenger vehicles, light-commercial vehicles or trucks is to hybridize the powertrain of the vehicle. These vehicles, often referred to as a HEV, use a combination of an electric and internal combustion (IC) powertrain to propel the vehicle (Schematic diagram in Figure 1.1b), which gives the HEV promising benefits over a conventional vehicle. The main advantages of HEV are the pure electric driving mode, electric driving (eDRV), the recuperation of energy during braking and increased operating efficiency of the ICE, which all contribute to a higher overall system efficiency compared to conventional ICE vehicles (more details on this hybrid powertrain and its advantages can be found in Appendix A.2). PHEVs offer even bigger advantages, because they can be externally recharged from the power grid and their upscaled electrical components allow the electric driving mode to be used longer and more frequently (more about the

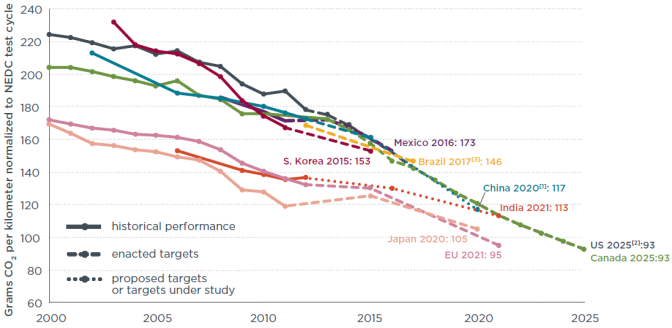

(a) Comparison of CO_2 regulations standards for passenger cars around the world. Normalized to the NEDC cycle. Adopted from [7].

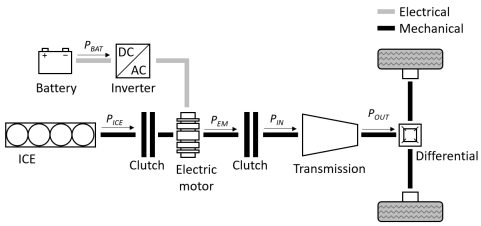

(b) Schematic diagram of a P2 parallel HEV topology.

Figure 1.1: Passenger vehicle legislation around the world and schematic overview of a HEV.

different types of HEVs in Appendix A.3). The higher overall system efficiency and lower exhaust emissions make the PHEV a promising vehicle concept that enables automotive manufacturers to meet their emission targets and provides lower operation costs to car owners. The HEVs became widely available in 1999 with the introduction of the Toyota Prius [9] and over the past years more and more models were introduced. Currently, (second half of 2017) more than 30 PHEV models are available in Germany [10] and most large automotive manufacturers have at least one PHEV model in production, or announced the introduction of PHEV model in the near future.

Since the electric powertrain of the HEV has so many advantages, the question arises whether the hybrid powertrain is actually an useful solution, rather than opting for a powertrain concept that removes the ICE from the vehicle all together. There are two vehicle concepts that feature an ICE-free powertrain and have therefore completely zero-emissions: pure battery electric vehicle (BEV)s and hydrogen fuel cell electric vehicle (FCEV)s. Both these vehicle concepts, however, have major obstacles that prevent them from full scale acceptation at this moment. For BEVs the main issue is the limited energy density of the batteries, which leads to a limited amount of energy available in the vehicle and therefore a limited driving range of the vehicle. Also expensive manufacturing of the batteries, low charging speeds compared to refueling a conventional car and the insufficient number and capacity of (high power) charging stations are major obstacles before BEVs are ready for full scale acceptation [11–13]. For FCEVs, the expensive manufacturing and immature technology of fuel cells as well as the absence of an established fuel infrastructure form the main issues that prevent full scale introduction of these vehicle types at this moment [11–13] Since the hybrid electric powertrain technology and the required infrastructure are already mature enough for mass acceptance at this moment, the HEV is an appropriate solution for the near future and the next decades according to different market predictions [3, 13–16]. The HEV is an intermediate solution, which helps to smooth the transition between the conventional and complete zero-emission vehicles and is likely to be broadly around in the next 30 years. Its market share however, will eventually be overtaken by other technologies with even lower emissions (like BEVs and/or FCEVs) in the long term future.

1.3 Predictive powertrain control

A HEV makes use of a hybrid powertrain that combines two power sources (an EM (electric motor with inverter)) and an ICE), which introduces a new degree of freedom to the vehicle: the distribution between electric and combustion traction power. This ratio is called the power split or power distribution of the hybrid powertrain and has a large influence on the overall efficiency of the complete vehicle. The distribution of electric and combustion power is managed by a control system which is often referred to as the supervisory controller of the hybrid powertrain. The main objective of the supervisory controller is to coordinate the power sources and optimize the power flow such that a high overall efficiency is achieved. Determining the best power split at each point in time in order to achieve the highest combined efficiency is not trivial and calculating the optimal strategy for the long term route is a complex task

To control the hybrid powertrain, conventionally only limited information on the driving conditions is available, because detailed and accurate prediction of long term future conditions, driving situations and control actions was not possible [17]. Consequently this means only general, predetermined strategies can be applied, which only use information on the conditions on the current instance and very little to no preview of the conditions ahead. In literature it is recognized and shown that knowledge on future driving conditions enables the use of predictive optimal control strategies that can significantly improve the overall efficiency of the vehicle compared to conventional control methods [18], [19]. Technological developments in navigation systems as well as recent developments in communication technology (vehicle-to-X (V2X)), advanced driver assistance system (ADAS) functions and autonomous driving functionality make it possible to obtain information on the future driving conditions with sufficient accuracy and enable the introduction of predictive advanced control methods in actual vehicles [17], [18], [20]. In Figure 1.2, the information systems of the vehicle are graphically illustrated.

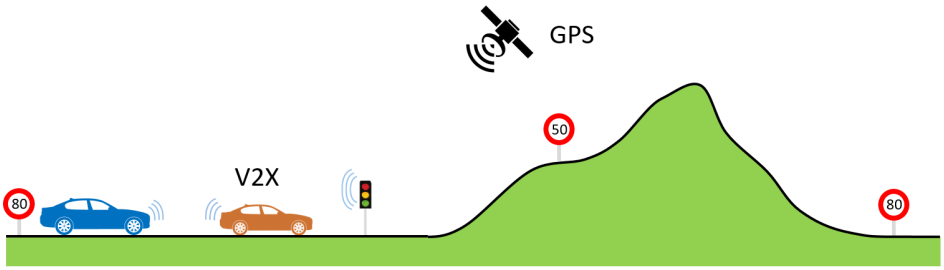

Figure 1.2: To obtain knowledge on the future altitude and velocity profile, the vehicle can make use of different information sources such as: navigation systems with Global Positioning System (GPS), V2X communication and ADAS functionality.

1.4 Research objective and goals

AVL List GmbH is an Austrian-based automotive consulting firm that specializes in the development of powertrain systems as well as instrumentation, test systems and associated softwares. This thesis is written in close collaboration with AVL and contributes to a wider field of ongoing research activities with respect to predictive powertrain control and concept ADAS functions. In this research a new approach is proposed for the online (i.e. to be calculated in real-time on the actual vehicle hardware) supervisory control of PHEVs based on a predictive optimal control strategy that utilizes preview of future conditions. Although predictive supervisory controllers have been relatively well established in literature, the necessary conditions for feasibility, drivability and implementation in real-life applications is still to be explored to a further extent. The aim of this research and its main contribution is to develop a new method for the supervisory control system of a PHEV, which can include these conditions in the control strategy, while also minimizing the fuel economy. The conditions that are considered in this work are the number of ICE starts, the variations in ICE torque and the update frequency the control method. This leads to the following research objective:

The objective of this research is to develop and implement a predictive optimal control method for PHEVs that can minimize the fuel consumption, while taking into account the necessary conditions for feasibility, drivability and implementation in real-life applications.

The research objective does however not include the development, dimensioning or optimization of the physical components of the hybrid powertrain, but rather tries to improve the overall efficiency of the PHEV by the use of more intelligent control strategies. To reach the objective of this research, the following goals need to be achieved throughout the research project:

- Develop control-oriented vehicle and powertrain models
- Develop a global controller that can determine a long horizon energy management strategy, with a battery depletion trajectory as output.

- Develop a novel local controller that can determine a short horizon power management strategy that tracks a long horizon reference trajectory, while minimizing fuel consumption and taking into account the feasibility, drivability and implementation conditions
- Validation and performance analysis of the developed methods

1.5 Simulation and validation approach

To demonstrate the effectiveness of the proposed method, the developed techniques are implemented in a co-simulation environment consisting of the tools Matlab, CarMaker and Cruise, in which the method is applied on an existing high fidelity simulation model of a PHEV. Although the proposed methodology is not limited to passenger vehicles, a specific type of HEV, specific hybrid topology, or specific use cases and drive cycles, the developed method will be evaluated and validated in multiple drive cycles using simulations with a high fidelity model of a P2 parallel PHEV (more on the hybrid topologies in Appendix A.4). The vehicle model, all vehicle parameters and the combustion powertrain of this PHEV model are based on a Volkswagen Jetta HEV, where the electrical components (EM and battery) are taken from other production PHEVs. The PHEV model used in these simulations consists of a EM of 80 kW in P2 configuration with a 110 kW ICE and a battery pack of 4.2 kWh, which are common specifications of PHEVs. The full details of the PHEV model can be found in Section 3.2. In order to evaluate the performance of the developed control method and its impact on the fuel economy of the vehicle, the control strategy is compared with a variation of other control methods that function as a benchmark. As the minimal performance reference for the developed control method, a conventional heuristic controller is used to demonstrate the potential gains of the proposed method compared to the standard control methodology. A DP based control strategy will determine the theoretical global optimal solution with the best possible performance. Next to these two control strategies, an Equivalent Consumption Minimization Strategy (ECMS) and model predictive control (MPC) control method are implemented as well, with the intent to gain a better perspective on the performance of the proposed method and provide additional reference material to improve the comparability of this work with literature.

1.6 Outline next chapters

This report starts with a deeper orientation on the supervisory controller of a hybrid electric vehicle in Chapter 2. This chapter gives an overview of the main tasks of the supervisory controller, different control methods that can be used and proposed a novel method to determine the best local control strategy. In Chapter 3 the vehicle architecture is discussed, control models are developed and high fidelity simulation environment is described. Chapter 4 discusses the proposed control methods and their implementation. In Chapter 5 the results of these simulations are presented and discussed. The conclusions of this work are drawn in Chapter 6, where also some recommendations for future works are presented. Finally, the reader is referred to the Appendices for further reference on the different types of HEV and their key characteristics in Appendix A and Appendix B for a study on the average performance of different control methods in literature.

2

Literature review and preliminaries

The combination of the two power sources in a hybrid powertrain introduces a new degree of freedom to the vehicle: the distribution in power between the two sources. To coordinate the power flow in the hybrid powertrain, a supervisory control system is required that determines the best power distribution between the two power sources.

In this chapter the main tasks for the supervisory controller and different methods to determine the control strategy are introduced based on literature research. An architecture for the supervisory control system is proposed, as well as a methodology for a novel control method that can take into account feasibility conditions.

2.1 Hybrid vehicles

The control strategies developed in this work will be applied on a PHEV with a P2 parallel topology (more on the hybrid topologies in Appendix A.4), which is a popular choice for hybrid vehicles because it is a cost effective approach with a high operating efficiency under most conditions, while maintaining a compact and easy integrable design (as discussed in Appendix A.4). The hybrid powertrain is a very promising concept that can offer significant improvement of the overall efficiency in comparison to conventional powertrains (more on this in Appendix A.2). This follows mainly from the fact that the two individual powertrains (electric and IC) have their key strengths in different areas and can therefore compensate each other's weaknesses to form a more superior powertrain concept. This principle of synergy is generally speaking the fundamental concept behind most supervisory controllers for hybrid powertrain and allows the highest overall efficiency of the complete powertrain to be achieved [12]. For parallel hybrids, the basic approach is to operate the electric powertrain in areas where the IC powertrain efficiency is relatively low and use the ICE as the power source in conditions where the efficiency of the ICE is relatively high [21]. Alternatively, if both individual solutions are infeasible or suboptimal, the supervisory controller can opt to apply load-point-moving (LPM) strategies by making use of both power sources in parallel (actively moving the operating point of the ICE (e.g. by negative EM torque) to achieve a higher overall efficiency. More on this in Appendix A.2).

2.2 Supervisory control

The freedom to choose any distribution of the tractive power request over the two power sources of a HEV at every point along the route introduces an additional degree of freedom that needs to be controlled: the power split [18]. The level of optimality of the control strategy of supervisory controller has a big influence on the overall performance of the complete vehicle[17]. Moreover, a potent HEV concept can perform poorly if operated by an inappropriate control strategy [18, 22]. However, determining the optimal strategy over the complete route that leads to a power split at every point along the route is a non-trivial

task. The‘main objective of the supervisory controller is to control the power split in such a way that the energy flows are optimized to obtain the highest overall efficiency along the complete trip. Within its overarching objective, two main tasks of the supervisory controller can be distinguished in controlling the hybrid powertrain [23–26]:

- **Energy Management Control:** Long term depletion strategy of the battery over the global time scale.
- **Power Management Control:** Short term detailed control strategy of the hybrid powertrain over a local time scale.

2.2.1 Two main tasks

The first main task is the long-term depletion strategy of the battery, referred to as the Energy Management Control (EMC) strategy or LH strategy. The main objective here is to determine how the energy in the battery can be most efficiently used or generated along the route in order to meet the targeted energy level of the battery (referred to as SoC) at the end of the trip and achieve the highest overall efficiency of the vehicle. For PHEVs, the target is typically to arrive with an empty battery at the end of the trip, but in principle any target SoC can be used. Since charging and discharging significant fractions of the battery takes a relatively long time (it has slow dynamics in comparison with the velocity dynamics of the vehicle [18, 26]) and the end-of-trip SoC target is given, the EMC strategy for depleting the battery is typically determined for the complete trip [25, 26]. The prediction horizon (the time in the future up to where predictions are made) is the entire trip length.

The second main task of the supervisory controller is the short-term detailed control strategy of the HEV, referred to as the Power Management Control (PMC) or SH strategy. Its main objective is to determine the best driving mode and power split for the current conditions and subsequently to supply according detailed control inputs to the subcomponents [24, 25]. This optimal driving mode and power split ideally minimize the fuel consumption, while also complying with the LH EMC strategy. The minimization of the fuel consumption is however, not the only objective of the local PMC control task. The final control strategy should also meet certain criteria in terms of feasibility and drivability in order to result in acceptable behavior for application in practice. Since the supervisory control system does not directly control the vehicle speed (more on this in the next section), the drivability of a control strategy is mainly characterized by the level of noise-vibration-harshness (NVH) [12]. For a HEV, the NVH level is for a largest part determined by the way the ICE is used and can be reduced by avoiding aggressive ICE transients (frequent shifting of the operating point), reducing the number of ICE starts and keeping the ICE on for a minimal amount of time once it has been turned on [27–29]. The level of acceptable drivability can vary a lot between different HEV, because it strongly depends on the brand and type of vehicle (e.g. luxury of sportive). Once the optimal strategy has been determined in terms of fuel consumption, drivability and agreement with the LH EMC strategy, the driving mode and power split can be translated to a set of detailed control inputs and supplied to the subcomponents, which consists of:

- Desired ICE torque
- Desired EM torque
- Desired brake pressure hydraulic brakes
- Desired gear

Since the PMC directly controls the vehicle power sources, it is required to operate at a frequency that is at least higher than the velocity dynamics of the vehicle which is about 10-20 Hz (more on this in Section 2.8.1). The PMC typically operates on an instantaneous basis or over a short horizon. The prediction horizon for short horizon control is in the order of 30-60 seconds.

2.2.2 Classification of control strategies

In literature different control strategies are proposed to fulfill the supervisory control task of the HEV. These control strategies can be categorized into two main categories: heuristic-based and optimization-based methods.

Conventionally, the control of hybrid powertrains relies only on information on the instantaneous driving conditions, vehicle states and power demand, because detailed and accurate information on future conditions and future control actions is not available [17]. Consequently this means only general, predetermined heuristic strategies can be applied, which only use information on the instantaneous conditions and no preview of the conditions ahead. The decision making in heuristic based control strategies follows from predefined logical "if-then-else" rules, maps and lookup tables or fuzzy logic techniques and determine the detailed control inputs based on the instantaneous states of the powertrain (e.g. engine speed, SoC, power demand) [1, 17, 22, 30, 31]. The rules and maps are constructed in such a way that their outputs correspond to a predetermined desired behavior. Besides relying only on instantaneous information, heuristic control strategies have additional strengths: they are robust, have a low computational demand and are fail safe in situations of sensor- or component-failure [27, 31]. If the vehicle parameters and drive cycle are known and the heuristic rules and maps are calibrated towards this cycle, the performance of heuristic methods in terms or fuel-economy can be near-optimal [17, 24]. However, the performance of heuristic control strategies is moderate for more complex cycles or drive cycles the heuristics are not directly calibrated toward, which both apply to normal use by the consumer.

The second main category of control strategies are optimization based methods. In literature it is recognized and shown that more intelligent, predictive, control strategies can significantly improve the overall efficiency of the vehicle compared to heuristic control methods [18], [19]. First of all, because there is only a finite number of heuristic rules and maps and their complexity is limited, it is not possible to perfectly emulate the desired behavior for every possible situation with a heuristic basis. The heuristics therefore have to be calibrated such that their resulting behavior has the best compromise for a certain set of representative driving conditions, where the performance loss resulting from the compromise depends on the number of heuristic rules in the heuristic basis and their complexity. Optimization based methods on the other hand, are typically free to chose any value (or any discretized value) for its optimization variables and are thereby able to directly minimize the actual objective function at that point in time (within their numerical accuracy).

Predictive optimization based methods are able to adopt control strategies that are optimized over a long term perspective, rather than only from an instantaneous point of view. Based on information of future conditions, these methods predict the future states of the HEV and adjust their current strategy accordingly to best anticipate on future events and conditions. The main difference in comparison to instantaneous optimization methods is that the instantaneous optimal solution does not ensure LH or global optimality whereas predictive optimization control strategies are able to achieve or approximate the maximal performance in the perspective of the complete route or section of the route. Predictive, optimization based control strategies are therefore able to achieve the largest improvements of the overall efficiency of the vehicle compared to conventional control strategies.

Next to the intelligent control of the battery depletion strategy and the driving mode and power split of the hybrid powertrain, it is recognized that smart adaptation of the velocity of the vehicle can bring large gains in the overall efficiency as well [26] (e.g. adaption of the deceleration profile). However, in this research and most other works, the velocity of the vehicle will be considered as a pure input and not as part of the control problem, because the vehicle velocity is subjected to many constraints from higher level decisions (e.g. road curvature, speed limits, safe interaction with other road users and infrastructure such as traffic signs). The management of these constraints and trade-offs between contradicting high-level objectives on the vehicle level (or even multiple vehicles) would be a different kind of problem that is no longer mainly about powertrain control and therefore can only be controlled by an overarching, high level control system and not by the controller of the hybrid powertrain.

Another variable that can be included in the optimization of the control strategy of the hybrid powertrain is the selection of the active gear. However, the gear-shifting strategy is typically not included in the supervisory optimal control problem, because the selection of the best gear is a relatively trivial task that is often determined by a separate heuristic control system [32–34]. Since the ICE and transmission efficiency increase with higher torque, the general strategy is to select the highest gear that is within the allowable

operating range and still acceptable in terms of drivability and NVH [1, 17].

2.2.3 Estimation of the future power demand and information sources

In order to solve an optimal control problem, knowledge on the future driving conditions is required on top of information on the instantaneous conditions and vehicle states. Since the main objective of the supervisory controller is to control the energy flows from the two power sources, the predictive EMC and PMC strategies require knowledge of the future power demands of the vehicle along the route. Information on upcoming power demands is however not directly available and has to be calculated using other information sources on future conditions. For this reason, the main purpose of acquiring information on future conditions is to calculate the future power demands of the vehicle. Some variables have only a small influence on the future power demands and can in most cases be neglected or assumed constant (e.g. wind power and direction). Reasonably accurate estimations of the future power demand profile can be calculated using the two variables with the highest contribution [17]:

- Future velocity and acceleration profile of the vehicle
- Future road gradient profile of the route

Next to information on future conditions, also a model of the vehicle (e.g. vehicle dynamics model) and knowledge on the vehicle parameters (such as mass, rolling resistance, aerodynamic drag, etc) are required to calculate the future power demand profile. The vehicle model is described in detail in Chapter 3.

It should be noted once more that without accurate information on the future power demand profile, predictive control strategies can never reach a high optimality. However, in practice, the future power demand profile can never be predicted with perfect accuracy. Due to (small) errors and discrepancies in the prediction of future conditions, vehicle parameters and vehicle model, the future power demands can only be estimated with a certain accuracy, but can never be 100% accurate in applications in practice. This however does not mean that the accuracy of the predictions is insufficient to achieve a close approximation of the optimal solution, which is still achievable if the predictions matches the required accuracy for their application. Analogue to the division of the two main tasks of the supervisory controller (EMC and PMC), the predictions of future conditions can be divided in long horizon estimations that are mainly used for energy control strategies and short horizon estimations used for the powertrain control strategies.

Assuming the vehicle parameters and vehicle models are known with a high accuracy, the main error sources in the estimation of the future power demand originate from the predictions of the future driving conditions. The prediction of the future terrain profile is highly suitable for both short horizon and long horizon predictions, because altitude information is available with high accuracy independent of the prediction horizon and is not subjected to change (as long as the route is not altered). The technology in GPS, Geographical Information System (GIS) and navigation systems that enables accurate prediction of the future road gradient profile is already available in modern passenger vehicles [17, 24, 35]. The accurate prediction of the future velocity profile on the other hand is much more difficult, especially in cases where the vehicle is driven by a human driver, and is one of the main reasons why predictive control of HEVs has not found its application in practice yet. Three main aspects in determining the future velocity profile can be distinguished:

1. The desired cruising speed and speed limits for every point along the prediction horizon have to be known.
2. The driving style of the vehicle and/or driver has to be known, which includes the velocity during corners, junctions, and any other conditions where the vehicle velocity is lower than the cruising speed or speed limits, as well as the the acceleration level between two desired speed targets.
3. The velocity limitations due to traffic and other road users at every point along the prediction horizon have to be known.

The estimation of the vehicle velocity profile using the first aspect is relatively easy for both long horizon and short horizon predictions, because the velocity information is known a priori, the information does not change and the information can be extracted with a high accuracy. Assuming the driving style of the vehicle is constant, the estimation of the vehicle velocity profile using the second point is also feasible for

both long horizon and short horizon predictions, because the velocity information can be directly calculated from sub-information that is known a priori (e.g. road layout), the sub-information does not change (as long as the conditions do not change) and the sub-information can be extracted with a high accuracy. Although the assumption is highly valid for autonomously driving vehicles (or systems like Adaptive Cruise Control (ACC)), the assumption on the constant driving style for a human driver is more questionable, which would lower the accuracy of predicted velocity profile. It is concluded that the first two aspects of velocity profile prediction (even though some of the predictions are based on estimations) is feasible and information on the future velocity profile can be obtained with relatively high accuracy independent on the length of the prediction horizon. This makes the information suitable for both the short and long horizon predictions of the future velocity profile [17, 18].

The third point however, has none of the previous properties, which makes the estimation of the future velocity profile difficult and inaccurate: the future traffic conditions and future behavior of individual road users are not based on a priori known (sub-)information, but have to be based on extrapolations of instantaneous and historic data and are therefore also strongly subjected to change. For these reasons, the information on future velocity limitations due to traffic and other road users has a poor accuracy that gets increasingly worse with longer prediction horizons, which makes the information only suitable for very short term predictions. Recent developments in communication technology (V2X) and vehicle sensor technology (e.g. camera vision and radar) however, have created the possibility to make predictions on the short horizon velocity profile with reasonable accuracy [17, 18, 35]. These short horizon predictions include the prediction of the behavior of other road users using forward calculating models based on sensor and communication data and has already been introduced to passenger vehicles for application in autonomous driving functionality or ADAS functions (such as ACC). For long horizon prediction of the future traffic conditions however, still only rough predictions can be made that have a poor accuracy (e.g. predicted traffic congestion by navigation systems). The prediction of the different subcomponents of the future power demand profile is summarized in Table 2.1.

Table 2.1: Overview of main components that make up the future power demand and their characteristics.

Prediction of:	Known a priori:	Subject to change:	Accuracy:	Source:
Road gradient	Fully	No	Very high	Navigation system
Cruising speed & speed limits	Fully	Largely not	High	Navigation system
Speed depending on driving style	Partly	Largely not	High	Navigation system and ADAS (if no human driver)
SH speed limitations due to traffic	No	Partly	Reasonable	V2X and ADAS
LH speed limitations due to traffic	No	Strongly	Poor	Navigation system

2.2.4 Formulation of the optimization problem

Before the optimal control strategy for the HEV can be determined, the objective of the supervisory controller has to be formulated as an optimal control problem. Analytical solutions to the optimal control problem of a HEV typically don't exist due to the large number of constraints and nonlinearities [32]. For this reason, numerical methods have to be used in order to determine the optimal solution. To enable the application of numerical methods to the optimal control problem, the HEV can be expressed as an discrete dynamic system whose states evolve over time depending on the applied control actions [1, 9, 35, 36]:

$$x_{k+1} = f(x_k, u_k) \tag{2.1}$$

where k takes integer values $0, 1, \ldots$ that correspond to the time steps of the discretized time vector (e.g. constant sampling times of 1 s), x_k is the state vector at time k (e.g. vehicle speed, battery SoC or gear) and u_k is the vector of control variables chosen at time k (e.g. requested ICE torque, EM torque or brake pressure). In order to determine the optimal control strategy for the HEV, a mathematical optimization problem has to be formulated, which searches the optimal control policy, $\mathbf{u}$, over the next N time steps that minimizes the cost function, J, (e.g. fuel consumption) starting at initial conditions x_0:

$$\mathbf{u} = \left[u_0, u_1, \ldots, u_{N-1}\right] \tag{2.2}$$

$$J(x(0), \mathbf{u}) = L_N(x(N)) + \sum_{k=1}^{N} L_k(x(k), u(k)) \tag{2.3}$$

where L_k are the instantaneous costs per time step and L_N are the terminal costs associated to the final conditions and states. In practice, many of the states and control inputs of the HEV are bounded and dependent on the specific conditions and states at that point in time. The boundary conditions can be formulated as inequality constraints to ensure safe and smooth operation of the vehicle:

$$T_{\text{ICE\_min}}(k) \leq T_{\text{ICE}}(k) \leq T_{\text{ICE\_max}}(k) \tag{2.4a}$$
$$T_{\text{EM\_min}}(k) \leq T_{\text{EM}}(k) \leq T_{\text{EM\_max}}(k) \tag{2.4b}$$
$$SoC_{\text{min}} \leq SoC(k) \leq SoC_{\text{max}} \tag{2.4c}$$

where ω_{in} is the input speed of the gearbox, engine and motor, T_{ICE} is the torque of the combustion engine, T_{EM} is the torque of the electric motor, SoC is the state of charge of the battery. The total power output of the vehicle after all losses and resistances should be controlled such that power demand profile over time is satisfied throughout the trip.

2.3 Heuristic control strategies

With the formulation of the optimal control problem for the HEV, several methods that can provide a suitable control strategy for this problem can be explored. As described in Section 2.2.2, heuristic control methods are still commonly applied in production HEV for the supervisory control of the hybrid powertrain, because they are robust, easy to implement have low computational demands and do not require access to information on future conditions [17, 22, 27, 31]. The heuristic controller typically use a hierarchical architecture to make two main decisions [21, 27]:

1. **Desired driving mode:**
   Determine whether the electric driving mode (ICE off) or ICE-based driving (ICE on) is desired.
2. **Desired power distribution:**
   In the case of ICE-based driving, determine what distribution of power between the two power sources is desired.

The heuristic rules are static (non-changing) thresholds and tables that are pre-constructed from engineering expertise, insight or optimization methods in an attempt to represent a predetermined desired control strategy as closely as possible. This predetermined set of rules incorporates all component limitations (e.g. torque limits) to prevent infeasible control actions and the decision logic to select the most preferable driving mode and power distribution for the instantaneous conditions and system states.

A major disadvantage of heuristic control strategies is that their performance in terms of fuel economy strongly depends on the calibration set (the implemented threshold values and maps) and the optimal calibration set itself can vary strongly between different drive cycles and driving conditions [17, 27]. Although the performance of heuristic controller can be near optimal the calibration is optimized towards a known drive cycle and set of the vehicle parameters [17, 24, 30], the performance is often moderate for more complex and unknown drive cycles. For this reason, heuristic controllers are unable to fully exploit potential of the hybrid powertrain under normal driving conditions in practice (where both the drive cycle and vehicle parameters are unknown).

2.4 Global optimization strategies

Due to the moderate performance of heuristic control strategies for unknown drive cycles, researchers explored the application of optimization based control method for hybrid powertrain control. In literature, the research towards finding the optimal control strategy for hybrid vehicles using knowledge on the future conditions started off as one large optimization problem over the full long-term route [1]. The research was mainly focused on determining the maximal potential performance improvements of predictive control strategies and to lesser extent on the development of control methods feasible for online applications[1, 9, 37]. Most of these works assumed information on the future conditions to be not subjected to change

and available with perfect accuracy over the complete prediction horizon. Because conditions will certainly change in real environments, the optimal control inputs calculated for long term future conditions are infeasible for direct application [1, 9, 37]. Also the computational limitations of the targeted implementation hardware were ignored, which makes the online application of full route optimization of detailed control inputs infeasible due to the extremely high computational demands of global optimization strategies. It can be concluded that due to their extremely high computational demand, as well as the absence of sufficient accuracy and detail of the information on future conditions, these control methods are not suitable for online application. Global optimization strategies however do have a high theoretical value, since, if calculated with hindsight, they can provide the true global optimal solution which can be used as a benchmark for the performance evaluation of more online applicable control methods. Also in this work, global optimization methods are use to assess the performance of other control methods.

2.4.1 Dynamic Programming

One of the numerical methods that can solve a global optimal control problem of the HEV is DP, which is a commonly used method for the global optimization of the energy management problem of HEVs. DP is a powerful optimization approach that is guaranteed to find the global optimal solution to constrained , nonlinear, non-convex and integer programming problems [1, 22, 35, 38]. The method is based on Bellman's principle of optimality, which makes it possible to split a n-variable problem into n simplified one-variable subproblems and solve them backwards from the terminal conditions [1, 36, 38]. The optimal control policy is determined by using the sequence of control inputs that minimize the instantaneous cost functions for each subproblem:

$$J_k^*(x_k) = \min_{u_k}[L_k(x_k, u_k) + J_{k+1}^*(x_{k+1})] \tag{2.5}$$

where J_k^* is the minimal cost from the initial state x_k at time k to the end and L_k are the instantaneous costs for the corresponding state and control action.

In order to solve this optimization problem numerically, the state and control variable space are discretized in finite grids. Dynamic programming guarantees the global optimal to the optimization problem is found, although the accuracy is limited to the level of discretization of the time, state and control space. Increasing the discretization will improve the quality of the approximation of the true optimal control policy, but the computational burden increases exponentially with the number of states and control variables. This syndrome is known as "the curse of dimensionality" [9, 22, 36].

2.5 Local optimization strategies

Because global optimization strategies were deemed infeasible for application in practice, new control methods for the local optimization of control strategies were researched that were better suitable for online applications. The main focus of this research was to develop methods with lower computational demands than global optimization strategies and lower dependency on fully detailed, highly accurate information on future conditions [1]. In local optimization methods the global optimal control problem of the HEV is simplified to the minimization of an instantaneous or short horizon based cost function, rather than the minimization of the cost function over the complete route. This means that instead of looking for the control policy that minimizes the global optimal control problem, it is assumed that the combination of control inputs that minimize the instantaneous or short horizon control problem provides a solution that is close to the global optimal solution [1, 32]. Technically, an instantaneous method is the same as a short horizon based method with a prediction horizon of 1 time step.

The simplification of the global optimal control problem to an instantaneous or short horizon based set of optimization problems offers a great reduction in computational demands and reduces the dependency on information about future conditions. However, depending on the complexity of the drive cycle, the performance of local optimization strategies is not as good as global optimization strategies (assuming the future conditions are accurately known in this case) . The main problem with local optimization strategies is that they are short-sighted and cannot relate the optimality of the control inputs at the current instance to

the long term optimal control problem [31, 37]. In other words, the optimal solution on a local basis does not ensure the optimal solution in the LH or global control problem and is therefore for most drive cycles not able to achieve the maximal performance in the perspective of the complete route. However, local optimization strategies can be supported by a globally optimized reference trajectory for the powertrain states (i.e. SoC) as proposed in Section 2.6. In this case, solutions close to the global optimum can be found. In practice however, the global optimal reference trajectory cannot account for local events in the far future, which is the reason why the local strategy has to provide some flexibility to tolerate LH reference errors. In this section two local optimization strategies will be discussed: ECMS and short horizon based strategies.

2.5.1 Equivalent Consumption Minimization Strategy (ECMS)

ECMS was introduced by Paganelli in 1999 as a numerical method that can solve the local optimal control problem of the HEV [1]. It's main principle is that the use of electric energy is equivalent to using a certain quantity of fuel [1, 22, 31]. The sum of the actual fuel consumption by the ICE and equivalent fuel consumption by the EM can subsequently be minimized. This optimization problem is simplified to the minimization of the instantaneous (rather than integral) equivalent fuel consumption, with cost function J:

$$\begin{aligned} &\underset{u(k)}{\text{Minimize:}} && J(k,u(k)) = \dot{m}_{f,\text{equiv}}(k,u(k)) = \dot{m}_{f,\text{ICE}}(k,u(k)) + s(k)P_{el}(k,u(k)) \\ &\text{Subject to:} && \text{Component constraints as defined in Equation (2.4)} \end{aligned} \tag{2.6}$$

where $\dot{m}_f$ is the mass flow of (equivalent) fuel, P_{el} is the electric power charged to or drawn from the battery and s is the equivalence parameter.

The equivalence parameter assigns a cost to the use of electric energy and plays a key role for the power distribution between the two power sources [1, 22, 24, 39]. It represents the chain of efficiencies for fuel transformed into electric power and vice versa and therefore its true value changes for each operating condition of the powertrain (drivetrain speed, power demand, SoC). In its most simple form the equivalence parameter is a constant value that is approximately valid for every driving condition and corresponds to the relative energy consumption between the IC and electric powertrain. Finding the true value of the equivalence parameter as a function of time that leads to the global optimal solution is challenging, since it depends on and is highly sensitive to the complete future driving conditions and powertrain states [1, 32, 40]. One method to obtain the optimal value of the equivalence parameter at every point in time is to directly derive it from a global optimal solution (e.g. determined by DP). However, due to uncertainties in the prediction of future conditions, the errors in the derived value of the equivalence parameter will eventually lead to divergence from the true optimal control strategy under the actual conditions. Another method to find an appropriate value for the equivalence parameter is to constantly adapt it based on the deviation of the current battery SoC from a certain predetermined reference SoC trajectory. These methods are grouped under the term Adaptive Equivalent Consumption Minimization Strategy (A-ECMS) [1, 40]. The reference SoC trajectory in these strategies can be a linear reference, or a certain optimized trajectory that is obtained from, for example, global optimization methods. In literature often proportional feedback or proportional-integral (PI) control are proposed to ensure the reference trajectory is tracked [24–26, 40].

ECMS as a local optimization method offers low computational demands and does not explicitly depend on information on future conditions: all future dependency is lumped in the equivalence parameter [1, 33]. Its solution can be close to the global optimal solution with appropriate adaptation of the equivalence parameters (e.g. derived from global optimal solution or if closely tracking an accurate globally optimized SoC reference). However, since the control problem is still solved on an instantaneous basis, the global optimality of the solution is still not ensured. Next to that, instantaneous methods can only penalize deviations from the prescribed reference SoC and can never ensure a hard constraint target value is exactly achieved. Again, since the global optimal reference trajectory cannot account for the local event in the far future, exactly tracking the reference does not lead to the true optimal solution.

2.5.2 Model Predictive Control (MPC)

MPC became popular in 1980's as a control method for the control of chemical processes [41, 42]. Nowadays, MPC is also frequently used in literature for automotive applications because of its ability to handle constrained multi-variable control problems [19, 30, 30, 31]. The general objective of MPC is to compute a future control policy that optimizes the future plant response with respect to a certain cost function and a set of constraints. MPC is often solved in receding horizon fashion [19, 30, 31, 41], which means the optimization is performed within a limited time window, called the moving horizon window. Although the optimal control policy is completely described within the entire horizon, only the first control action is supplied to the plant, discarding the rest of the planned control actions. To optimize the future response of the plant, the future behavior and response of the plant to control inputs are predicted using the predicted future driving conditions and an internal vehicle model. For application in HEVs, MPC can be applied to minimize the equivalent fuel consumption and, if available, to track the desired LH global SoC trajectory.

$$\begin{aligned} &\underset{u(k)}{\text{Minimize:}} \quad J(k) = \sum_{i=1}^{N_p} w_1 (SoC_{\text{ref}}(k+i) - SoC(k+i))^2 + w_2 \dot{m}_{f,\text{equiv}}(k+i, u(k+i)) \\ &\text{Subject to:} \qquad\qquad \text{Component constraints as defined in Equation (2.4)} \end{aligned} \tag{2.7}$$

where SoC is the battery SoC level, SoC_{ref} is the LH SoC reference trajectory, $\dot{m}_{f,\text{equiv}}$ is the consumption of equivalent fuel, N_p is the prediction horizon and w_1 and w_2 are weight factors to balance the two terms of the cost function.

Using MPC over a short prediction horizon to solve the local optimization problem can be seen as a good compromise between global control methods (like DP) and instantaneous methods (like ECMS) [31, 37]. In comparison to the global optimal DP method, MPC is less computationally demanding and does not require complete future information over the entire drive cycle (only over the prediction horizon), which potentially enables its use in real-time applications. Compared to ECMS, MPC is less short-sighted and less sensitive to its initial conditions, since it can better anticipate on future events and plan according future control actions in advance (depending on the prediction horizon). In contrast to ECMS, the MPC approach has the ability to include hard constraints in its control strategy, rather than only reference tracking based on the penalization of deviations.

Due to the nonlinear component characteristics and discrete system states discrete (e.g. ICE on/off and driving modes) , the non-simplified optimal control problem results in a discrete nonlinear constraint optimization problem, which requires complex solving algorithms (such as mixed integer nonlinear programming (MINLP) solvers) [43]. The high computational demands required to solve a nonlinear hybrid (discrete) MPC form the biggest obstacle for online application in HEVs [31]. The most common way to use a MPC control method and work around this problem is to linearize the plant model, constraints and objective around its operating point. This way the problem can be converted into a quadratic problem, which can be solved at significantly lower computational costs [31]. However, these simplifications can be so strong that determined control policy is no longer optimal to the non-simplified optimal control problem. This was found by Borhan et al. [37], where the simplified quadratic solution was unable to provide noticeable improvements in fuel economy compared to a conventional heuristic control method.

2.6 Two-stage architecture

In the previous two sections, it was shown that global optimization methods are unsuitable for online application and local optimization methods can achieve only moderate performance for complex drive cycle due to their lack of perspective to the complete route. In the research for real-life applicable control methods with high performance for both the LH and SHcontrol strategy, it was recognized that as long as the SH solution complies with the general LH strategy, the influence of the detailed SH strategy on the LH optimality is small [23–26]. More practically said, as long as the SH control strategy does not deviate far from the LH control strategy, the detailed SH control inputs have only a minor influence on the optimality of the complete LH control problem. The reason for this is that the two control strategies control very distinct dynamics, which take place on different timescales as mentioned already in Section 2.2.1. By making use

of this property, it is possible to split the two main tasks of the supervisory control problem into two separate optimal control problems and solve them sequentially: first determining the LH strategy for optimal EMC and afterwards tracking this LH solution in the SH control problem for optimal PMC. Concluding, it can be said that since the cross-sensitivity influence of the SH solution on the LH strategy is small, it is possible to treat the optimal control problem for the supervisory controller of a HEV as an unidirectional problem. This allows the optimal control problem to be split in two separate optimal control problems that can be solved sequentially with dedicated solvers for each subproblem. Independently of the complexity and optimality of the LH solution, the LH reference SoC trajectory is used as the interface between the two controllers [19, 23–26, 30, 34]. In Figure 2.1 an overview of the architecture is displayed.

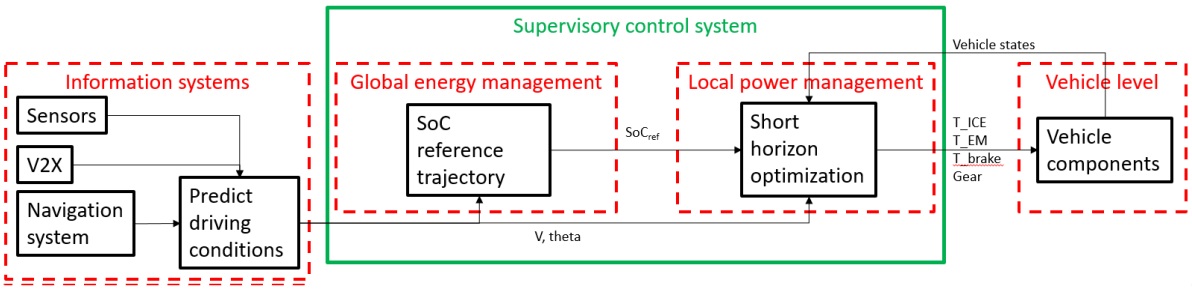

Figure 2.1: Overview of the two-stage control architecture and its interfaces.

The two-stage control method offers significant advantages over individual SH or complete route optimal control methods. Not only can the two-stage approach closely approximate the global optimal solution [19, 23–26, 30, 34], it also allows the use of separate solvers that are dedicated to the two control problems. These advantages make the two-stage control architecture a promising control approach for the application in practice. Within the two-stage architecture, the main intent of the LH optimization problem is no longer to supply the detailed control inputs, but instead, is to determine the battery depletion strategy over the complete route. This enables the use of LH estimation methods that approximate the global optimal solution with reduced computational demands, since the computational demands of a fully detailed global optimization method (like DP) are still too high for online calculation in real-world systems. Next to that, since only the LH battery depletion profile is required, it is also possible use estimation methods that require less accurate information on future conditions (e.g. a linear depletion profile is now an option). It should be noted, however, that the application of less advanced estimation techniques also reduces the optimality of the solution.

2.7 Long horizon estimation methods

The main objective of the LH or EMC controller is to determine the optimal depletion strategy of the battery that meets the desired SoC level of the battery at the end of the trip The optimality of this battery depletion strategy is an important factor in the overall efficiency of the PHEV, where the true global optimal control policy results in the minimal fuel consumption. As mentioned before in Section 2.4, determining the true global optimal solution for the LH problem is infeasible since neither the level of detail in predictive information, nor computation resources are available to calculate this solution. For these reasons, LH estimation methods are introduced to approximate the global optimal battery depletion strategy. The level of knowledge on future conditions these estimation methods are based on can be classified in three different levels. In this section these knowledge levels will be introduced and state of the art control strategies based on each of these levels will be described.

1. No trip information
2. Distance information
3. Distance, altitude and velocity information

2.7.1 No trip information

In this knowledge level of future conditions, the only available information is the vehicle states and power demand at the current instance. With complete absence of information on upcoming conditions (including the trip length and traveled distance) the global optimal LH battery depletion profile could have any possible shape and length. Statistical data shows however that on average a significant amount of trips are shorter that than the all-electric driving range of the PHEV [44–46]. Based on this observation and the absence of any knowledge on the shape and length of the ideal depletion strategy, it is best to adopt an EMC strategy that strongly focuses on utilizing the electric driving mode with minimal use of the ICE. If however, after a battery depletion phase the battery SoC level is low (because the trip turns out to be longer than the all-electric range, the EMC strategy has to be adapted for the remaining of the trip. In these cases a mixed strategy is adopted that keeps the SoC of the battery within an operating window for the remaining of the trip (charge sustaining). This two-phase control strategy is referred to as the charge depleting - charge sustaining (CDCS) strategy, based on the two distinctive phases [13]. Although variations of the emphasis on maximizing the use of the electric driving mode are possible, supervisory controllers based on the CDCS EMC strategy are widely used in production HEVs [13, 19, 21, 22, 30, 32, 35].

2.7.2 Only distance information

For long horizon estimation methods that have access to the traveled distance and length of the trip, the distance to the final SoC target is given at any point in time. However, the optimal depletion profile could still have any possible shape. In cases where the trip length is shorter than the all-electric range of the vehicle (and assuming the trip has conditions similar to the cycle this range was based on), the supervisory controller could adapt an EMC strategy that maximizes use of pure electric driving [30]. If the trip is longer than the all-electric range and no further knowledge on future conditions is available, it is best to assume the conditions along the trip have the same average power demand and therefore it is best to distribute the available battery energy linearly over the trip [19, 30, 32]. Since distance information is available in any modern HEV with a navigation system, these depletion strategies could be a promising alternative to the CDCS strategy. This approach is also proposed in various works in literature and shows significant improvements over CDCS strategies [19, 30, 32]. The relative performance of the strategy in comparison to strategies with access to higher levels of information, however, strongly varies between the works and different simulation cases.

2.7.3 Distance, altitude and velocity information

If the planned route is known and information is available on the altitude and velocity conditions along this route, it is possible for the supervisory controller to estimate the future power demand at each point in time (as discussed in Section 2.2.3). Once the future power demand is known, optimization methods can be applied to determine the optimal (or an estimation of the optimal) depletion strategy. As mentioned in Section 2.4, many works rely on global optimization methods like DP to determine the LH strategy, but the computation of the optimal solution has too high computational demands for online applications. Literature has proposed several approaches however, that can estimate the global optimal LH with low computational cost and lower accuracy requirements on the predictive information.

Ambuhl and Guzzella [24] propose a LH estimation method that uses a power-based segmentation approach to determine a SoC reference signal for a HEV without plug-in functionality. The objective of the estimation method is to maximize the recuperation energy and to minimize the rate of change of the SoC. The method discretizes the route into variable-sized segments based on the direction of the power flow (negative or positive torque request) over which a linear change in SoC is assumed. A quadratic programming (QP) algorithm is used to determine the SoC change per segment and the LH SoC trajectory is constructed afterwards. Tianheng et al. [25] propose a LH estimation method that uses a mathematical relation to determine a SoC reference signal for a PHEV. The fundamental assumption of the method is that segments with frequent accelerations or low driving speeds are suboptimal for ICE operation and therefore are preferred to be driven electrically. The method discretizes the route into long segments (7 to 12 km) over which a linear SoC change is assumed. A mathematical relation is used to translate the predicted energy demands into a change in SoC based on average and standard deviation of the velocity

over the segment and the LH SoC trajectory is constructed afterwards. Vajedi et al. [19, 40, 47] propose a LH estimation method that uses a power-based clustering approach to determine a SoC reference signal for a PHEV. The method clusters route segments into groups based on their average power demand and subsequently determines the optimal power split for each cluster such that the fuel consumption of the HEV over the complete trip is minimized while satisfying the final SoC target. Once the power split for each segment is known, the LH SoC trajectory can be constructed. Heppeler et al. [26, 34] propose a LH estimation method that uses a power-based classification approach to determine a SoC reference signal for a HEV without plug-in functionality. The objective of the estimation method is to maximize the amount of equivalent fuel saved by the application of the electric driving mode and LPM strategies and to minimize the loss of recuperation potential. The route is split into variable-sized segment based on four different use cases that together span the complete range of power demands. A DP algorithm is used to determine the SoC change per segment and the LH SoC trajectory is constructed afterwards. Taghavipour et al. [30] propose a LH estimation method that uses a velocity-based segmentation approach to determine a SoC reference signal for a PHEV. The method splits the route into variable-sized segments based on the velocity profile and subsequently calculates the average power demand per segment. Using the `fmincon` function in Matlab, the optimal power split for each segment is determined that minimize the fuel consumption of the HEV over the complete trip while satisfying the final SoC target. Once the power split for each segment is known, the LH SoC trajectory can be constructed.

Each one of these works applied a two-stage control architecture to control the powertrain of the HEV, for which they all used a LH SoC reference trajectory as the interface between the two control stages. For the planning and application of control actions of the local range, both ECMS and MPC methods were applied.

2.8 Adaptive heuristic control

During the literature review, it was recognized that the local control methods proposed by literature often fail to take into account all conditions that are necessary for feasible online application of the control method. In this section, the main principle of a novel adaptive heuristic control method is proposed that updates the calibration set of a conventional, non-predictive, heuristic controller based on predictive information on the near-future driving conditions in order to the lower fuel consumption and/or better with the LH control strategy.

2.8.1 Problem with optimization based methods

In the previous sections of Chapter 2, it has been recognized that minimizing the fuel consumption is not the only criteria a supervisory control system of a HEV should take into account: also feasibility, drivability and computational considerations should be included.

First of all, the feasible domain of control inputs is constrained by component limitations as introduced in Equation (2.4). Any infeasible control request will be saturated and result in a vehicle response that differs from the desired behavior. These quasi-static component limitations (described in more detail in Chapter 3) however, do not include the dynamic delays of the powertrain components. Especially for the turbocharged ICEs there can be a significant lag in the output torque response to load steps [9, 17]. For this reason, large variations in the requested ICE torque are undesired. The torque-buildup-time of the ICE used in this simulation model is around 0.9 seconds to go from low torque (<25%) to high torque (>75%). Next to that, as discussed in Section 2.2.1, the supervisory controller has to consider the effect of the vehicle on the driver and avoid control policies that result in unacceptable behavior in terms of drivability (e.g. avoid aggressive ICE transients, frequent ICE starts and constrain minimal ICE-on-time). And thirdly, the computational resources during online application are limited. Due to these constraints, control methods with high computational demands are infeasible for online application. These three conditions (feasibility inputs, drivability, computational constraints) will be referred to as the feasibility conditions for online application.

When analyzing works in literature, it has been found that most works in literature do not take into account (all of) these feasibility conditions for online application. It was found that most works in literature do not mention any drivability conditions in their search for the optimal control strategy. As a result, the optimal control problems that are solved in literature do not constrain the number of ICE starts in any way. Since these works in literature do not see this behavior as important characteristics, there is no detailed information on the typical usage of the ICE and assessing the drivability of the control strategies is difficult. However, three examples have been found in literature that likely do not satisfy the drivability considerations: In the work of Heppeler et al. [26] and the work of Taghavipour et al. [30], a figure is depicted that shows high frequent ICE starts and shut downs with very short phases where the ICE is on. In the work of Zhang et al. [48], a comparison is made between a conventional heuristic control method and an ECMS-based method. The results show that very short ICE-on phases are present and the number of ICE starts is at least 3 times higher than that of the heuristic control method. As discussed in Section 2.2.1, it can be concluded that the usage of the ICE should be constrained in order to limit the number of ICE starts, length of the ICE phases and aggressive ICE transients. It should be noted that, since the ICE status is a discrete state, the complexity of MPC-based optimization problems would increase significantly when these constraints are taken into account, leading to significantly higher computational demands. .

Next to the drivability conditions, the computational demands are not completely taken into account in most works in literature. For acceptable control of the ICE and EM, the control frequency of the supervisory controller should at least be higher than the requested changes in the acceleration of the vehicle. Typical frequencies for velocity control in for example ACC applications is 10 Hz [49, 50], and typical response times to throttle inputs (tip in/out) should be within 50 ms [51, 52]. This means (at least parts of) the supervisory controller should operate at 20 Hz and calculate the new control actions within a 50 ms time period. A computation time of 50 ms is a relatively short time to solve complex optimization tasks, especially since the computational resources on-board a vehicle are significantly less than the available resources in a PC. In literature nevertheless, often complex optimization are applied to solve the optimal control problem for the hybrid powertrain control. Although very little information is given on the actual computational demands of the methods proposed in literature, it is believed that the available computational resources in online applications are often strongly over-estimated. The A-ECMS and MPC control methods applied in this work take respectively 90 ms and 1750 ms to compute (introduced in Section 4.5 and evaluated in Section 5.5).

Optimization based methods could still be feasible for online applications, but there seems to be a trade-off between the computational demands and the accuracy (nonlinearity) of the models, the length of the prediction horizon and the inclusion of discrete states for drivability considerations. Although optimization based methods (and in particular nonlinear MPC-based methods) are believed to be infeasible for direct control of hybrid powertrain in online applications, hierarchical optimization based control method that operate parts of the control tasks at different control frequencies could be feasible. In such a system an optimization based control method for trajectory planning would be operated at a low update frequency and a control system for direct control with low computational demands would operate at a high update frequency. In the next section, an adaptive heuristic control method is proposed that makes use of this approach.

2.8.2 Proposal adaptive heuristic control

In strong contrast to the optimization based methods proposed by literature and their corresponding problems with the feasibility conditions stand heuristic control methods. As extensively described in Section 2.2.2 and Section 2.3, they are characterized by their low computational demands and take into account the necessary conditions to achieve an acceptable level of drivability. Although its performance can be near optimal for drive cycles they are optimized towards, the main disadvantage of heuristic control methods is that the performance is often moderate for unknown drive cycles.

Rephrasing the previous statement, it could be said that, the performance of a heuristic controller is potentially near optimal for any route, as long as its calibration is optimized towards the route's driving conditions.

Conventionally, it is not possible to recalibrate the heuristic controller for every route, since the driving conditions are unknown. However, by recognizing that the prediction of the future driving conditions is feasible over a short horizon (as described in Section 2.2.3), the recalibration of a heuristic controller over a short horizon period becomes possible. It is important to note that, the resulting set of driving conditions for a recalibration over the short horizon is extremely short (i.e. in the order of 60 seconds) and that the conditions are typically relatively constant with low diversity over a short horizon compared to a set of driving conditions over the complete route. For these two reasons (a low number of samples and relatively constant conditions), the performance of a heuristic control method after recalibration on a set of driving conditions over the short horizon can be very close to the optimal strategy.

Instead of conventionally optimizing the calibration set towards a complete route, in this work a novel control method is proposed that optimizes a new calibration set towards each short horizon interval, which is only a small section the route (i.e. in the order of 60 seconds). As the basis of this method, a conventional heuristic controller is used that determines the control inputs based on the instantaneous conditions and includes all the required functionality in terms of feasibility and drivability criteria. Its set of calibration parameters is adapted by a recalibration process based on the upcoming driving conditions over the next short horizon interval. The heuristic rules are adapted by the recalibration process (described in more detail in the next section) such that the most desired behavior is obtained in terms of energy management, fuel economy, drivability and feasibility. If a LH battery SoC reference is available, the optimal calibration set can be determined that is able to track this LH reference. More practically speaking, a recalibration of the calibration set means that the threshold values and maps of the default calibration are modified to obtain a more optimal vehicle behavior. The complexity and shape of the maps can be altered if desired and the number of variables that are modified is in principle free.

The proposed adaptive heuristic control method with a heuristic controller as its basis has very low computational demands for the direct control logic, which means that the control system that actually sends the control inputs to the various subsystems can be computed at a very high frequency. The calculation of the optimization tasks (recalibration and LH) can be spread out over a longer time period to keep the computational costs low. Like conventional heuristic control methods, the adaptive heuristic approach provides a high level of robustness that will always make sure the requested control inputs are feasible and will adapt the strategy if the driving conditions are different from expected (e.g. turn ICE on if the deliverable electric power is insufficient). The core control logic of the proposed control method relies on proven technology that is already widely applied in production HEVs. Since the recalibration process can be seen as an additional system on top of an existing control system, it is not required to modify the existing interface between the supervisory controller and other systems (such as the Engine Control Unit).

2.8.3 Methods for recalibration

Although the basic principle of adaptive heuristic control is relatively simple, implementing an automated process that finds the optimal calibration set is not a trivial task, because there is no direct relation between the calibration parameters and the resulting vehicle response. The goal of this recalibration process is to find a more optimal calibration set for a known heuristic controller and the predicted conditions over the given SH interval.

One might argue that the best way to find the optimal calibration set is to extract the calibration set from a detailed MPC solution over the SH that includes all objective terms and all feasibility and drivability constraints for acceptable behavior in practice. However, in order to make direct extraction of the calibration set possible without the need for further modifications, the MPC optimal control problem has to include the complete heuristic logic (including every rule and every map) of the heuristic controller. The resulting optimal control problem is a highly complex optimization problem that includes discrete states and nonlinear relations (even more than the normal non-simplified MPC problem). Setting up and solving this optimization problem is a difficult task and requires complex solvers like MINLP solvers that become more computationally demanding with increasing length of the SH prediction horizon [43]. The complexity and computational demands of this approach make it a less ideal method for determining the new calibration

set. Rather than solving a discrete and nonlinear MPC problem, one might opt to solve a less complex optimal control problem (e.g. without discrete states or a quadratic programming problem). Direct extraction of the calibration set is not possible in this case, because the solution to the simplified optimal control problem does not include the complete heuristic logic. A secondary translation step is therefore required that applies strong modifications to the simplified MPC solution in order to translate it into a control policy that allows the new calibration set to be extracted. However, modifying the solution to the simplified optimal control problem does no longer ensure the modified solution is optimal or feasible and makes also this approach a less ideal method for determining the new calibration set. Summarizing, the MPC-based recalibration methods determine a sequence of control actions for each point in time over the SH interval and subsequently obtain a new calibration set for the heuristic controller by either direct extraction or a translation process.

Reevaluating the goal of the recalibration method (finding a more optimal calibration for a known heuristic controller and the given SH interval) shows that the MPC-based recalibration methods is actually a rather cumbersome and indirect method for a goal that is much simpler. Rather than solving a MPC problem and extracting a calibration set, it is possible to directly test different calibration sets and evaluate their performance. Using an intelligent search method, look for the calibration set that performs best in terms of the objective while satisfying the constraints and LH SoC strategy. Depending on the required number of candidate calibrations that need to be evaluated, this approach is easy to set up and potentially low in computational demands (in contrast to a detailed MPC). Also, since the exact behavior of a candidate calibration is directly assessed, it is guaranteed the heuristic controller with its final calibration will behave as expected (in contrast to a simple MPC with a subsequent translation step). The solution space and complexity of this intelligent search method strongly depends on the desired number of logical rules that need to be recalibrated and their complexity. However, as described in Section 2.3, the heuristic controller makes only two main decisions: the desired driving mode and the desired power distribution and therefore, the complexity of this problem is expected to be relatively low.

2.8.4 Summary of adaptive heuristic control

It was found that optimization based control methods in literature only focus on the minimization of fuel consumption over the SH interval, but do not take into account all conditions for online application (feasibility of control inputs, drivability conditions and computational resources). In contrast to optimization based methods, heuristic control methods include all of these conditions. The main disadvantage of heuristic method is, however, that their performance in terms of fuel economy is low for unknown cycles.

To improve the performance, an approach is proposed that uses the predicted upcoming driving conditions to update the calibration set of a heuristic controller for each SH interval. Since the basis of method is conventional non-predictive heuristic controller that includes all functionality of feasibility and drivability. Besides that, this control method would not require modifications to existing interfaces of the supervisory control systems and other control systems. Its computational demands are very low, which enables it to operate at a high frequency. The calculations for the recalibration process can be spread out over longer time period to keep computational costs low.

The main goal of the recalibration process is to find a more optimal set of calibration parameters for the known heuristic controller. An intelligent search method is proposed that determines best calibration parameters by testing different candidate calibration sets and directly evaluating their behavior and performance. This approach is easy to set up and potentially low in computational demands (subject to the number and complexity of the calibration parameters).

In Figure 2.2 the adaptive heuristic control method is graphically displayed. The combination of the intelligent search method and heuristic controller make up the ”Local power management” system in Figure 2.1.

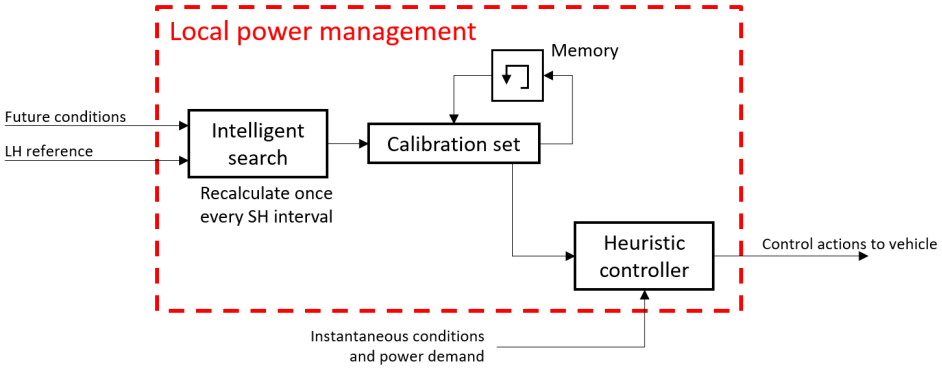

Figure 2.2: Overview of the adaptive heuristic control method.

3

Vehicle modeling

Predictive control methods make use of internal system models to predict the response of the system to future control actions and external inputs. In this chapter, the topology and components of the simulation vehicle are described. A control-oriented model is developed that is suitable for online calculations while maintaining sufficient accuracy. Finally, the validity of the developed control-oriented models is evaluated by comparing its behavior to the high fidelity model.

3.1 Model types

The availability of suitable vehicle and component models is essential in the development of predictive supervisory control methods. First of all, even if the true optimal control policies can be determined, the feasibility and optimality of the calculated control inputs are only as good as the prediction model they are based on. Next to the quality of the predictions, a suitable plant model is also required for simulation based (Model-in-the-Loop testing) evaluation and validation of the developed control methods, to ensure the methods can be successfully applied to a real dynamic system. Several different types of models are incorporated in the development process of control methods, which can be divided into two main groups: high-fidelity models and control-oriented models.

High fidelity models are highly detailed and try to model the behavior of the real system as accurately as possible but as a result are often complex and computationally expensive to run. Control-oriented models on the other hand find their main purpose in online controller models and have to be simple enough for fast calculation, while still providing sufficient accuracy to characterize the system. In this work, control-oriented models are used in the predictive supervisory control system to predict future demands and the vehicle's response to control inputs. A high-fidelity model is used as the plant model to evaluate the effectiveness of the control method, as well as reference for the validation of the control-oriented models. Also, because the high fidelity model takes more and higher order system dynamics into account, the application on this simulation model is closer to the application on an actual vehicle.

3.2 Vehicle topology

Although the method is not limited to a specific type of HEV or specific hybrid topology, in this research a PHEV simulation model is used as a platform for the evaluation and validation of the developed control methods. The vehicle model, all vehicle parameters and the combustion powertrain of this PHEV model are based on a Volkswagen Jetta HEV, where the electrical components (EM and battery) are taken from other production PHEVs. The vehicle is a front-wheel driven PHEV based on a P2 parallel architecture (Appendix A.4), where both the ICE and EM are mechanically coupled to the drivetrain and wheels. A controllable clutch is integrated in the design that allows the ICE to be decoupled from the powertrain and makes it possible to operate the vehicle in pure electric driving mode. The electric energy required

by the EM is supplied by a high voltage Lithium Polymer battery. Also the EM is able to apply negative torque during which energy is stored in the battery (e.g. during regenerative braking). In cases where the regenerative braking power is insufficient or unavailable, hydraulic brakes can be applied to decelerate the vehicle. The vehicle architecture and all its major components are illustrated in Figure 3.1. The vehicle has specifications similar to an average midrange passenger vehicle with a total mass of 1635 kg. The engine has a maximum power of 110 kW and a maximum power of the electric motor of 80 kW, which are jointly connected to a 7-speed automatic transmission. The battery has a capacity of 4.2 kWh operating at a nominal voltage of 407.2 Volt and can be externally charged using the plug-in functionality.

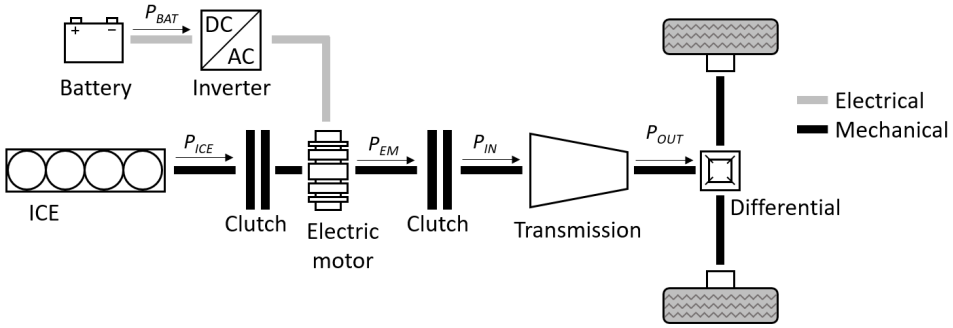

Figure 3.1: Topology of a P2 parallel hybrid powertrain.

3.3 High fidelity model

In order to evaluate the effectiveness of the developed control method and strategies, an accurate and reliable simulation model is required that represents all the relevant aspects of a real-world vehicle, its powertrain and environmental conditions. In this work, a co-simulation toolchain is used to create a high-fidelity vehicle model of the PHEV [53, 54]. The simulation toolchain, depicted in Figure 3.2, combines the following simulation tools:

- **IPG CarMaker:** to include 3D vehicle dynamics (in contrast to the control oriented model, including lateral and pitch dynamics). IPG CarMaker provides an accurate vehicle environment including road characteristics and environmental conditions. It also offers a velocity control system that mimics the behavior of a human driver. Next to that, IPG CarMaker is able to visualize the vehicle, some vehicle states and its environment.
- **AVL Cruise:** to extent the powertrain modeling capabilities. AVL Cruise provides detailed models of the hybrid powertrain, including the EM, ICE, battery, transmission and various subsystems.
- **Matlab/Simulink:** is used for the development and implementation of the supervisory controller of the powertrain.

The high fidelity model was developed by AVL. The models of the powertrain components (transmission and ICE as well as the EM and battery) where obtained by tests on a chassis dynamometer and other test benches, which is one of the core businesses of AVL. Other key parameters, such as the vehicle mass and aerodynamic drag coefficient are publicly available.

3.4 Control oriented model

As mentioned earlier in this chapter, the level of complexity and corresponding computational costs of high fidelity models are too high for application in online controller models. Instead, control-oriented models have been developed that require less computational resources, while still providing sufficient accuracy for online evaluation. Since the main goal of the supervisory controller is to determine control policies to control the power and energy flow in the PHEV, the main goal of the control-oriented is to capture the power related system characteristics with high accuracy. The first main simplification that is made in the control-oriented models is the omitting of all lateral and pitch dynamics of the vehicle. This simplification

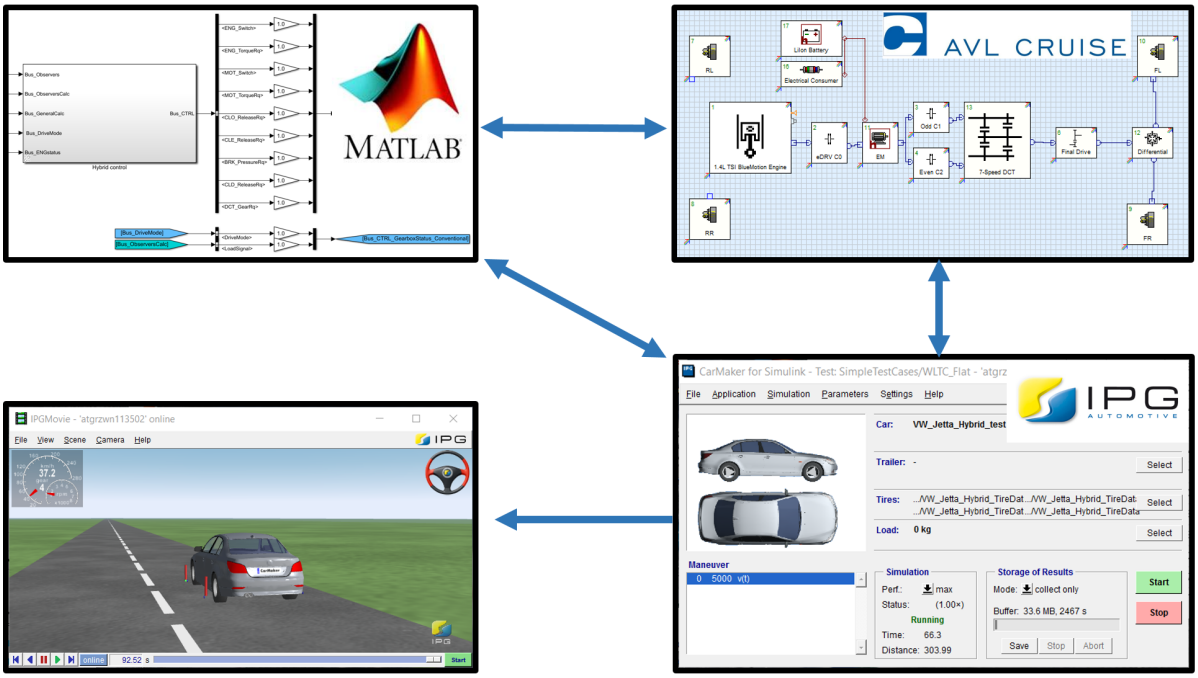

Figure 3.2: Overview of the simulation environment (Top left: Matlab/Simulink, Top right: AVL Cruise, Bottom right: IPG CarMaker, Bottom left: IPG Movie)

is reasonable since neither exerts a significant influence on the energy consumption [17]. Since the main interest is energy consumption, the system can be treated as quasi-stationary [18] and therefore, can be assumed the vehicle has only one controllable state: the state of charge SoC of the battery. For the evaluation of the drivability, the ICE status can be an additional state, but this state is not controllable for most of the control methods (the ICE is in these cases started when it is needed and turned off if it is no longer needed). Furthermore, the model has two inputs: the power demand (which is prescribed by the velocity and road inclination profile) and the power split (which is controllable and determines the distribution between the electric and combustion power source).

3.4.1 Longitudinal model

In order to determine the power demand of the vehicle a longitudinal vehicle dynamics model is applied. The main external longitudinal forces acting on a vehicle can be seen in Figure 3.3a. The corresponding resistive forces and vehicle's power demand are given by:

$$P_d = (F_{ax} + F_d)v \tag{3.1a}$$

$$F_d = \underbrace{\frac{1}{2}\rho A C_d v^2}_{\text{Aerodynamic drag}} + \underbrace{mg\cos\theta(C_{r,a} + C_{r,b} * V)}_{\text{Rolling resistance}} + \underbrace{mg\sin\theta}_{\text{Inclination}} \tag{3.1b}$$

$$F_{ax} = m_{\text{eff}}(G) \cdot \dot{v} \tag{3.1c}$$

where the power demand, P_d, is the result of the sum of the resistive forces, F_d, and the the inertial forces, F_{ax}, multiplied by the velocity of the vehicle, v. The resistive forces are build up by three components: the aerodynamic drag, rolling resistance and the forces due to the gravitational force and inclination of the road. Here, ρ is the air density, A is the frontal area, C_d is the aerodynamic drag coefficient, m is the vehicle's mass, g is the gravitational constant, $C_{r,a}$ and $C_{r,b}$ are rolling resistance coefficients based on the SAE J2452 rolling resistance model [55] and θ is the road inclination angle.

3.4.2 Drivetrain model

The inertia force in Equation (3.1) follows from the requested acceleration and the effective mass, m_{eff}, modeled by the combination of the mass of the vehicle and gear-dependent, G, rotational inertias of the drivetrain, J:

$$m_{\text{eff}}(G) = m + \frac{J_{\text{eff}}(G)}{r_{\text{wheel}}^2} \tag{3.2a}$$

$$J_{\text{eff}}(G) = J_{\text{before}} \cdot i_{\text{TRS}}^2(G) + J_{\text{after}} \tag{3.2b}$$

where the gear-dependent combined rotational inertia, $J_{\text{eff}}(G)$, is divided by the square of the wheel radius, r_{wheel}. The combined rotational inertia is build up by the inertias before the transmission, J_{before}, (e.g. ICE, EM, clutches and part of the drive shafts) multiplied by the current transmission ratio, i_{TRS} and the inertias after the transmission, J_{after}, (e.g. wheels, differential and part of the drive shafts). A schematic overview of the drivetrain is displayed in Figure 3.3b.

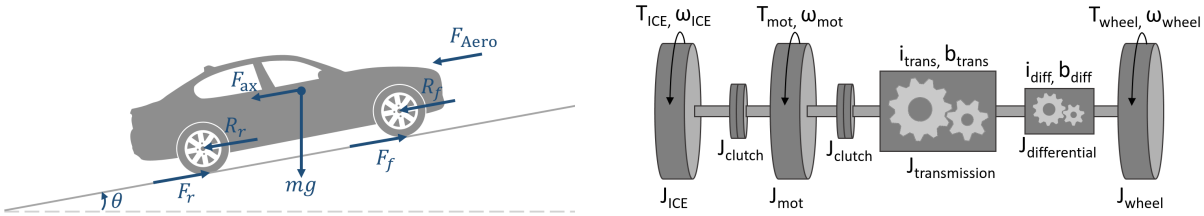

(a) Longitudinal forces acting on a vehicle on an inclined road.

(b) Transmission ratios, inertias and friction losses in the drivetrain.

Figure 3.3: Longitudinal and drivetrain model of the PHEV.

In addition to rotational inertias, the components in the drivetrain (in particular the transmission and differential) introduce friction losses (b_{trans} and b_{diff}) as well. In the control-oriented model the friction losses of the complete drivetrain are combined in a single component that introduces friction and is modeled as a 3D table that depends on the rotational input speed, input torque and active gear: $T_{\text{fric}}(k) = f(\omega_{\text{in}}(k), T_{\text{in}}(k), G(k))$. This table is generated from measurement data obtained from quasi-stationary testing and assumes a well-lubricated system operated under warmed-up conditions. As mentioned before in Section 2.2.2, the gearshifts are determined by a heuristic rule set and are a function of the velocity and torque request: $G(k) = f(v(k), T_{\text{out}}(k))$.

3.4.3 ICE and EM model

In a similar fashion as the friction losses in the drivetrain components, the fuel consumption characteristics of the ICE are modeled in 2D table, which is often referred to as the brake specific fuel consumption (BSFC) map [9] and is displayed in Figure A.1b. Here the fuel consumption of the ICE, $\dot{m}_{f,\text{ICE}}$, is a function of the rotational input speed,ω_{in}, and output torque of the engine, T_{ICE}: $\dot{m}_{f,\text{ICE}}(k) = f(\omega_{\text{in}}(k), T_{\text{ICE}}(k))$. Also this map is the result of quasi-stationary state measurements and assuming warmed-up and well-lubricated conditions. Similar to the fuel characteristics of the ICE, the power losses from the conversion from electrical to mechanical power in the inverter and electric motor are modeled as a 2D table, based on quasi-stationary measurements (displayed in Figure A.1a). The power losses in these two components are combined in a single component that introduces the power losses, $P_{\text{losses, EM}}$, and is a function of the rotational input speed and output torque of the motor, T_{EM}: $P_{\text{losses, EM}}(k) = f(\omega_{\text{in}}(k), T_{\text{EM}}(k))$.

3.4.4 Battery model

In literature many different circuit models of the high voltage battery have been proposed, which vary strongly in complexity and accuracy to model the voltage dynamic of the battery [1, 9, 17]. For applications

that focus mainly on efficiency considerations of the battery, the voltage dynamics can be strongly simplified and the use a Thevenin-based equivalent electric circuit model (Figure 3.4) is sufficiently accurate [1]. In this work such a model is used to model the battery, where the open-circuit voltage, V_{oc}, and internal resistance, R_{in}, are a function of the SoC . The variations in battery SoC are calculated by the integration of the battery current, I_{BAT}:

$$\Delta SoC = \sum_{k=1}^{N} \dot{SoC}(k) * T_s = -\frac{1}{Q_0} \sum_{k=1}^{N} I_{\text{BAT}}(k) * T_s \tag{3.3a}$$

$$I_{\text{BAT}}(k) = \frac{V_{\text{oc}}(SoC(k)) - \sqrt{V_{\text{oc}}(SoC(k))^2 - 4R_{\text{in}}(SoC(k))P_{\text{EM}}(k)}}{2R_{\text{in}}(SoC(k))} \tag{3.3b}$$

with the initial conditions $SoC(k = 1) = SoC_0$, where Q_0 is the nominal battery capacity and a positive battery current stands for discharging the battery. To prevent battery rapid battery aging, the operation range of the SoC is limited by the manufacturer to a minimal and maximal bound. For the battery in this simulation model the bounds are: $SoC \in [SoC_{\text{min}}, SoC_{\text{max}}] = [0.10, 0.975]$. The cooling systems of the battery and EM in passenger vehicles are typically always sufficiently sized to maintain a relatively constant operating temperature (once warmed up). For this reason, temperature effects are neglected in this work [24–26].

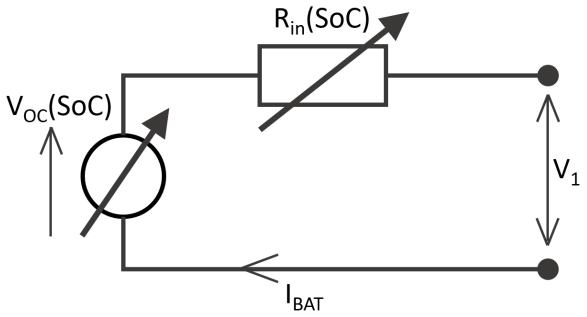

Figure 3.4: Equivalent circuit model of the battery.

3.4.5 Definition power split

As described in Chapter 2, the final goal of the supervisory controller of a HEV is to find the optimal power distribution between the ICE and EM over time. The power distribution at any point in time is prescribed by the power split control variable, which uses the definition as shown in Equation (3.4a). With this definition it is possible to use a $PS \in [-1 \quad 1]$ domain for the power split under all conditions and allows for LPM actions up to the component limitations of the EM under all conditions (including standstill).

$$\text{Definition:} \quad PS(k) = \frac{-P_{\text{EM}}(k)}{P_{\text{input}}(k)} \qquad P_{\text{input}}(k) < 0 \tag{3.4a}$$

$$PS(k) = \frac{P_{\text{EM}}(k)}{P_{\text{input}}(k)} \qquad P_{\text{input}}(k) \geq 0 \text{ and } PS(k) \geq 0 \tag{3.4b}$$

$$PS(k) = -\frac{T_{\text{EM}}(k)}{T_{\text{EM, min}}} \qquad P_{\text{input}}(k) \geq 0 \text{ and } PS(k) < 0 \tag{3.4c}$$

$$\text{Subject to:} \quad -1 \leq PS(k) \leq 1 \tag{3.4d}$$

where PS is the power split at any point in time, P_{EM} is the mechanical power output of the electric motor, P_{input} is the power demand before the transmission, T_{EM} is the output torque of the electric motor and $T_{\text{EM, min}}$ is the maximal negative torque output of the electric motor in regenerative mode at standstill. The behavior of the vehicle and corresponding driving modes is graphically displayed in Figure 3.5.

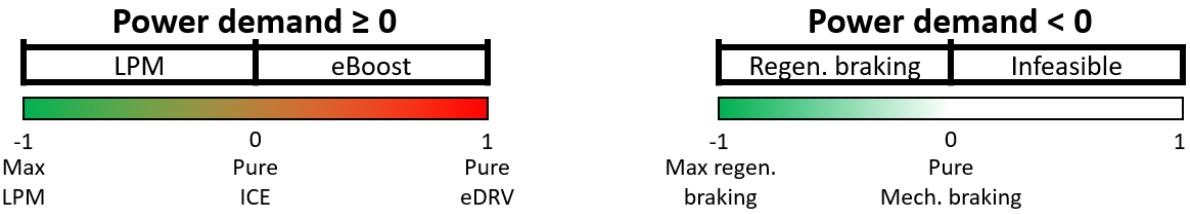

Figure 3.5: The definition of the power split graphically displayed.
With this definition, a power split of -1 is defined as maximal LPM or regenerative braking. With a power split of 0, the EM is not in use, meaning pure ICE driving or pure mechanical braking. A power split of 1 is defined as pure electric driving, while any power splits between 0 and 1 (indicating positive power consumption) are infeasible during braking.

3.5 Validation of control-oriented model using high fidelity model

The accuracy of the prediction models is important to achieve a high level of feasibility and optimality of the determined control policies. In real-world control applications, obtaining a good model description of the plant can be a challenging task, even if the underlying physical principles are known. Since the parameters of the plant are often not accurately known (e.g. rolling resistance of the tire), parameter estimation techniques can be applied to find a representative characterization of the complex system using the control-oriented (simplified) model.

In this work, a high-fidelity model is used to evaluate the developed control methods, which has been extensively tested and validated on the real-world vehicle. Since the high-fidelity model and all its input parameters are in principle known in this case, many parameters of the control-oriented model (e.g. vehicle mass, aerodynamic drag coefficient) are known as well and do not require further parameter estimation. Due to the limited computational resources in online applications however, simplifications have to be made in the control-oriented model (e.g. tire and battery modeling), which can introduce discrepancies between the control-oriented and high-fidelity model. The main goal of the developed predictive control strategies is to maximize the fuel economy of the HEV, which means the cumulative fuel consumption and battery SoC are the key variables of interest and require the highest prediction accuracy. By applying parameter fitting to minimize the errors between the control-oriented and high-fidelity model and focusing on the general trends and steady-state behavior of the fuel consumption and battery SoC, highly accurate predictions with respect to the fuel economy of the vehicle can be achieved. This process and the accuracy of the control-oriented model with respect to the high fidelity model will be discussed in the next section.

3.5.1 Parameter estimation and model validation

Simulating the fuel consumption and battery SoC of the HEV over time is the result of cascade of sub-models, which were described in Section 3.4. In order to make accurate predictions of the fuel consumption and battery SoC, each of these sub-models requires a high accuracy as well (e.g. a significant error in the propulsion torque, will often lead to a significant error in the fuel economy as well). Four different sub-models can be distinguished that have the following main goals:

1. **Longitudinal model:** Obtain the demanded wheel drive torque, which requires good modeling of the resistive forces.
2. **Drivetrain model:** Obtain the demanded input torque, which requires good modeling of the drivetrain friction losses and inertial effects.
3. **ICE and EM model:** Obtain the fuel consumption and electric power consumption, which requires good efficiency modeling of the ICE and EM.
4. **Battery model:** Obtain the change in SoC, which requires a good resistive cell model.

To achieve good correspondence between the control-oriented and high fidelity model, a hierarchical approach is used to fit and validate each sub-model from the first to fourth level. Any significant long-term discrepancies of each sub-model are minimized by iterative fittingThis way, accurate predictions of respectively the propulsion torque, input torque, ICE and EM efficiencies, battery SoC and fuel consumption

can be made, which can be used in the predictive control strategies. The parameter fitting approach uses results generated by simulations of both the control-oriented model and high-fidelity model over the same drive cycle. However, since the vehicle states in the two models are not necessarily the same, the controllers would not apply the same control actions and the results of the simulations are unsuitable for direct comparison. In order to obtain the same control actions in both models and make direct comparison possible, two distinctive operating modes are simulated: operation as a conventional vehicle where only the ICE can be applied for propulsion and operation as a pure-electric vehicle where only the EM can be used.

In Figure 3.6a, the velocity profile of the Worldwide harmonized Light vehicles Test Cycles (WLTC) profile is displayed, as well as the velocity profile of the high fidelity model. The high fidelity model is able to track the desired velocity profile closely, as can be seen in Figure 3.6b. The control-oriented model is driven over the resulting velocity profile of the high fidelity model, with the same gear shifting profile prescribed. Since the control-oriented model only makes forward predictions of the vehicle's behavior, its velocity and gear shift profile are exactly equal to the high fidelity model.

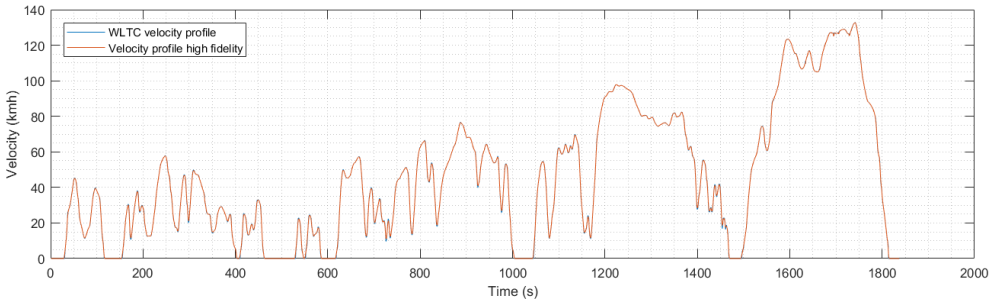

(a) Velocity profile from the drive cycle and the high fidelity model.

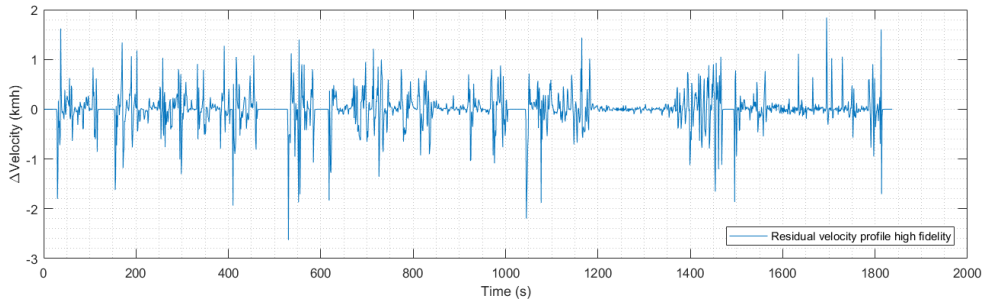

(b) Residual of the velocity profile as tracked by the high fidelity model.

Figure 3.6: Comparison of the velocity profiles from the drive cycle and the high fidelity model.

In Figure 3.7 and Figure 3.8, a comparison between the simulation results over the WLTC drive cycle over a flat road for both the high-fidelity and control oriented model is presented. Because the battery SoC is too low after 1650 seconds, only the interval between 0 and 1650 seconds is depicted. Figure 3.7a and Figure 3.7b display a comparison of both simulation models for the input torque (before transmission) over time, which is the final output of the second sub-model. It can be seen that the correspondence between the two simulation models is high and no steady-state offsets are present. The most extreme differences in input torque from Figure 3.7b (all errors larger than 50 Nm) are superimposed over the gear shifting profile in Figure 3.7. It can be seen that all short duration peaks in the high-fidely model are the result of the control actions during shifting, which is not accounted for in the control oriented model. The resulting fuel consumption and change in battery SoC over time are displayed in Figure 3.8. Also here it can be seen that the two models correspond very well and no significant (cumulative) errors are present. It should be noted that the displayed results are long term forward predictions (of more than 1000 seconds), where the predictions over the SH have much higher accuracy. Based on the simulation results it is concluded that the accuracy of the control oriented model is high enough to make reliable predictions of the future fuel consumption and battery depletion of the PHEV and suitable to be used in predictive control applications.

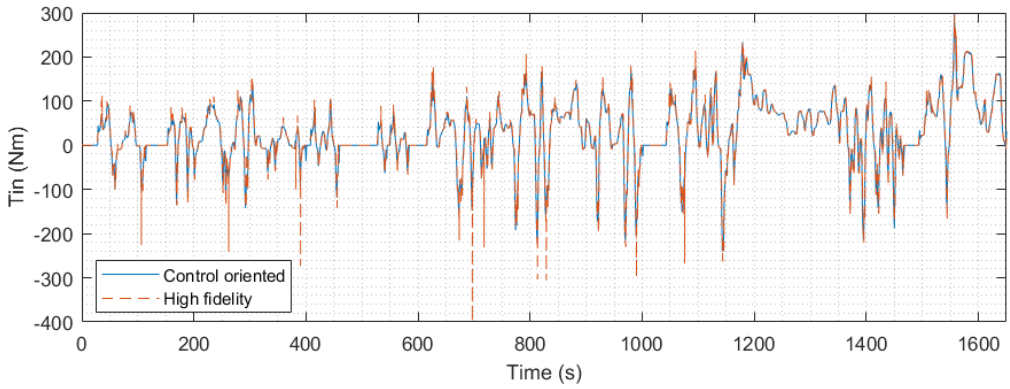

(a) Transmission input torque over time.

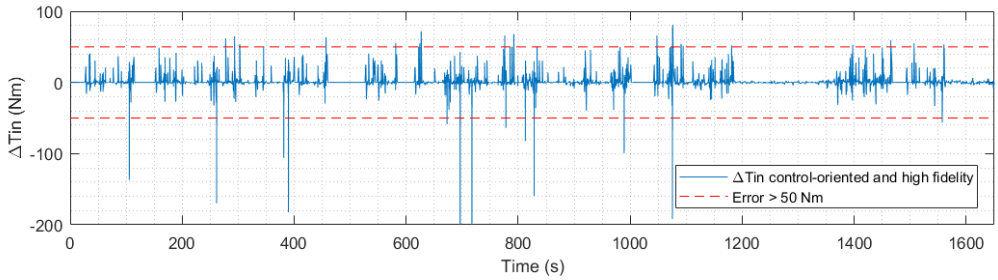

(b) Difference in the transmission input torque between the two models.

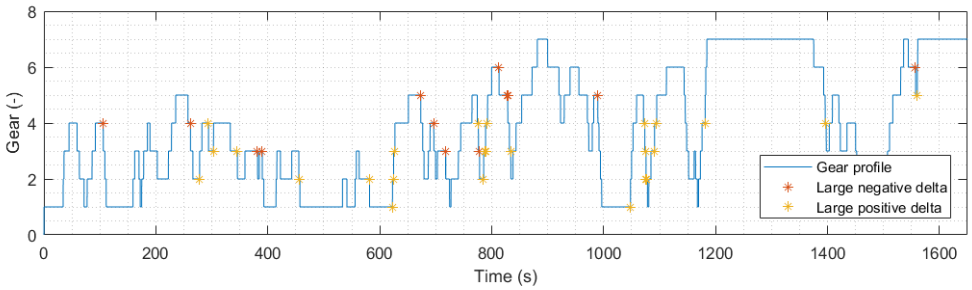

(c) Active gear profile over time

Figure 3.7: Comparison of the transmission input torque over time. The models show a high level agreement, which demonstrates the longitudinal model and drivetrain model can provide accurate forward predictions. The short duration peaks align with the gearshift points, which are not accounted for in the control-oriented model.

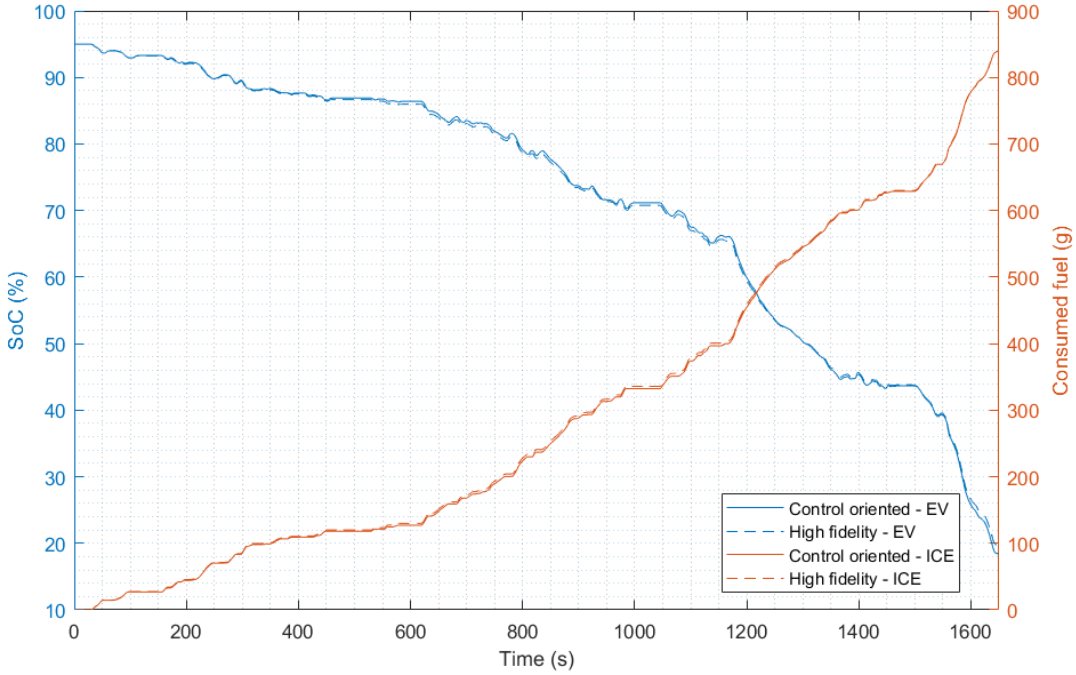

(a) Battery SoC and cumulative fuel consumption over time.

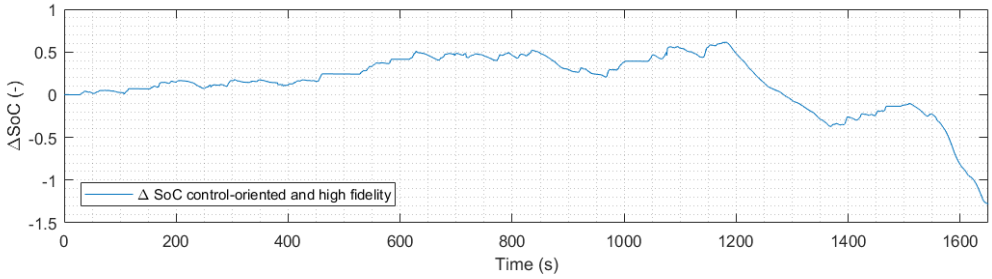

(b) Difference in battery SoC between the two models.

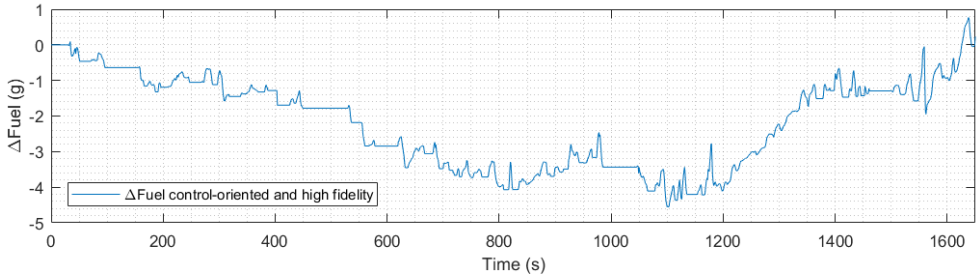

(c) Difference in cumulative fuel consumption between the two models.

Figure 3.8: Comparison of the battery SoC and cumulative fuel consumption over time. The models show a high level agreement, which demonstrates the ICE, EM and battery model can provide accurate forward predictions.

4

Development control methods

A two-stage control architecture for the supervisory control system of a PHEV is adopted, which splits the global range battery depletion strategy and local range detailed powertrain control in two separate systems.

In this chapter, the implementation of different methods for the global controlas well as local control are discussed. A LH estimation method is proposed that can approximate the global optimal solution closely with drastically reduces computational demands. Also the implementation an adaptive heuristic control methods is proposed to determine the local control strategy. Finally, an overview of the final controller architecture is presented.

4.1 Governing objective, main tasks and architecture

The main objective of the supervisory controller is to control the distribution between the electric and combustion power source in such a way that energy flows are optimized to obtain the highest overall efficiency along the complete trip. The level of optimality of the control policies determined by the supervisory controller has a big influence on the overall performance of the complete vehicle.

The supervisory control system proposed in this work makes use of a two-stage control architecture that splits the overarching objective into two separate optimal control problems with dedicated solvers for each subproblem: the long term or global energy management control and the short term or local power management control (as introduced in Section 2.2.1 and Section 2.6). The global control method manages the overall distribution of the battery energy based on rough information on the future conditions. Its main objective is to control the energy in the battery such that it is used at instances where it contributes the most to the overall efficiency of the vehicle. The local control method on the other hand makes use of detailed information over a short horizon to optimize the powertrain operation at the short horizon in terms of driving mode and power split. Its main objective is to obtain detailed control strategies that provide a low equivalent fuel consumption, comply with the LH strategy and offer an acceptable level of drivability.

In Section 4.3 different LH control methods are described and the detailed implementation of a LH estimation method based on distance, altitude and velocity information is proposed in Section 4.4. A linear battery depletion strategy based on only distance information will be used as a reference to evaluate the improvement in performance. Different local control methods are discussed in Section 4.5 and the detailed implementation of an adaptive heuristic method for the local control is proposed in Section 4.6. The conventional heuristic control method will be used as a reference to evaluate the improvement in performance of the proposed methods. Multiple other local control strategies (ECMS, MPC) that are frequently used in literature are implemented as well to gain a better perspective on the performance of the proposed methods and provide additional reference material to improve the comparability of this work with literature. Dynamic programming is used as a method to provide an upper benchmark of the optimal solution to the optimal control problem if, with hindsight, the future information is known in full detail. This method will be

applied to the global optimal control problem, the local optimal control problem and the complete optimal control problem as a whole.

4.2 Information sources

As mentioned in Section 2.2.3, predictive EMC and PMC methods require knowledge on the future power demands along the route to plan their control strategies accordingly. In the prediction of the future power demand profile, the two variables with the highest contributions are the future velocity (and acceleration) profile and the road gradient or altitude profile. The vehicle models described in Section 3.4 are used to estimate the corresponding future power demand profile. In Section 2.2.3 it was also described that the obtainable prediction accuracies of the future driving conditions depend on the signal and the length of the prediction horizon. In particular the accuracy of long range velocity predictions is poor, because the conditions are strongly subjected to change. For long range predictions of the future velocity profile systems like GPS, GIS and navigation systems can be used, where for the short range more accurate systems like ADAS and V2X system can be used.

Although the prediction of future driving conditions and the implementation in a predictive information system is not a trivial task, these information systems are not part of the scope of this work. Instead, it is assumed such a predictive information system is present and the information sources are available to the supervisory controller. The outputs of the predictive information system are implemented as a set of predefined data vectors and are available to the supervisory controller as sampled data vectors with steps of 1 second. It is assumed that the highly accurate altitude information and velocity information with a rough level of detail are known over the entire route. Detailed velocity information is also available, but only over the SH prediction horizon.

4.3 Global control strategy

The optimality of the global battery depletion strategy is an important factor in the overall efficiency of the HEV. In mathematical terms, a EMC control policy needs to be determined that minimizes the total fuel consumption of the vehicle within the predetermined initial and final SoC levels while respecting all component limitations of the powertrain components:

$$\underset{u(k)}{\text{Minimize:}} \quad J(u(k)) = \sum_{k=1}^{N} \dot{m}_{f,\text{ICE}}(k, u(k)) \tag{4.1a}$$

$$\text{Subject to:} \quad SoC(0) = SoC_{\text{init}} \tag{4.1b}$$

$$SoC(N) \geq SoC_{\text{final}} \tag{4.1c}$$

$$SoC_{\text{min}} \leq SoC(k) \leq SoC_{\text{max}} \tag{4.1d}$$

Component constraints as defined in Equation (2.4)

where $\dot{m}_{f,\text{ICE}}$ is the instantaneous fuel consumption, SoC is the battery SoC level and SoC_{min} and SoC_{max} are the bounds of the usable battery SoC range.

Once the optimal LH EMC depletion strategy is determined, it will be supplied to a SH PMC method where it is used as a reference trajectory that needs to be tracked. To provide some flexibility to the SH PMC method however, it is also required to supply an upper and lower bound of the reference trajectory. Although more advanced methods exist, in this work constant bounds of ±1% SoC are used. As described in Section 4.2, the EMC controller will use complete and highly detailed distance and altitude information, but has only access to a rough velocity profile with limited accuracy for the long horizon prediction. In this work a prescribed final SoC target is used, but it should be noted that, for actual application in personal vehicles and especially in cases where no interaction with the driver is desired, determining this target is not always trivial.

4.3.1 Calculation methods

As described extensively in Section 2.7, the number and accuracy of available calculation methods for the LH EMC solution strongly depends on the availability and quality of information on future conditions. In this work, a linear over distance battery depletion strategy is described, as well as a proposal for a method based on distance, altitude and velocity information.

Distance information only

As described in Section 2.7.2, the electric driving mode should be maximized for relatively short trips. If the trip, however, is longer than the all-electric driving range of the HEV, it was reasoned it is best to distribute the battery energy linearly over the trip. The global battery depletion strategy and SoC reference can be calculated according to the following relation:

$$SoC_{\text{ref}}(t) = SoC_{\text{init}} - \frac{SoC_{\text{init}} - SoC_{\text{final}}}{x_{\text{total}}} x(t) \tag{4.2}$$

where SoC_{ref} is the reference SoC value at each point in time, SoC_{init} is the initial SoC level, SoC_{final} is the target SoC value at the end of the trip, x_{total} is the total traveling distance and $x(t)$ is the traveled distance up to time t.

Distance, altitude and velocity information

In applications where the planned route is known, an approximation of the future driving conditions along the route can be obtained, which enables the estimation of the future power demand at each point in time (see Section 2.7.3). The estimation of the future power demand can be used by optimization methods to calculate or estimate the optimal depletion strategy. In the Section 4.3.3 a DP algorithm is introduced that requires complete information on the future driving conditions, but can be very useful to calculate in hindsight the truly global optimal solution to the optimal control problem if the complete future conditions had been accurately known in advance. In Section 4.4 a new LH estimation method is proposed that is suitable for online calculation of a LH battery depletion strategy that is close to the global optimal solution.

4.3.2 Levels of contribution

Realizing the EMC objective of finding the optimal battery depletion strategy is not a trivial task. It has been recognized that three main levels of contribution that benefit the overall efficiency of the HEV can be distinguished: recuperation potential, distribution of battery energy and operation efficiency. A good LH strategy needs to perform well on all three levels or find the best compromise if the three levels are contradicting each other.

Recuperation potential

The most important factor that benefits the overall efficiency of the HEV is the maximization of recuperated energy during sections where regenerative braking is possible. By ensuring all energy that is potentially available for regeneration (the complete recuperation potential) is captured, the overall amount of electric energy that is available during the trip is maximized and the electric driving mode can be utilized in the maximum number of instances. Recuperation potential is lost in situations where the supervisory control system finds itself in a state where the battery SoC is too high to allow for complete recuperation of the gravitational energy potential of the vehicle and therefore has to use the hydraulic brakes to follow the prescribed velocity profile. There are two cases where a HEV could loose a portion of the recuperation potential: decelerations and downhill sections.

The energy available in a deceleration of the vehicle is relatively small compared to the total amount of energy stored in the battery of a PHEV (in the order of 2-3% for a 80 to 0 km/h deceleration on a flat road for the vehicle introduced in Chapter 3). Since these decelerations are aways preceded by an acceleration phases (which offer the opportunity to reduce the SoC), these situations are not likely to result in the loss

of recuperation potential. Downhill sections on the other hand contain a much more significant fraction of the total amount of energy stored in the battery of a PHEV (in the order of 10% per 100m of altitude for the vehicle introduced in Chapter 3). In particular during mountainous trips with large altitude differences, the supervisory controller is prone to lose part of the recuperation potential. In Figure 4.1 an example is given to illustrate the regenerative braking sections and the significance of capturing the complete recuperation potential.

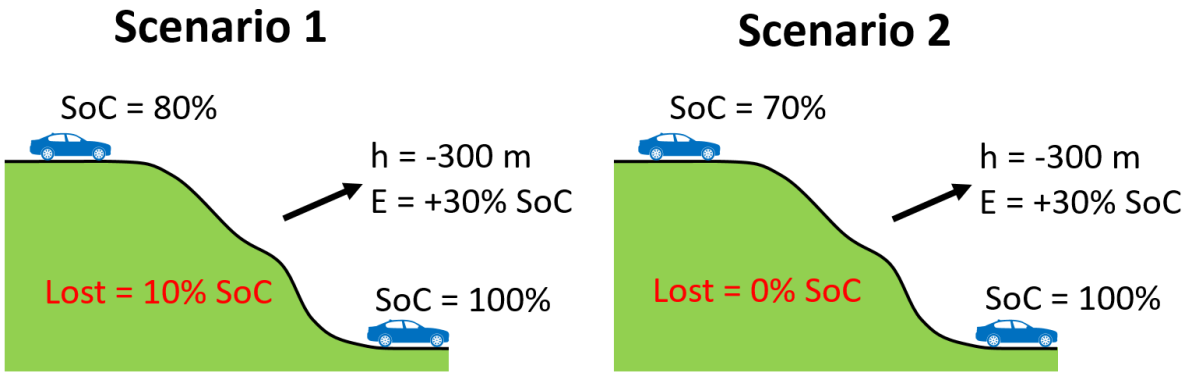

Figure 4.1: Level 1 contribution: recuperation potential.
In this example, a downhill road section of 300 meters is present, during which a significant portion of the battery SoC can be regenerated. The two scenarios illustrate that a smart selection of the SoC at the start of the section (in this example < 70%) can prevent the loss of recuperation potential.

Distribution of battery energy

The second factor that has an important influence on the overall efficiency of the HEV is the well-reasoned distribution of the battery energy over the route. During trips that are longer than the all-electric range of the HEV, intelligent selection of the driving mode along the trip allows the electric driving mode to be utilized at instances where it offers the largest improvements compared to other driving modes. Also the applied LPM strategies should be tailored such that it provides the best trade-off between fuel consumption and gained electric energy for the complete trip. Generally speaking, it is wise to operate the electric powertrain in low speed and low power demand conditions and operate the ICE supported by LPM strategies in all other conditions. In Figure 4.2 an example is given to illustrate the power split selection and the significance of making well-reasoned selections.

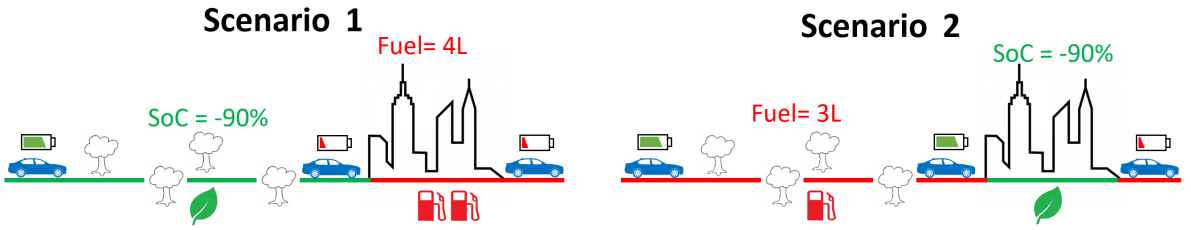

Figure 4.2: Level 2 contribution: distribution of battery energy.
In this example, a highway road section followed by an urban section are present. In scenario 1, the highway section is driven electrically and the urban section ICE-based and vice versa in scenario 2. The two scenarios illustrate that, due to the relatively low operating efficiency of the ICE in stop and go traffic in the urban section, the overall fuel consumption of the vehicle can significantly benefit from smart distribution of the battery energy.

Powertrain operation efficiency

The third factor has the least significant influence on the overall efficiency of the HEV of the three contribution levels, but can still provide improvements in fuel consumption in cases where the application of the first two factors still leaves freedom to adjust the control strategy. The principle is based on the fact

that the average operating efficiency of the electric powertrain is generally the highest in the higher battery SoC regions (e.g. for the Lithium-Polymer battery in this simulation model: 98% efficiency at 95% SoC and 96% efficiency at 10% SoC at 30 kW discharge power). This is mainly due to the decreasing nominal battery voltage for lower SoC, and, as a result, the higher currents and thus higher losses that occur for the same power flow. By recognizing this effect and maintaining higher SoC regions (as long as this does not compromise solutions of the first and second level of contribution), the supervisory controller can obtain a higher average efficiency of the electric powertrain which makes it possible to extent the use of the pure electric driving mode. In Figure 4.3 an example is given to illustrate the benefits of operating the electric powertrain in regions with higher efficiency.

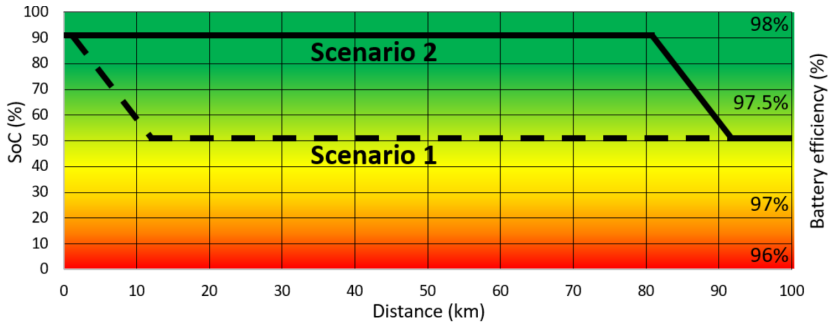

Figure 4.3: Level 3 contribution: Powertrain operation efficiency.
In this example, the driving conditions during the route are constant. In scenario 1, a strong depletion phase is followed by a charge sustaining phase and vice versa in scenario 2. Due to the higher powertrain efficiency in scenario 2, the overall fuel consumption at the end of the trip will be lower than in the first scenario.

4.3.3 Dynamic programming method

Although in real-life applications it is impossible to know the complete future conditions in advance and computational resources are limited, it can be very useful to calculate in hindsight the control policies that would have been the truly global optimal solution to the optimal control problem if the complete future conditions had been accurately known in advance. Since these global optimal solutions provide the best performance that can theoretically be obtained, they are often referred to as the upper performance limit, or upper benchmark, when comparing them to the results of more online feasible control methods Section 2.4. The global optimal solution has perfect performance, or the perfect balance of performance, on all three levels of contribution introduced in Section 4.3.2.

As extensively described in Section 2.4.1, DP is one of these numerical methods and is able to provide the global optimal solution to many types of discrete optimal control problems (within its accuracy limits due to discretization and truncation errors). In this work, the general dynamic programming function developed by Sundtrom and Guzzella is applied as the solver algorithm to find the global optimal solution to the DP problem definition [56]. In general, a DP algorithm finds the solution to the optimal control problem by four main steps [1]:

1. **Feasible bounds:** Determine the boundary values of the state variable for each point in time that still allow the state at the final time step to be achieved

2. **Intermediate costs:** Calculate the intermediate costs of every control action, for every state value and each time step by progressing backwards from the final time step. The intermediate costs are stored in a separate matrix for each time step.

3. **Cost to go:** For each state value, determine the optimal set of control actions to reach this state value at time k from the final state at the final time step. By starting at the final time step and repeating the process until the initial time, the global optimal sequence of control inputs is found. The optimal costs to go are stored in the optimal control matrix.

4. **Forward calculation:** From the initial state, the model is evaluated in forward calculation by following the optimal costs to go in the optimal control matrix to determine the optimal control and state sequence.

4.4 Global estimation method

Although DP is guaranteed to find the global optimal solution to the optimal control problem, which is a very desirable characteristic of a solver technique, its online implementation is not feasible due to high computational burden (as explained in Section 2.4.1). For this reason, there is an interest for an estimation method that can find a close-to-optimal solution with significantly reduced computational demands. In this work, the goal is set to achieve a computation time of the LH estimation solution under 10 seconds on a PC with a 2.5 GHz CPU.

The main difference between a global optimization technique like DP and an estimation method is that unlike DP, not every time-instance can be individually regarded and optimized towards the complete optimal control problem. Instead, some assumptions have to be made in order to drastically reduce the number of variables and thereby lower the computational demands to solve the optimal control problem. Ideally, the estimation method greatly reduces the number of variables with minimal impact on the optimality of the solution. Two main principles can be distinguished: reducing the number of variables by courser discretization of the route and/or input variable; or clustering instances and assigning the same variable to instances that belong together.

In this section, a LH estimation method based on power-based clustering of instances is proposed that achieves a close-to-optimal solution with drastically reduced computational demands. Section 4.4.1 will describe the different types of route sections and the level of freedom in the control actions the supervisory control system has over these sections. In Section 4.4.2, the main principle of the LH estimation method will be described and Section 4.4.3 discusses how the objective of this method can be formulated as a mathematical optimization problem. Section 4.4.4 and Section 4.4.5 will discuss some additional steps that are required to obtain a close-to-optimal LH solution.

4.4.1 Different types of sections

The first step in the principle behind this global estimation method is the division of the route into different sections based on the level of freedom the control strategy has with respect to the control of the battery SoC in that section. In this work, three main types of sections are recognized:

- **Stationary sections**
  During stationary sections the vehicle is in stand-still and no traction torque for acceleration or deceleration of the vehicle is required. In these instances there are no control actions to optimize and it can be assumed it is always best to turn off the ICE. This type of time intervals are referred to as **stationary** sections.
- **Fixed (Regenerative sections)**
  The assumption is made that, during a regenerative section, the optimal control strategy always maximizes the recuperation of energy. This means the total amount of recuperated energy is always either equal to the complete recuperation potential of the regenerative section, or equal to the maximal amount of recuperated energy imposed by component limitations (e.g. maximal battery SoC). The assumption is reasonable, since (for the defined optimization problem) no situations exist where the recuperation of essentially ”free” energy is not desired and the assumption is supported by the global optimal results from DP later shown in Figure 4.4. Since the recuperated energy is always maximized, the supervisory controller does not explicitly control the change of SoC during these sections: given the SoC level at the start of a regenerative section, the braking power profile and the component limitations, the final SoC at the end of the regenerative section is also given. This type of time intervals are referred to as **fixed** sections.
- **Free (eDRV, pure ICE, LPM or eBoost sections)**

The remaining type of sections fall in a category where different propulsive driving mode are possible (eDRV, pure ICE, LPM or eBoost sections). As a result, the supervisory controller is able to explicitly control the change in battery SoC between pure eDRV and maximal LPM and has the possibility to completely turn off the ICE if it is not required for the propulsion of the vehicle. This type of time intervals are referred to as **free** sections.

4.4.2 Main principle

Based on the classification made in the previous section, it follows that the global estimation method only has to solve the optimal power split for the instances in the free sections, as the optimal value is intrinsically found for the stationary and regenerative sections. The main principle the proposed global estimation method is based on is the following simplification: If two instances during a trip have the same power demand, they also have the same optimal power split. The main intent of the proposed simplification is to reduce the number of optimization variables in the optimal control problem. However, depending on the discretization step size of the power demand, the number of variables can still be very high. For the proposed LH estimation method it is chosen to cluster the instances into 11 clusters that share similar power demands and subsequently assign one power split value to all the instances in a cluster.

The validity of this approach is supported by Figure 4.4, which displays the global optimal distribution of power splits determined by the DP optimization method and the final result of the proposed method. For most of the power demands it is clear that there is a relative small spread of power split values most of the instances are grouped around, but also a number of instances with power split values that deviate far from expected trend, which contradicts the previous stated assumption. At this point it should be noted again that generalizations indeed introduce errors relative to the global optimal solution, but without a number of assumptions, the global estimation method cannot reduce the computational resources required to solve the optimal control problem. Next to that, it is important to note that there is in principle no need to stay close to the global optimal control policy (other local minima are acceptable), as long as the final cost (in this case the total fuel consumption) is close to the global minimal value. In other words, although the estimated optimal sequence of control actions may look very different from the global optimal control policy, this doesn't matter if the final fuel consumption is close to the global minimal fuel consumption (assuming a model with high enough accurate enough predictions of component limitations is used).

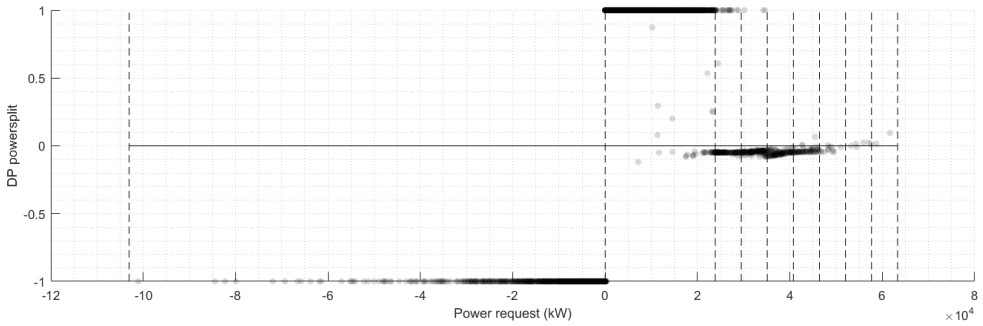

Figure 4.4: Power split assigned to each time instance of the Graz drive cycle according to the DP solution. The color intensity corresponds to the number of data samples at that location. Power split definition according to Equation (3.4a) and Figure 3.5.

Referring back to the classification in Section 4.4.1, all the fixed (regenerative) instances can be clustered into one group and can be preassigned with the optimal power split value of -1 (since regeneration of energy is always to be maximized). Next to that, all the stationary instances can also be clustered in a single group and, although they don't require any control actions, can be preassigned a power split value of +1. For the free instances, the corresponding cluster and optimal power split for each cluster are not trivial and need to be determined by the estimation method. To simplify this process and restrict the number of possible solutions drastically, it is assumed that the optimal control policy is characterized by a clear

transition from the pure electric driving mode to ICE-based driving modes at a certain power level, referred to as P_{eDRV}. This implies that all instances with power demands lower than P_{eDRV} are driven electrically and all instances with power demands higher than P_{eDRV} are never driven electrically. In Figure 4.4 it can be seen that such a transition is also present in the global optimal distribution of power splits, but the power level this transition happens is not as distinct and is subjected to a certain amount of overlap. It should be noted that the value of P_{eDRV} has a big influence on the overall optimality of the global estimation. However, without a predetermined global optimal solution it is unknown where at what power level this P_{eDRV} lies, since it strongly depends on drive cycle, initial and final SoC target and vehicle characteristics. In Section 4.4.4 a method is proposed to determine this power level, but for now it can be assumed the optimal P_{eDRV} power level is known.

Assuming the proposed transition simplification is valid, all the electrically driven instances (that lie between 0 and the P_{eDRV} power level) can be clustered into one group and assigned a single power split value of +1. The remaining instances with power demands higher than P_{eDRV} will all be driven with the ICE enabled, but can have different amounts of electric boost (eBoost) or LPM strategies. The span of power demands between P_{eDRV} and the maximum power demand P_{max} is linearly divided into a prescribed number of clusters, n. More intelligent clustering techniques might be possible, but are not considered in this research. The number of clusters used to discretize the span of power demands determines the trade-off between optimality of the global estimation method and the computational resources required to solve the problem. An overview of the different clusters and their assigned power split value is given in Table 4.1.

Table 4.1: Definition of the clusters and the power split assigned to each cluster.

Cluster number:	Power demand (kW)	Power split:	Type:
1	$P(k) = 0$	+1	Stationary
2	$P(k) < 0$	-1	Regenerative
3	$0 > P(k) \geq P_{\text{eDRV}}$	+1	eDRV
4 to n	$P_{\text{eDRV}} > P(k) \geq P_{\text{max}}$	To be determined	ICE on

4.4.3 Optimize power split per cluster

Once each instance has been assigned to their corresponding cluster, the optimal power split for each cluster, $\mathbf{x} = [PS_1, PS_2, ..., PS_n]$, needs to be determined in order to obtain the optimal EMC battery depletion strategy that minimizes the total fuel consumption. This objective can be formulated as a n-dimensional optimization problem (where n is the number of clusters) that minimizes a cost function. This cost function consists of two terms, where the first minimizes the fuel consumption and the second aids the convergence of the optimization problem. It is subjected to a set of hard constraints that ensure the SoC remains within the upper and lower bound and that the SoC at the end of the trip is higher than or equal to the target SoC:

$$\underset{\mathbf{x}}{\text{Minimize:}} \quad J(\mathbf{x}) = \sum_{k=1}^{N} w_1 \dot{m}_{\text{f,ICE}}(k, \mathbf{x}) + w_2 (SoC(N, \mathbf{x}) - SoC_{\text{final}})^2 \tag{4.3a}$$

$$\text{Subject to:} \quad \mathbf{x}_{\text{min}} \leq \mathbf{x} \leq \mathbf{x}_{\text{max}} \tag{4.3b}$$

$$SoC(0) = SoC_{\text{init}} \tag{4.3c}$$

$$SoC(N) \leq SoC_{\text{final}} \tag{4.3d}$$

$$SoC_{\text{min}} \leq SoC(k) \leq SoC_{\text{max}} \tag{4.3e}$$

Component constraints as defined in Equation (2.4)

where $\mathbf{x}$ is the vector of power splits from the third to the n-th cluster and has to lie within the domain $[-1 \quad 1]$, $\dot{m}_{\text{f,ICE}}$ is the instantaneous fuel consumption of the vehicle, $SoC(N)$ is the battery SoC at the end of the trip, SoC_{final} is the targeted final SoC level, SoC_{min} and SoC_{max} are the bounds of the usable battery

SoC range and w_1 and w_2 are weight factors to balance the two terms of the cost function.

Since detailed knowledge on the powertrain components and the operating conditions is available, it is possible to recognize a priori that certain domains in the solution space that will not satisfy the component constraints and are therefore infeasible. For this optimization problem it can be deduced that the lower bound of optimization variables (which dictates the maximum level of LPM strategies that can be applied for each cluster) follows from either the maximum power output power of the ICE or the maximum absolute generative power of the EM. By predetermining the actual lower bound of the optimization variables and thereby limiting the solution space, the convergence of the optimization process can be improved, which reduces the computational demands. A similar approach can be applied to the upper bound of the optimization variables by recognizing that eBoost (power splits between 0 and 1) are only desired if the ICE is operated near its maximal output torque. The final optimization problem that needs to be solved is a n-dimensional problem that is a function of n continuous optimization variables. Although for the complete problem local minima can exist, the individual optimization variables typically have a convex relation to the cost function (displayed in Figure 4.5). These characteristics allow for efficient solving of the optimization problem by a gradient-based optimization method. In this work, the `fmincon` function [57] using the interior-point algorithm in Matlab is applied to determine the optimal power splits value for each cluster.

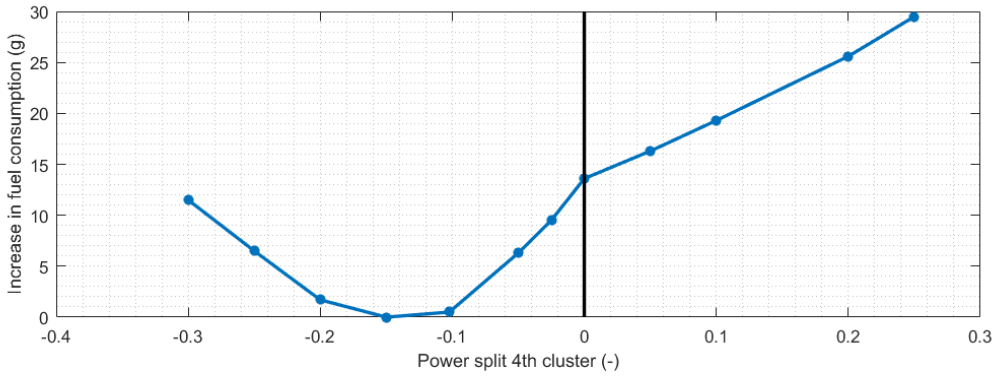

Figure 4.5: Objective function plot of the power split of the fourth cluster. The power split value of this cluster is prescribed, while the power splits of the other clusters are optimized.

4.4.4 Determine size of eDRV cluster

The transition between the electrically and ICE-based driven clusters given by the power level P_{eDRV} (Section 4.4.2) has a big influence on the overall optimality of the global estimation . An optimization method is required to determine the optimal power level, since it strongly depends on drive cycle, initial and final SoC target and vehicle characteristics. For example, while trips shorter than the all-electric range of the vehicle ideally have all time instances in the eDRV cluster (Table 4.1), other cycles might have a very limited amount of electric energy available and therefore only a few instances in the eDRV cluster.

Fundamentally, it can be reasoned that the optimization of the size of the eDRV cluster is a convex problem. Since the two bounds operate the ICE in its most extreme regions (the bottom and top region of Figure A.1b), any intermediate strategy should be able to achieve a higher overall operating efficiency than the most extreme cases. A plot of the objective function using a brute force method displayed in Figure 4.6 supports this idea and shows the P_{eDRV} is indeed a convex function. The first step in finding the optimal size of the eDRV cluster is to determine the minimal and maximal size the cluster can have, while still satisfying the constraints of the optimization problem. By recognizing the bounds of the optimization problem are the result of two characteristic operation strategies of the powertrain, they can be determined a priori without the need for any optimization of the power splits and therefore with low computational cost:

- **Lower bound:**
  The lower bound of the eDRV cluster follows from a control strategy that applies no LPM strategies

(only pure ICE operation) in the ICE-based clusters (clusters 4 to n), where the cluster power splits $PS = [1, -1, 1, 0, 0, 0, 0, 0, 0, 0]$ are assigned. Since the only sources of energy are the initial battery energy and energy recuperated during regenerative braking, this control strategy will result in the minimal amount of available electric energy. Since the available electric energy is minimal, the number of instances the electric driving mode can be used is minimal, which dictates the minimal P_{eDRV} power level that still meets the final SoC constraint for this strategy. Of course control strategies with even less or no instances in electric driving (P_{eDRV} lower than the lower bound) are feasible, but they do not use the complete available energy in the battery and thus do not minimize the fuel consumption.

- **Upper bound:**
  The upper bound of the eDRV cluster on the other hand follows from a control strategy that applies maximal LPM strategies in the ICE-based clusters, which follows (similar to Section 4.4.3) from either the maximum power output power of the ICE or the maximum absolute generative power of the EM, represented as LB. The cluster power splits $PS = [1, -1, 1, LB, LB, LB, LB, LB, LB, LB]$ are assigned in this case. The maximal amount of electric energy is available in this control strategy, which dictates the maximal P_{eDRV} power level that still satisfies the final SoC constraint. Any power level of P_{eDRV} larger than this upper bound uses too much electric energy and cannot satisfy the final SoC constraint.

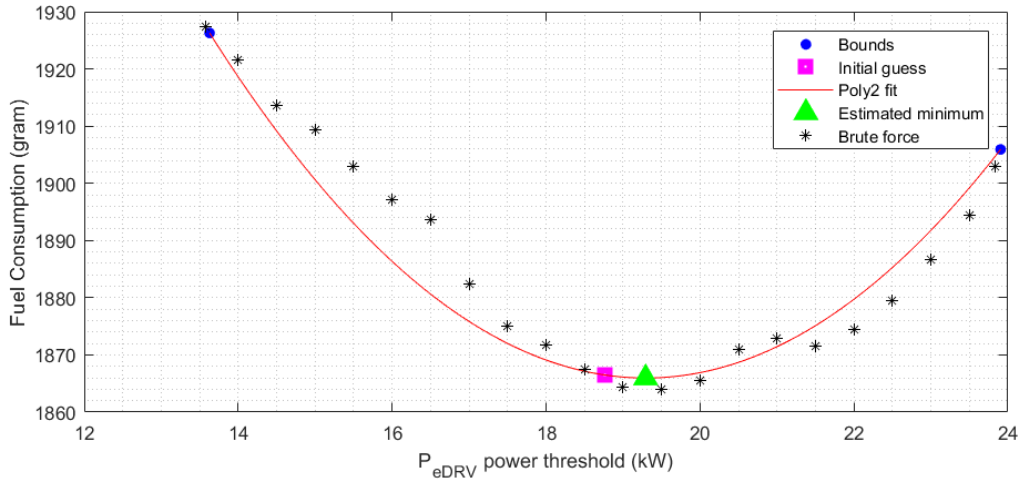

Figure 4.6: Objective function plot of the P_{eDRV} optimization problem obtained by a brute force method. The second order polynomial fit demonstrates accurate estimations of the optimal value of P_{eDRV} can be made by a simple estimation approach.

Depending on the available computational resources and desired optimality, one can opt for different methods to determine the size of the eDRV cluster: using a brute force method, application of an (gradient-based) optimization problem, or a simplified estimation approach. It can be recognized in Figure 4.6 that the objective function is relatively flat around the optimal point (between 20 and 22 kW) and therefore a perfect estimation of P_{eDRV} is not crucial to achieve a low fuel consumption, as long as it is in the flat region. For this reason, in this work a simple estimation approach is chosen that can determine a near-optimal value for P_{eDRV} with low computational cost.

It is recognized that a second order polynomial function can relatively accurately approximate the objective function, which is displayed in Figure 4.6. The minimum of this second order polynomial function can be calculated very quickly using its analytic derivative and provides a good approximation of the optimal value of P_{eDRV}. The fitting of a second order polynomial function requires three data samples and since the bounds of the function and the corresponding fuel consumption at these power levels are already determined, only one computationally expensive function evaluation is required to fit the second order polynomial function (because there is no characteristic operation strategy of the powertrain at any other location in the domain and the power splits have to be optimized to find this point, which is computationally expensive and takes around 3 seconds to compute). Because further information on the shape of the

convergence function is not available, the mean of the two bounds is taken as the third data sample and the best initial guess for the minimum of this function. Once the size of the eDRV cluster is determined, the optimal power splits for clusters can be calculated and the resulting SoC profile is taken as final battery depletion strategy.

4.4.5 Preventing loss of recuperation potential

The approach proposed in the previous sections mainly takes the second and third contribution level (Section 4.3.2) into account, but does not perform well in terms of the level 1 contribution. In extreme drive cycles, where large regeneration sections are present in the route (and thus large portions of the battery can be recuperated), the problem over the complete route divides itself in two or multiple subproblems. In this type of routes the optimal battery depletion strategy can have very different average electric power consumptions for these separated subproblems and as a result, very different optimal power splits can be found for the same power level. For example, the first part of the route can make maximal use of the electric driving mode, while the second part uses a mix of electric and ICE based driving modes. Although the problem can be solved using the proposed clustering approach, the optimality of the solution is often low, because the underlying principle of this approach is not able to divide the problem into two or multiple subproblems and therefore is prone to lose part of the complete recuperation potential (This happens in the example in Figure 4.7). It should be noted here that the problem lies in clustering process (the assigning process of the correct cluster to each instance), not the method as a whole and if the clustering process can be improved, highly optimal solutions can still be obtained. Without knowledge on the optimal depletion strategy, however, it is not trivial how the overall problem is split in multiple subproblems and which instances are assigned to the wrong cluster group. It was recognized that the instances where the problems occur can be found by comparing the SoC trajectories of the upper bound and lower bound from the P_{eDRV} problem with the recuperation-curve, as demonstrated in the example in Figure 4.7.

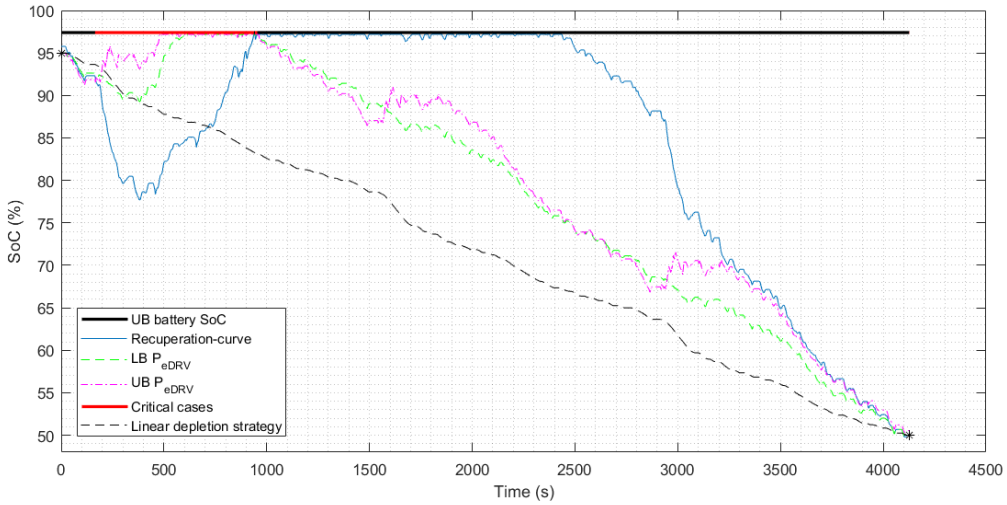

Figure 4.7: The recuperation-curve represents the SoC values that still allow the capturing of the complete recuperation potential. In this example (3F drive cycle), all instances between 194 and 954 sec (where the braking phase is between 391 and 954 sec) exceed the recuperation-curve and thus recuperation potential is lost.

The recuperation-curve represents the upper SoC value at each point in time that still allows the complete recuperation potential to be captured over the entire remaining of the trip while still meeting the final SoC target. Any SoC value above this curve is either limited by the upper SoC limit and miss part of the recuperation potential, or will not meet the final SoC target and not use the complete available energy in the battery. The recuperation-curve can be calculated by backward simulation of the vehicle from the final SoC target where only complete operation in the electric driving mode is used (and thus maximal electric energy is consumed). With the definition of the recuperation-curve, three different situations can be distinguished:

1. Both the upper and lower bound are smaller than the recuperation-curve for all instances. In this case, no limitations by the upper SoC bound are encountered and the full recuperation potential is captured. The level 1 contribution is completely satisfied and there is no need to reassign any of the instances to new clusters.
2. One of the bounds is larger than the recuperation-curve for some instances, while the other is not. In this case, one of the bound evaluations encountered limitations by the upper SoC bound and was unable to capture the full recuperation potential. However, since the other bound did not exceed the recuperation-curve at the same instances, it can be assumed that the problem has enough freedom and will be automatically solved by the power split optimization of the clusters. There is no need to reassign any of the instances.
3. Both the upper and lower bound are larger than the recuperation-curve at the same instances. In this case, it is clear that the initial clustering needs to be modified in order to increase the use of the electric energy in the early stages and allow the complete recuperation potential to be captured. It is not trivial however, to which instances this applies. In general, complete operation in the electric driving mode is not a good solution and a mix of electric and ICE-based operation is required.

The latter situation is a challenging case to solve, since the overall problem is in these cases truly divided into two or multiple subproblems. One could argue that the estimation of the battery depletion strategy should therefore also be solved as individual subproblems, however, it is unclear where the start and what the final SoC target for each subproblem would be. Dividing the estimation of the battery depletion strategy into subproblems would, however, drastically increase the complexity of the overall problem, which is the reason why in this work a different approach is proposed. Instead of splitting the optimization problem into subproblems, a decent correction of the original clustering result can be made by forcing all instances to the eDRV cluster where both the upper and lower bound exceed the recuperation-curve. This way, at the very moment these instances become crucial to the level 1 contribution, the capture of the complete recuperation potential is ensured. The proposed approach offers a simple and fast method to ensure the complete recuperation potential is captured, but potentially more optimal (in terms of level 2 and 3 contributions) distributions of the battery energy over the first subproblem could exist that will lead to a lower overall fuel consumption. The assumption is made that optimal power split over the different subsections are still close to each other and can therefore still be solved as one optimization problem with minimal impact on the level 2 and level 3 contributions. In this case the performance loss is small and the optimization of power splits can still determine the best power splits are found for any slightly sub-optimal clustering sets.

4.4.6 Summary of the proposed global estimation method

In the previous sections it was explained that three different types of sections can be distinguished: stationary, fixed and free sections. For the stationary and fixed sections the optimal control policy can be predetermined, but there is a need to optimize the control strategy for the free sections. In order to reduce the number of optimization variables, a method is proposed that clusters instances into groups based on their power demandThe underlying principle of the method is based on the assumption that two instances with the same power demand, have the same optimal power split. The optimal power split for each cluster is determined using a gradient based optimization algorithm. The solution space of the optimization problem (and therefore the computational demands) can be significantly reduced by a priori determining the infeasible regions of the solution space.

The clustering method relies on a known size of the eDRV cluster (in which all instances are driven in the electric driving mode), but without knowledge on optimal depletion strategy, the size of this cluster is unknown. A simple and quick estimation method is proposed to determine the optimal size of the eDRV cluster which is based on fitting a second order polynomial function. Since the upper and lower bound of the eDRV cluster can be determined with low computational cost, only one computationally expensive function evaluation is required to get an approximation of the optimal size of the eDRV cluster.

The capturing of the complete recuperation potential is not automatically ensured by the proposed clus-

tering method. It is recognized that the loss of recuperation potential is caused by instances that lie above the recuperation-curve (SoC values at any point in time that ensure the complete recuperation potential can be captured). Rather than a complex method that splits the problem in multiple subproblems, a quick and elegant method is chosen, that assigns all instances that exceed this recuperation-curve to the eDRV cluster, thereby ensuring the complete recuperation potential is captured. The distribution of the instances is however potentially not the most optimal strategy in terms of the distribution of the battery energy over the route. For most cases the performance loss is small however and any errors can be compensated for by the optimization of the power splits per cluster.

In Figure 4.8, a flowchart is depicted that graphically displays the different steps in the global estimation method.

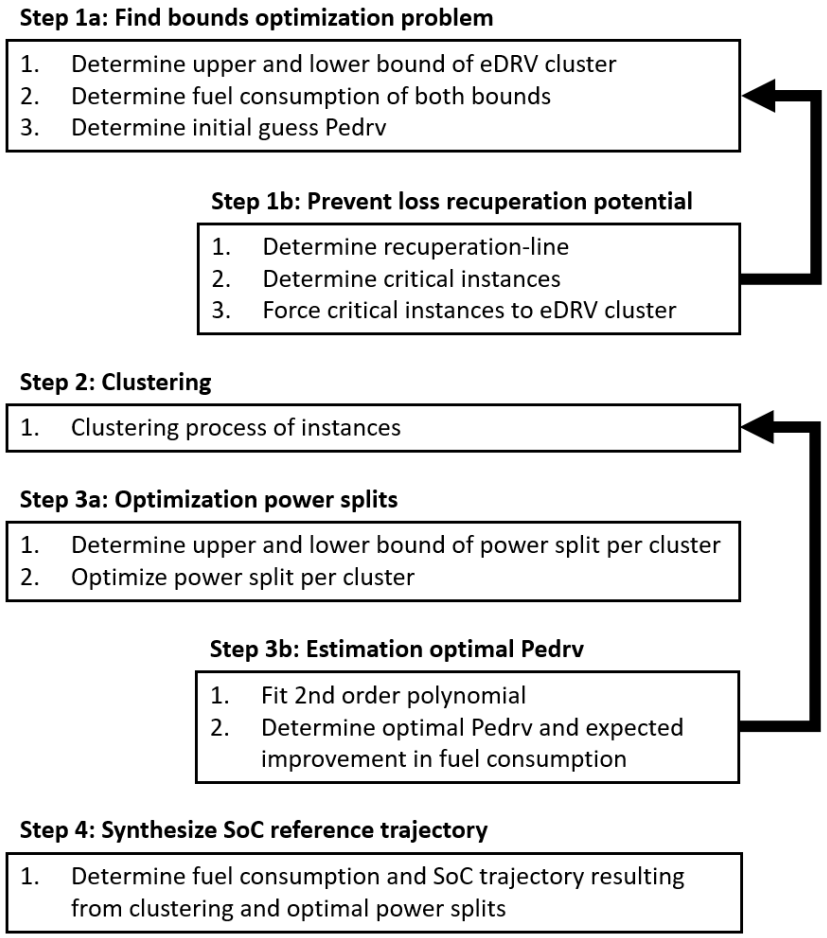

Figure 4.8: Flowchart of the steps in the global estimation method.

4.5 Local control strategies

Although the global estimation method (EMC) ensures a high overall efficiency of the HEV from a global perspective, an additional control system is still required to determine a fully detailed powertrain control strategy over the local timescale (PMC). Due to high computational loads and unavailability of accurate future velocity information over the complete route, global estimation methods typically determine only a low detailed powertrain operation strategy (like a battery SoC reference), rather than a fully detailed strategy over the complete route. This however, leads to the introduction of errors in the strategy by global estimation method relative to the truly global optimal solution [34], which needs to be taken care of the local control strategy.

Local optimal control methods on the other hand offer the possibility to optimize the detailed powertrain operation on the local timescale based on accurate and up-to-date information. For these reasons, local control methods are potentially much better in determining the best control policy over the SH horizon than the original LH SoC reference . However, since local control method lack the insight of the impact of their current control actions on the complete route, their local control policy should still be in accordance with the LH strategy. To allow some flexibility to tolerate LH errors, local control strategies are often permitted to deviate from the LH SoC reference trajectory. In the case of instantaneous methods (such as A-ECMS), the deviations are subsequently limited by PI reference tracking [24–26, 40], or in the case of MPC-based methods, limited by quadratic penalization costs [19, 30, 31, 37]. Since SoC at the end of horizon, and therefore the consumed amount of battery energy, is in this case no longer prescribed and can vary between strategies, the evaluation of the fuel economy of different strategies based on the direct comparison of the fuel consumption is no longer valid. For this reason, the aim of the local control methods is to minimize the equivalent fuel consumption, which relates the consumption of battery energy to the consumption of conventional fuel. The objectives of the local control method are, however, not only the minimization of the equivalent fuel consumption and tracking the LH reference trajectory. The local control strategy should also take into account considerations for feasibility and drivability criteria as introduced in Section 2.2.1.

In this section, different common local control methods are introduced, starting with the introduction of a conventional heuristic controller in Section 4.5.1. The instantaneous optimization ECMS method and the predictive optimization MPC method are introduced in respectively Section 4.5.2 and Section 4.5.3. In Section 4.6 a novel adaptive heuristic control method is proposed as the final approach for solving the SH control problem.

4.5.1 Heuristic control logic

As described in Section 2.2.2 and Section 2.3, heuristic control methods are still commonly applied in production HEV. Although their performance is often only moderate for drive cycles their calibration is not directly optimized towards, it is still useful to know the performance of conventional heuristic control strategies. The results of the heuristic method can be used as a lower performance limit or lower benchmark when evaluating the performance and relative improvement of the proposed control strategies.

The selection of the instantaneous control inputs in the heuristic controller follows from logical rules, maps and lookup tables based on the instantaneous power request and the instantaneous states of the vehicle and powertrain and can be divided into two categories: component rules and calibration rules. Component rules represent the component limitations (e.g. torque limits) and prevent the heuristic controller from requesting infeasible control actions. Although feasible, not all the remaining control actions are equally desirable in terms of certain criteria like energy management, fuel consumption and drivability. For this purpose, the calibration rules are set up to represent these criteria and instantaneously decide upon the most preferable driving mode and power distribution based on the instantaneous conditions and system states. The calibration heuristics are static (non-changing) thresholds and tables that are pre-constructed from engineering expertise, insight or optimization methods to represent the desired control strategy as closely as possible.

The calibration set of the heuristic controller employed in this work takes into account more objectives than just the instantaneous minimization of the (equivalent) fuel consumption of the vehicle. First of all, the calibration set also incorporates the objective to obtain an acceptable level of drivability for the passengers of the vehicle, for which different forms of considerations can be considered (as discussed in Section 2.2.1). The measures applied in this heuristic controller try to limit the number of ICE starts, by enforcing a minimal ICE-on-time of 10 seconds. Next to this constraint, an ICE torque target curve, T_{LPM}, for LPM strategies is implemented. This curve varies slowly over the rotational speed of the ICE, which operates the ICE on a more constant torque level and limits the transients of the ICE.

Next to the drivability measures, the heuristic control method needs to control the LH EMC battery depletion strategy as well, since without predictive information about the future power demands of the trip,

intelligent planning strategies are not possible. Instead, the EMC strategy has to be intrinsically controlled by calibration rules that constraint the use of electric energy as a function of the battery SoC. In this work the amount of electric power, P_{eDRV}, that can be used is implemented as a function of SoC ($P_{\text{eDRV}} = f(SoC)$), which allows the electric driving mode to be used more frequently for instances with high SoC and less frequently for instances where the battery SoC is low. This rule is the main calibration rule that controls the selection of the driving mode of the vehicle as described in Section 2.3. The map of the heuristic rule that constrains the electric power is displayed in Figure 4.9a. Figure 4.9b displays the implemented calibration rule that controls the torque target, T_{LPM}, of the ICE and thereby the power distribution between the ICE and EM.

The only inputs to the heuristic controller are the instantaneous vehicle and powertrain states and the instantaneous power demand. No vehicle models are used in the heuristic controller, except for the component limitations, which are modeled as static maps. A heuristic control algorithm based on standard P2 parallel PHEV methodology is applied to determine the desired control actions. Its heuristic calibration set was reverse-engineered and fine tuned by AVL based on chassis dynamometer measurements of the original VW Jetta vehicle. The algorithm finds the preferred control inputs to the current conditions by four main steps:

1. **Feasibility electric driving:** Determine whether the electric driving mode is feasible and whether it is desired according to the calibration heuristics.
2. **ICE-status:** Decide whether the ICE should be on or off.
3. **Power distribution (Traction):** If traction torque is requested and the ICE is on, determine the desired output torque of the ICE.
4. **Power distribution (Braking):** If braking torque is requested, determine whether regenerative braking is sufficient and apply hydraulic braking pressure if necessary.

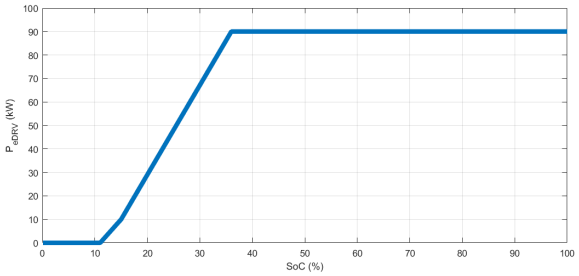

(a) P_{eDRV} recalibration rule that determines the power threshold for electric driving.

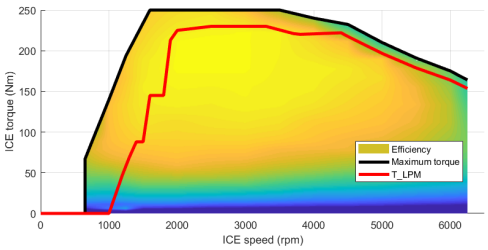

(b) T_{LPM} recalibration rule that determines the torque target for the operation of the ICE.

Figure 4.9: The two main calibration rules that jointly determine the desired driving mode and power split.

4.5.2 ECMS

One of the instantaneous optimization based control methods is ECMS, which is described in Section 2.5.1. Rather than determining the optimal control policy for a certain horizon or timespan, ECMS determines the next control action (power split) by minimizing the equivalent fuel consumption for the next time instance:

$$\begin{aligned} &\underset{u(k)}{\text{Minimize:}} && J(k,u(k)) = \dot{m}_{f,\text{equiv}}(k,u(k)) = \dot{m}_{f,\text{ICE}}(k,u(k)) + s(k)P_{el}(k,u(k)) \\ &\text{Subject to:} && \text{Component constraints as defined in Equation (2.4)} \end{aligned} \tag{4.4}$$

where $\dot{m}_f$ is the instantaneous (equivalent) fuel consumption, P_{el} is the electric power drawn or supplied to the battery and s is the equivalence parameter.

The equivalence parameter assigns a cost to the use of electric energy and plays a key role in the selection of the power distribution. The equivalence parameter represents the chain of efficiencies for fuel trans-

formed into electric power and vice versa and therefore it theoretical value changes for each operating condition (speed, power demand, SoC) of the powertrain and drive cycle. Since its optimal value can only be known with hindsight, in many applications in literature the equivalence parameter is continuously adapted to comply with a LH SoC reference based on PI feedback control, which is also applied in this work. The discretization step size of the power split variable is a trade-off between the acceptable computational costs and the numerical accuracy. A self-developed algorithm for this control method finds the solution to the optimal control problem by five main steps:

1. **Update equivalence parameter:** Determine the value for the equivalence parameter for the current time instance based on the current SoC and reference SoC using PI feedback control.
2. **Domain control inputs:** Identify the acceptable range of control inputs that satisfy the instantaneous constraints for the prescribed power request and given states of the system.
3. **Discretization:** Discretize the range of the control input into a finite number of control candidates.
4. **Calculate cost:** Evaluate the cost function based on the equivalent fuel consumption of each control candidate.
5. **Select best candidate:** Select the control action that minimizes the cost function for the next instance.

4.5.3 MPC

MPC is a predictive optimization based control method as described in Section 2.5.2. Rather than determining the optimal control action for only the next instance, the optimal control problem is solved over a short horizon in receding horizon fashion. For each horizon, the optimal sequence of control actions is searched that minimizes the equivalent fuel consumption while tracking the LH reference trajectory. In this work the upper and lower bound of the LH SoC reference are ensured with a hard constraint, while deviations from the target final SoC are penalized by a penalty term in the objective function to provide flexibility to the tolerate errors in the LH reference trajectory. The optimal control problem can be formulated as the following optimization problem:

$$\underset{u(k)}{\text{Minimize:}} \quad J(k) = \sum_{i=1}^{N_p} w_1 \dot{m}_{f,\text{equiv}}(k+i, u(k+i)) + w_2 (SoC_{\text{final}} - SoC(k+N_p))^2 \tag{4.5a}$$

$$\text{Subject to:} \quad SoC_{\text{min}}(k+N_p) \leq SoC(k+N_p) \leq SoC_{\text{max}}(k+N_p) \tag{4.5b}$$

Component constraints as defined in Equation (2.4)

where SoC_{ref} is the LH SoC reference trajectory, $\dot{m}_{f,\text{equiv}}$ is the consumption of equivalent fuel, N_p is the prediction horizon and w_1 and w_2 are weight factors to balance the two terms of the cost function.

One technique that can be used to solve the MPC problem is DP, which can be applied in a similar fashion as in Section 4.3.3. The computational resources required to apply DP on a MPC problem are reasonably low, because the solution space is relatively small (typically in the order of 2 seconds for a 60 second horizon, which makes it feasible for performance analysis, but infeasible for online application). However, DP is not suitable for the implementation of intermediate integral time constraints (integrals over only a part of the horizon) like the minimal ICE on time constraint. The reason for this is that in DP a state at a certain point in time is completely independent of all preceding control actions, which is clearly not the case for this type of integral constraints (the preceding conditions are important and backward calculation is not possible). Since adding a single instantaneous boolean condition to the unconstrained problem would already double the number of possible solutions, a multi-time step integral constraint very rapidly increases the complexity of the optimal control problem. Other methods like MINLP have been proposed in literature to solve discrete nonlinear optimal control problems and can in principle find optimal solution for this type of constrained optimal control problems [43]. However, the solving techniques are difficult to set up and very computationally demanding [31]. Since the MPC-based control methods are only implemented for performance evaluation in this work and are not the primary research goal, a MINLP control method was

not implemented in this work.

However, for the development and performance evaluation of the novel control method proposed in Section 2.8.2, it is still important to have a control method that can act as the upper performance benchmark. It chosen to base all performance and optimality evaluations on the unconstrained optimal control problem (which does not include the additional drivability and feasibility conditions) and assume the performance and optimality of the proposed adaptive heuristic method on the constrained optimal control problem is similar. This allows the control method to be evaluated with respect to other control methods, without the need for the implementation of a complex MINLP MPC method. The previously proposed DP-based MPC method will be used as upper benchmark in the unconstrained optimal control problem in this work.

4.6 Adaptive heuristic control

In Section 2.8.1, it was discussed that optimization based methods like MPC are infeasible for online application in actual real-world HEVs, because they are too computationally demanding, can request infeasible control actions and often ignore drivability conditions. Instead, an adaptive heuristic control method was proposed in Section 2.8.2 that adapts the calibration set of a conventional heuristic controller to a more optimal calibration set based on upcoming driving conditions and events. The proposed control method can benefit from the advantages of heuristic control, while still achieving a high level of optimality compared to the global optimal control policy. The objective of the recalibration process is to adapt the default calibration set to a more optimal calibration set, in order to obtain the most desired behavior in terms of energy management, fuel economy, drivability and feasibility. In combination with the LH battery SoC reference, the optimal calibration set can be searched that is also in accordance with the LH strategy.

4.6.1 Strategy for recalibration

In Section 2.8.3 it was reasoned that the application of fully detailed MPC-based recalibration methods is not suitable for the recalibration process, because they are a rather cumbersome approach and either result in a very complex optimization problem, or require strong modifications that may render the simplified solution no longer optimal or feasible. Instead of an MPC-based method, a new approach is proposed based on an intelligent search method that looks for a feasible calibration set that performs best in terms of a provided objective function (more on the problem formulation in the next section). Although the number of variables that are modified is (in principle) free and the complexity and shape of the maps can be increased if desired, it was described in Section 4.5.1 that there are two calibration maps, P_{eDRV} and T_{LPM}, that make the two main decisions on the driving mode and power split. Simple adjustments of these two calibration maps can therefore already completely change the final control strategy of the heuristic controller. Since the recalibration process can take into account the LH battery depletion strategy, there is no longer a need to incorporate SoC dependency in calibration maps (as introduced in Section 4.5.1) and the P_{eDRV} can be taken as a constant. In this work, the recalibration process is limited to overwriting the electric power threshold calibration map (P_{eDRV}) with a constant value and saturating the ICE torque target (T_{LPM}) calibration map with a constant value, which is graphically displayed in respectively Figure 4.10a and Figure 4.10b.

For the intelligent search process, the main task is the formulation of a candidate calibration set and assessing the optimality and feasibility of this calibration set. The first step in this process is to determine the control decisions over time of the candidate calibration set using an internal controller model. Subsequently, the vehicle response to these control actions is simulated over the SH interval using an internal plant model. The resulting SoC trajectory, fuel consumption and all other relevant states and inputs are assessed for their optimality and feasibility and afterwards, a new candidate calibration set can be formulated. The intelligent search approach can be implemented in an automated process by formulating it as an optimization problem, which is graphically displayed in Figure 4.11.

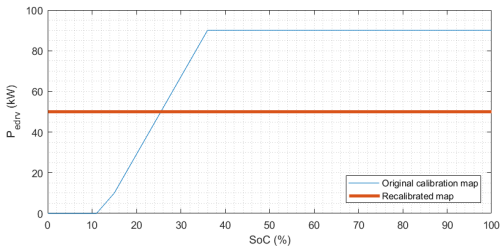

(a) Recalibration of the P_{eDRV} calibration map to a power threshold of 50 kW.

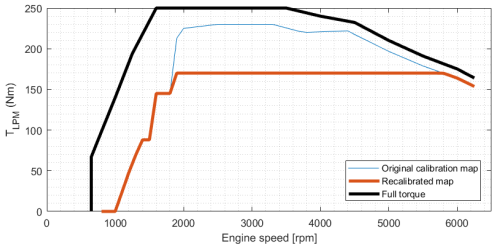

(b) Recalibration of the T_{LPM} calibration map to a torque of 170 Nm.**ADD full load curve**

Figure 4.10: Examples of the recalibration of both calibration maps.

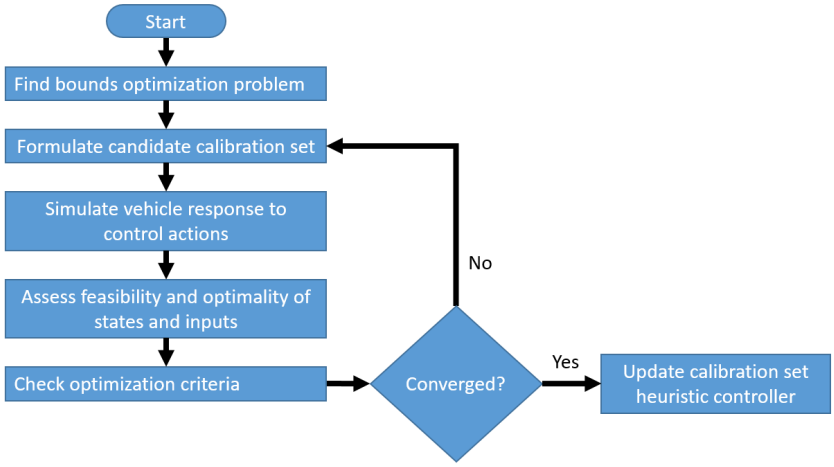

Figure 4.11: Flowchart of the steps in the SH intelligent search process.

4.6.2 Formulation as optimization problem

In order to formulate the recalibration process as an optimization problem, the objectives of the recalibration process need to be captured in a mathematical cost function and a set of constraint functions. The optimization problem has only two optimization variables $\mathbf{x} = [P_{\text{eDRV}} \quad T_{\text{LPM}}]$, which are constant over the entire SH interval. There are three separate sub-objectives that need to be taken into account in the optimization problem: minimize fuel economy, comply with LH SoC strategy, maximize drivability. Since the method relies on a conventional heuristic controller as its basis, many of the feasibility and drivability conditions are already directly ensured in the control strategy. More specifically, the feasibility of all control actions, the ICE-on-time constraint of 10 seconds and the reduction of aggressive ICE transient are intrinsically included as described in Section 4.5.1. . and the following terms are included in the final optimization problem:

- **Local fuel economy:**
  Minimize the consumption of equivalent fuel: $\sum_{i=1}^{N_p} \dot{m}_{\text{f, equiv}}(\mathbf{x}, k+i)$
- **LH strategy:**
  Stay within upper and lower bounds at the end of the horizon (implemented as a hard constraint): $SoC_{\text{f,LB}} \leq SoC(k+N_p, \mathbf{x}) \leq SoC_{\text{f,UB}}$
  Penalize deviations from the target SoC at the end of the horizon (implemented as penalty term): $(SoC_{\text{target}} - SoC(k+N_p, \mathbf{x}))^2$
- **Drivability:**
  Additional penalty term to reduce the number of ICE starts: $(\text{ICE}_{\text{starts}}(\mathbf{x}))$

The different objective terms can be mathematically summarized in a single cost function and the optimization problem is subject to:

$$\underset{\mathbf{x}}{\text{Minimize:}} \quad J(k,\mathbf{x}) = \sum_{i=1}^{N_p} w_1 \dot{m}_{\text{f, equiv}}(\mathbf{x}, k+i) + w_2 (SoC_{\text{target}} - SoC(k+N_p,\mathbf{x}))^2 + w_3(\text{ICE}_{\text{starts}}(\mathbf{x})) \tag{4.6a}$$

$$\text{Subject to:} \quad SoC_{\text{f,LB}} \leq SoC(k+N_p,\mathbf{x}) \leq SoC_{\text{f,UB}} \tag{4.6b}$$

where $\dot{m}_{\text{f, equiv}}$ is the instantaneous equivalent fuel consumption, SoC is the battery SoC level, SoC_{target} is the targeted SoC level at the end of the SH, $\text{ICE}_{\text{starts}}$ is the number of times the ICE is started, $t_{\text{min, off}}$ is the minimal time the ICE should remain off, $t_{\text{ICE off}}$ is the actual time of the ICE-off phase, $SoC_{\text{f,UB}}$ and $SoC_{\text{f,LB}}$ are the hard constraint bounds of the LH reference trajectory at the end of the horizon and w is a weight factor given to each term in the objective function.

4.6.3 Characteristics of the optimization problem

In order to come up with an efficient and robust optimization strategy for solving the optimization problem, it is key to understand the shape and characteristics of the objective and constraint functions. In Figure 4.12b and Figure 4.12a, contour plots of respectively the final SoC state and the cost function for a typical optimization problem are displayed. Based on comparison of numerous recalibration optimization problems, this optimization problem seems to be a representative problem for the recalibration task. Figure 4.12a display the final SoC states for different calibration sets, solved over the two optimization variables in a 100x100 grid. A pattern can be recognized where the top-left corner has the highest SoC values and the entire right border has the lowest SoC values. The two red curves represent the calibration sets that meet the upper and lower bound of the LH reference trajectory at the end of the horizon. The solution space between these two curves is the feasible domain of this optimization problem. The feasible domain forms a trench that roughly stretches from the bottom-left corner to the top-right corner. The general shape of the cost function that can be seen in Figure 4.12b is mainly the result of the cost from the equivalent fuel consumption and deviation from the SoC target, the other costs (ICE starts) have their main influence on a more local scale within the feasible domain of the solution space. When studying the cost function contour plot in Figure 4.12b it can be seen that the cost function is convex from roughly the top-left to bottom-right corner, forming a valley. Throughout this valley (across the axis from roughly the top-right to bottom-left corner), however, the cost function is typically not convex or monotonically increasing/decreasing. As a result of these two characteristics, the cost function contains multiple local minima within the feasible domain. In practice, the different local minima represent the number, length or starting time of the ICE on phases. In the exemplary optimization problem displayed in Figure 4.12b, the global minimum in the bottom-left corner represents 2 relatively long ICE on phases and the top right local minimum represents 3 relatively short ICE on phases.

The domain of the T_{LPM} variable always spans from 0 to 230 Nm (the maximal value of the torque target line) for every SH optimization problem. The domain of the P_{eDRV} variable spans between 0 and the maximal electric power demand over the SH interval for any arbitrary SH optimization problem. Due to the LH battery SoC constraint however, in many SH problems the electric and ICE-based driving modes have to alternate each other in order to achieve a feasible end of horizon SoC state, rather than pure electric or ICE-based driving. This leads to a reduced feasible domain of the P_{eDRV} solution space, since, for example, very low and very high values of the electric power threshold (i.e. <5.2 kW and >47.2 kW in the example of Figure 4.12b) cannot provide feasible calibrations. These bound can be estimated a priori in an attempt to reduce the complexity of the optimization problem.

4.6.4 Solving the optimization problem

In this work it is proposed to make use of the same boundary estimation method for the SH optimization problem as proposed in the LH estimation method (Section 4.4.4). Although more advanced methods

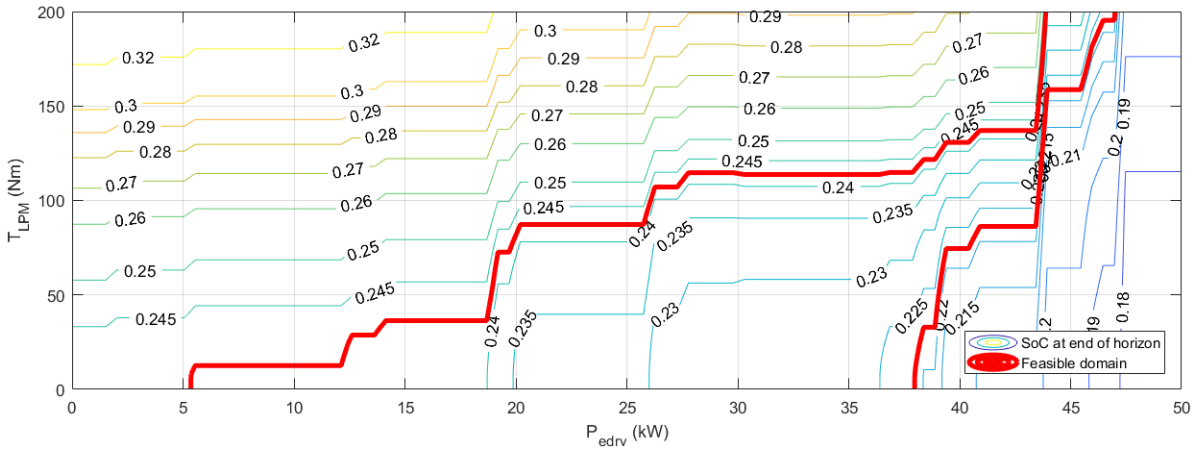

(a) The contour plot of the final SoC state illustrates the SoC value at the end of the SH interval. The feasible domain is outlined by the thick red curves, which correspond to the feasible bounds [0.222 0.242].

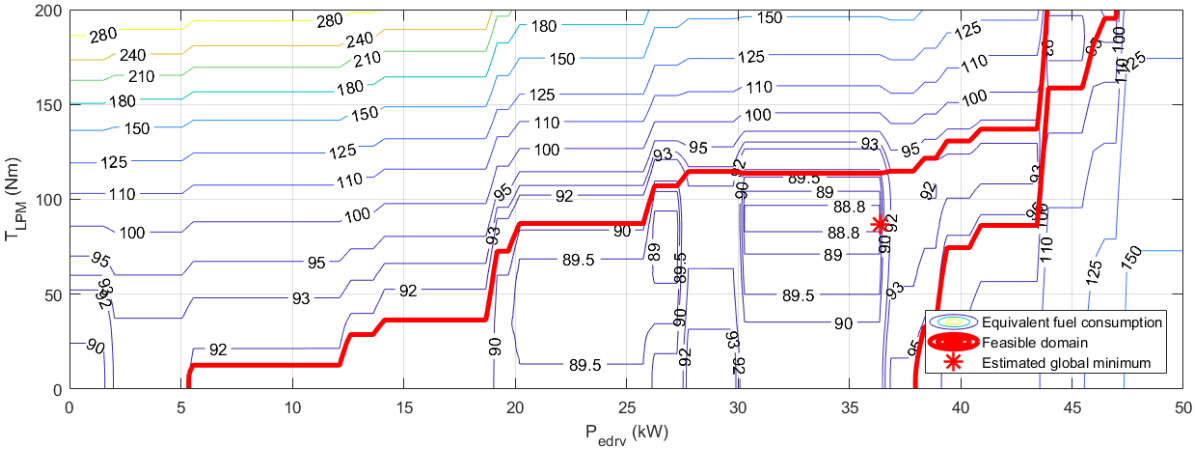

(b) The contour plot of the cost function illustrates the equivalent fuel consumption over the SH interval. The problem consists of two minima ($[25,\ 50]$ and $[36,\ 90]$) of which the latter is the global optimum with an equivalent fuel consumption of 88.7 grams.

Figure 4.12: Contour plots of the final SoC state and cost function for a typical recalibration problem.

can be developed, the reduced solution space in this work is defined by a rectangular boxdefined by the minimal and maximal feasible bounds of the P_{eDRV} variable and the original domain of the T_{LPM} variable. The bounds of the P_{eDRV} variable, similarly to the LH method, follow from two characteristic powertrain operation strategies:

- **Lower bound:**
  The lower bound is the minimal threshold of the electric power without applying any LPM strategies that just meets the upper SoC target. It represents the minimal amount of electric energy that has to be used since all strategies with lower P_{eDRV} thresholds cannot satisfy the upper bound of the LH SoC strategy and have unused battery energy left. In Figure 4.12a, this corresponds to the left-most point of the SoC bound at approximately 5 kW.

- **Upper bound:**
  The upper bound is the maximal threshold of the electric power that just meets the lower SoC target with maximal application of LPM strategies and full load operation of the ICE (or the limit of the EM). It represents the maximal amount of electric energy that can be used since all strategies with higher P_{eDRV} thresholds cannot satisfy the LH SoC strategy and have not enough battery energy left. In Figure 4.12a, this corresponds to the left-most point of the SoC bound at approximately 47 kW.

Once the reduced solution space is determined, an optimization process can be used to look for the optimal combination of the P_{eDRV} and T_{LPM} variable. Gradient-based solving techniques are generally a quick method to determine the exact location of a (local) minimum, but in the case of multiple local minima their convergence to a specific local minima strongly depends on the initial starting point of the algorithm.Since in the general case there is no way of knowing where and in which direction to start the gradient-based optimization process, there is a need for an optimization process that is more robust to local minima.

First- or higher order solving techniques (using derivative information) are intrinsically not robust to problems with multiple local minima, therefore zero-order (random or stochastic) methods or brute force methods are often applied [58]. However, once the rough location of the minimum has been found, the convergence rate of zero-order methods is relatively slow compared to first- and higher-order methods [58]. For this reason, it is common engineering practice to apply a two-stage, or hybrid, optimization process where a gradient-based method is applied once the zero-order method has pointed out a specific local minimum. A particle swarm optimization (PSO) method is a common optimization technique in literature [58] to solve optimization problems with multiple local minima, because it is a relatively efficient zero-order method [59, 60]. A PSO method is used for the application on the SH recalibration process, because the method proves to be robust, accurate and its computational demands are sufficiently low. In this work Matlab's `particleswarm` PSO algorithm [61] is applied to solve the optimization problem. It was found that the convergence of the PSO method is already sufficient for recalibration process and the application of a subsequent gradient-based optimization method as final step provides only very marginal improvements (typically in the order of 0.05 grams or 0.1% of the equivalent fuel consumption per short horizon).

4.6.5 Measures for robustness

For SH intervals where perfect knowledge of the future power demand and future driving conditions is available, the adaptive heuristic control method as proposed in the previous sections can determine the optimized calibration set and subsequently achieve the highly optimal vehicle response as planned. In practice however, the future conditions (in particular the future velocity profile and exact efficiency of the complete vehicle) can never be predicted with 100% accuracy and will therefore contain prediction errors. As result, the heuristic controller in practice will not respond exactly as planned during the recalibration process. Since one of the strengths of the heuristic control method is that the control actions can be computed at very high frequencies, the output torque of the ICE and EM are continuously adapted such that actual power demand is satisfied. For example, if the anticipated torque request was 90 Nm, but the actual torque request is 80 Nm, the output torque is simply lowered according to the heuristic rules.

The biggest problems occur, however, when the actual power demand does not match predicted power demand and subsequently, an incorrect driving mode is selected. In cases where the actual power demand is higher than prediction, a false ICE start might be triggered where this was not planned, or if the actual power demand is slightly lower than prediction, an ICE start might not be triggered at all and the interval is falsely driven electrically. As a consequence of this wrong drive mode, either too much battery energy remain and the SoC level is too high (in the case of a false ICE start), or too much electric energy is used and the SoC level will be too low (in the case of a missed ICE trigger). Although the optimal calibration set is recalculated every SH interval and thus the controller should be able to quickly converge back to the LH SoC reference profile, a deviation from the optimal path often leads to an increase of fuel consumption in the end.

To improve the robustness of the selected calibration set (in the sense that the actual vehicle response will be closer to the planned response), several measures have been applied to reduce the cases where an incorrect driving mode is selected. First of all, to reduce the effect of short-duration spikes (e.g. during gearshifts) on the selection of the driving mode, a minimal time threshold for the exceeding the P_{eDRV} power threshold is implemented. This way, any short peaks in the power demand (with a duration smaller than 1 second in this work) are filtered out and do not trigger false ICE starts. For SH intervals where no use of the ICE is planned, the P_{eDRV} power threshold can in principle be chosen anywhere between the maximal predicted electric power demand and the maximal power output of the EM. From a robustness

perspective, however, it is not recommended to pick a power level close to the maximal predicted electric power demand, since any slight prediction errors might trigger an ICE start in this case. On the other hand, selecting a P_{eDRV} power threshold equal to the maximal power output of the EM is also not wise, because scenarios might occur where very large disturbances in the predicted power demand are present (e.g. an unplanned overtake of the preceding vehicle). Since the impact on the local SoC planning would be very large in these cases, it is better start the ICE once the power demand exceeds a certain default power threshold. In this work, it chosen to adopt a default P_{eDRV} power threshold of 37 kW for SH intervals where no use of the ICE is planned, which adds robustness to both of the above described scenarios. In cases where the predicted electric power demand is close to or larger than default threshold, but still no use of the ICE is desired, a margin of 5 kW is used on top of maximal electric power demand to decrease the number of false ICE triggers. A similar measure is implemented to prevent false ICE shutdowns. In SH intervals where electric driving is not desired, the P_{eDRV} power threshold is selected below the minimal predicted electric power demand with margin of -5kW.

4.7 Final architecture overview

In this work, a supervisory control system for a HEV is proposed that makes use of a two-stage control architecture. The two main tasks of the supervisory controller, LH EMC and SH PMC, are split into two separate optimal control problems that are solved sequentially by solver that are dedicated to the specific subproblem. The final architecture of the control system is graphically displayed in Figure 4.13.

The supervisory control system uses forward prediction models to determine the best control strategies. The data inputs for the supervisory controller are received from the predictive information system, which typically includes GPS, GIS and navigation systems, as well as communication technology (V2X) and advanced vehicle sensors (camera vision, radar, ...), but is not part of the scope of this work. The predictive information system supplies altitude and velocity information to the supervisory control system, where the velocity information is only available with a rough level of detail for long term predictions.

The LH control method manages the overall battery depletion profile to prevent the loss of recuperation potential and aims to use the energy in the battery at instances where it contributes the most to the overall efficiency of the vehicle. A power-based clustering method is proposed that optimizes the power split for each cluster in an attempt to achieve the best approximation of the global optimal control strategy.

The SH control method manages the detailed powertrain operation over the SH to determine the best driving mode and power split in terms of equivalent fuel consumption and drivability. Rather than applying optimization based control approaches, a novel adaptive heuristic control method is proposed that relies on a conventional heuristic control method to determine the direct control inputs for the vehicle. An PSO-based search method is applied to adapt the calibration set of the heuristic controller based on upcoming conditions and events in order to achieve a better fuel economy compared to the default calibration set.

Prediction errors in the future power demand can lead to discrepancies between the planned and actual driving mode, which can lead to significant deviations from the optimal reference trajectory. To improve the robustness of the selected calibration set, several robustness measures have been introduced in the recalibration process. In most SH intervals it is possible to apply margins on top of the predicted power demands to prevent the selection of incorrect driving modes.

The control architecture also allows other SH control methods to be used (such as ECMS or MPC), because the interface and required input and output data for the different control methods is the same.

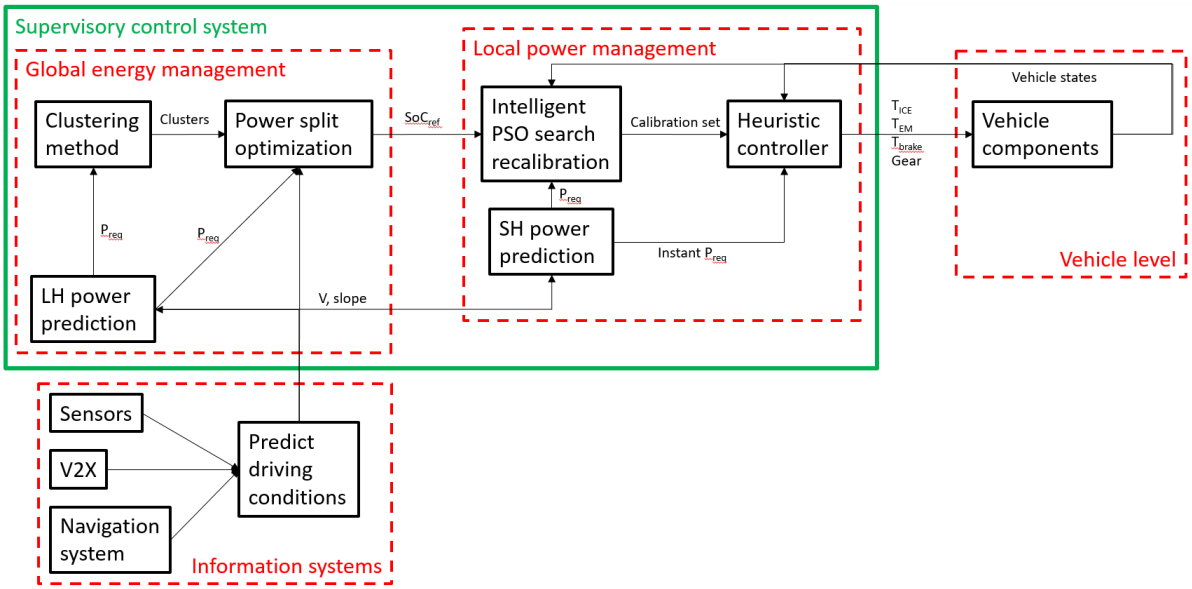

Figure 4.13: Overview of the final two-stage architecture of the supervisory controller and its interfaces

5

Results and evaluation

In this chapter the performance of the proposed control method is evaluated in comparison with existing methods. The evaluation is split up in different levels to obtain more meaning full assessments. The performance of the individual control stages is evaluated, as well as the performance of the complete control system as a whole. To assess its robustness, the proposed control method is applied in a high fidelity simulation environment.

5.1 Simulation approach

To assess the effectiveness of the proposed control method, the behavior and control actions of the proposed control method are evaluated in a set of simulation cases. The main goal of this simulation process is to determine what the impact of the individual control stages is on the overall fuel economy of the HEV, and how this performance of the individual control stages compares to other existing control methods. Furthermore, the simulation cases should demonstrate the ability of the proposed local control method to track a global SoC reference trajectory and to what extent the proposed method is able to incorporate feasibility and drivability conditions into its control strategies. Finally, the robustness of the combined control method to disturbances and predictions errors is of interest.

It is, however, difficult to make meaningful assessments of the performance of the individual control levels (global and local) when only comparing the final control actions of the controller as a whole. Since there are many potential error sources, it is impossible to trace back where performance losses originated and also the performance comparison to other control methods loses its relevance if the sources of performance loss are unclear. For this reason, a performance evaluation approach on three distinctive levels is proposed based on the solely the control-oriented simulation models, such that no disturbances are present. Firstly, the control strategies and relative performance of the global estimation method are assessed. Secondly, the control strategies of the proposed local control is assessed and compared independently of the LH strategy. Finally, the combined performance of the two control stages is evaluated. Once the performance of the complete control method is determined in a disturbance-free simulation environment, its effectiveness is evaluated in the presence of disturbances in the high fidelity simulation environment.

5.2 Simulation cases

To evaluate the effectiveness of the developed control methods, their performance is tested over in a set of simulation cases. The first simulation case is the Graz drive cycle. This drive cycle is an in-house drive cycle for emission testing by AVL, which meets Real Driving Emissions (RDE) cycle requirements and is therefore a highly dynamic and demanding cycle [62]. The drive cycle is a recorded cycle, which means there are a lot of velocity and altitude fluctuations. The velocity and altitude profile are displayed in

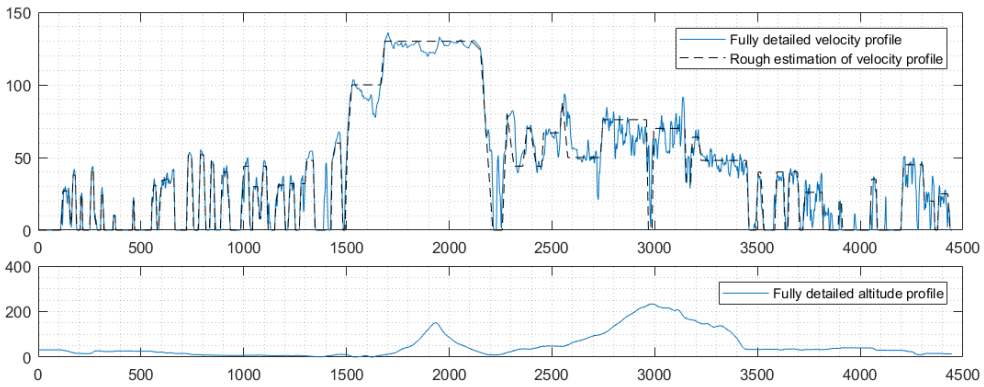

Figure 5.1: Velocity and altitude profile of the Graz cycle.

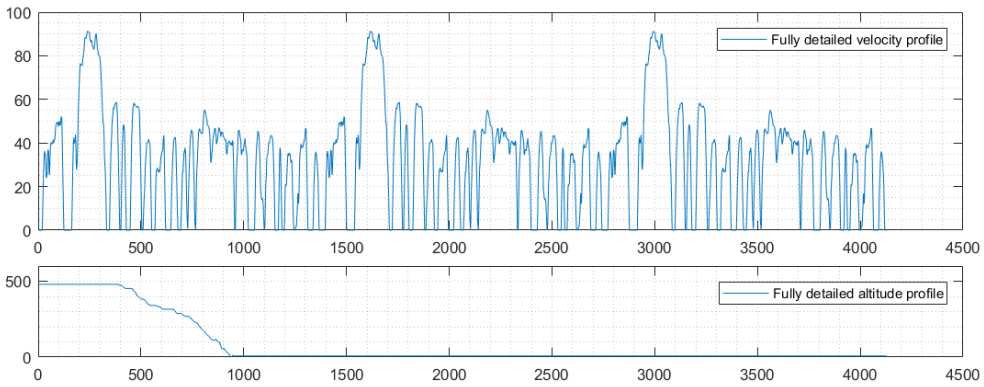

Figure 5.2: Velocity and altitude profile of the 3F cycle.

Figure 5.1. For the Graz drive cycle, a rough estimation of the velocity profile is created. The availability of this level of preview information is more realistic than the fully detailed velocity profile and can be used in the LH estimation method to determine the reference SoC trajectory.

The second simulation case is the 3F cycle. This drive cycle is a constructed by repeating the FTP-75 cycle three times. The FTP-75 drive cycle is an US drive cycle from the Environmental Protection Agency, which consists mainly urban driving [63]. Also this drive cycle is a recorded cycle, which includes a lot of velocity fluctuations. Originally, the drive cycle does not contain an altitude profile, but for this work a significant downhill section is added. This downhill altitude profile is taken from GPS data from a real downhill road in Austria between the GPS coordinates [46.668463, 15.009701] and [46.653374, 14.982247]. The velocity and altitude profile are displayed in Figure 5.2.

5.3 Evaluation LH control method

In this section, the performance of the global estimation method proposed in Section 4.4 is evaluated using Graz drive cycle and 3F drive cycle. The main goal is to assess the individual optimality of the proposed global estimation method over the complete route in terms of fuel consumption. All simulation are performed with the control-oriented simulation models only and for these simulation cases the LH estimation method has access to the complete detailed velocity profile.

As the first steps in the solving process, the instances were clustered into groups that share similar power demands and the P_{eDRV} power threshold was determined according to the method proposed in Section 4.4.4. For the Graz simulation case, the additional steps to prevent the loss of recuperation potential

were not required. A number of 10 clusters were defined, for which a linear distribution for cluster 4 to 10 is used and the optimal P_{eDRV} threshold was found to be 23.8 kW. The final clustering results for the Graz drive cycle are displayed in a histogram in Figure 5.3. Here the blue (dark) bars illustrate the distribution of the requested propulsion power, where each bar represents the cumulative time for the corresponding power demands. The gray (light) bars show the different clusters (10 in total) and their corresponding cumulative travel time.

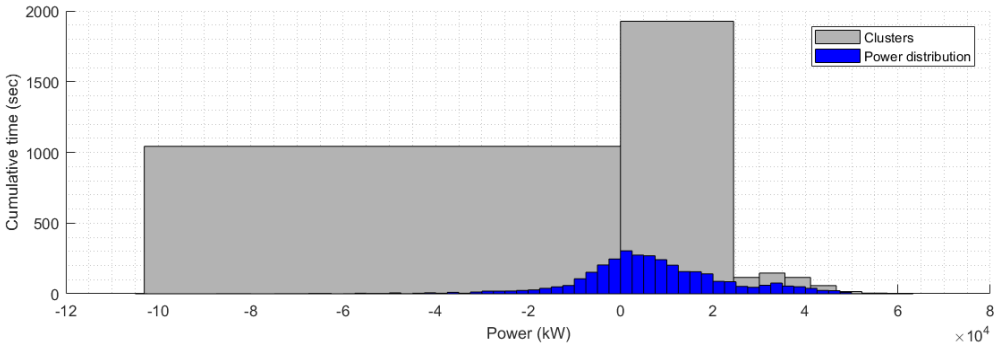

Figure 5.3: Distribution of the time instances over the 10 clusters for the Graz drive cycle. Cluster 1 is not depicted, since the power request is zero for all the instances in this cluster.

In the next step, the power split value for the clusters 4 to 10 are obtained by an optimization process that minimizes the total fuel consumption. The optimization results for the Graz drive cycle are summarized in Table 5.1 and graphically displayed in Figure 5.4a. It can be seen that the third cluster is driven electrically and the optimal power splits of clusters 4 to 10 are negative, which means the control method plans the use of LPM strategies in these instances to increase the load of the ICE and generate additional battery energy. The results of the DP method are displayed in Figure 5.4b as a benchmark of the global optimal solution. The figure illustrates that the transition from electric to ICE-based driving in the DP solution is relatively sharp defined for this simulation case and does indeed take place around 24 kW (as also determined by the LH estimation method). It can also be seen that the proposed power splits of the DP and proposed solution have a high level of agreement.

Table 5.1: Distribution of the clusters and their optimized power split value.

Cluster number:	Power demand (kW)	Power split:	Type:
1	$P_k = 0$	+1	Stationary
2	$P_k < 0$	-1	Regenerative
3	$0 > P_k \geq 23.8$	+1	eDRV
4	$23.8 > P_k \geq 29.5$	-0.0526	ICE on
5	$29.5 > P_k \geq 35.5$	-0.0412	ICE on
6	$35.1 > P_k \geq 40.8$	-0.0513	ICE on
7	$40.8 > P_k \geq 46.4$	-0.0392	ICE on
8	$46.4 > P_k \geq 52.0$	-0.0276	ICE on
9	$52.0 > P_k \geq 57.7$	-0.0111	ICE on
10	$57.7 > P_k \geq 63.3$	-0.0150	ICE on

Figure 5.5 displays the resulting battery SoC depletion profile and the fuel consumption profile of the global estimation method and the DP solution, as well as the linear over distance battery depletion profile. It can be seen that the shapes of the SoC trajectory and cumulative fuel consumption over time are very similar. Both control strategies drive the first 1650 seconds and last 1250 seconds (from 3200 seconds to the end) almost completely electrically, with minimal use of the ICE (which can be deduced from the low consumption of fuel). This makes sense, because the vehicle speeds are low and only small variations in the altitude profile are present during these intervals, as can be seen in Figure 5.6 where the velocity and altitude profile of the Graz drive are depicted again. During the intervals from 1700-1930 seconds

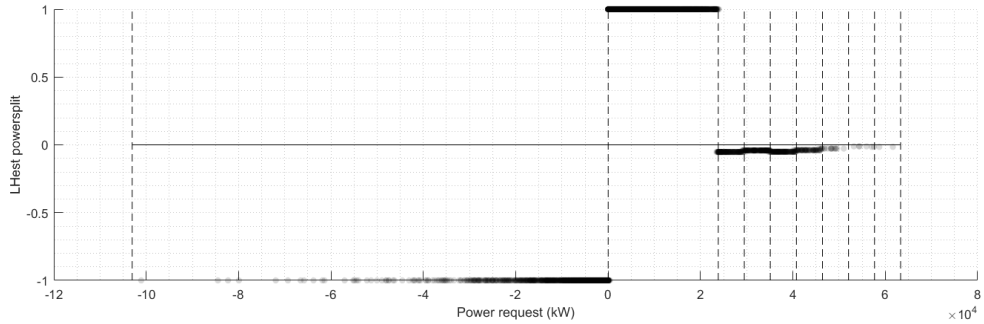

(a) The selected power split resulting from the global estimation method plotted over the propulsion power request.

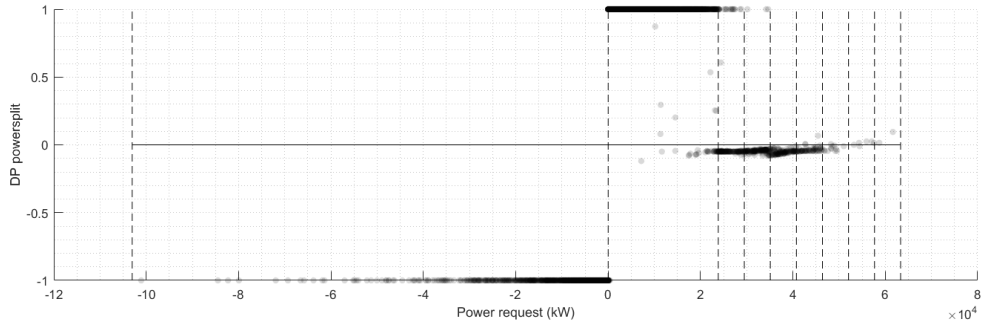

(b) The selected power split resulting from the dynamic programming optimization method plotted over the propulsion power request. This solution is the global optimal solution to the optimal control problem.

Figure 5.4: Graphical illustration of the selected power split values over the propulsion power request for a global optimal and global estimation method. The color intensity in these plots corresponds to the local sample density.

and 2700-3200 seconds on the other hand, both controllers make intensive use of the ICE with high fuel consumption. This can be explained by the fact that these intervals overlap with two long uphill driving phases, where the velocity is also relatively high. The resulting power demands are high in these sections, which leads to relatively high operating efficiencies of the ICE. Both the global estimation strategy and DP strategy deviate from the linear battery depletion strategy to obtain a more optimal depletion profile, where the most significant differences are aligned with the extremities of the altitude profile. In Table 5.2, the final SoC state and total fuel consumption are listed. The total fuel consumption of the estimation method is only 1 gram or 0.07% higher than the global optimal solution from DP for this simulation example.

Table 5.2: Comparison of the results for the Graz drive cycle from the dynamic programming solution and global estimation method.

	Dynamic programming	LH estimation
Final SoC (%)	15.0050	15.0076
Fuel consumption (gram)	1424.58	1425.57
Compensated fuel consumption (gram)	1424.53	1425.50
Optimality	-	99.93%

In the second simulation case, a large downhill section is present, which can potentially lead to the loss of recuperation potential as introduced in Section 4.3.2 and shown in Figure 4.7. To prevent this from happening, an additional step is applied in the LH estimation method to ensure recuperation potential is fully captured (Section 4.4.5). The results of the LH estimation method are listed in Table 5.3, where it can be seen that additional recuperation step was very effective, saving more than 200 grams (more than 30%) of fuel in this simulation case. In Figure 5.7, the battery depletion profile of DP and LH estimation

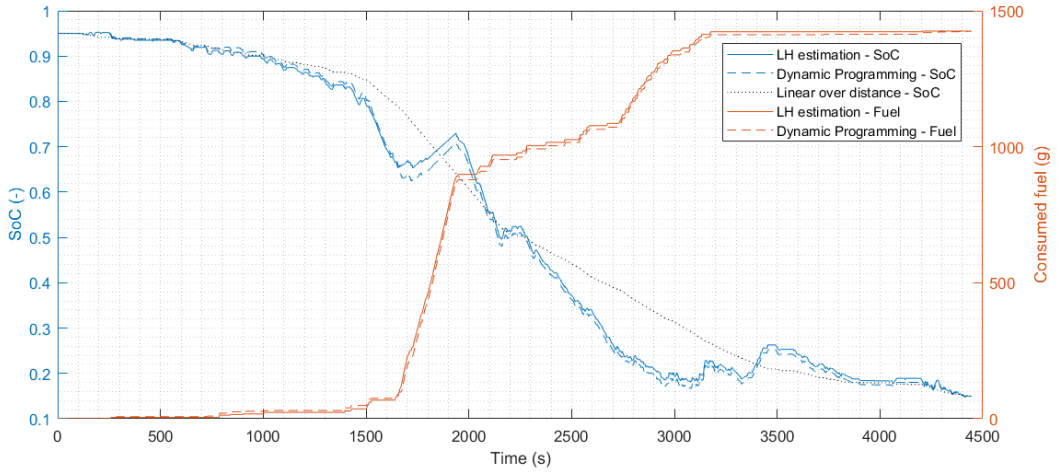

Figure 5.5: A comparison between the global estimation and dynamic programming solution of the battery SoC and fuel consumption over time.

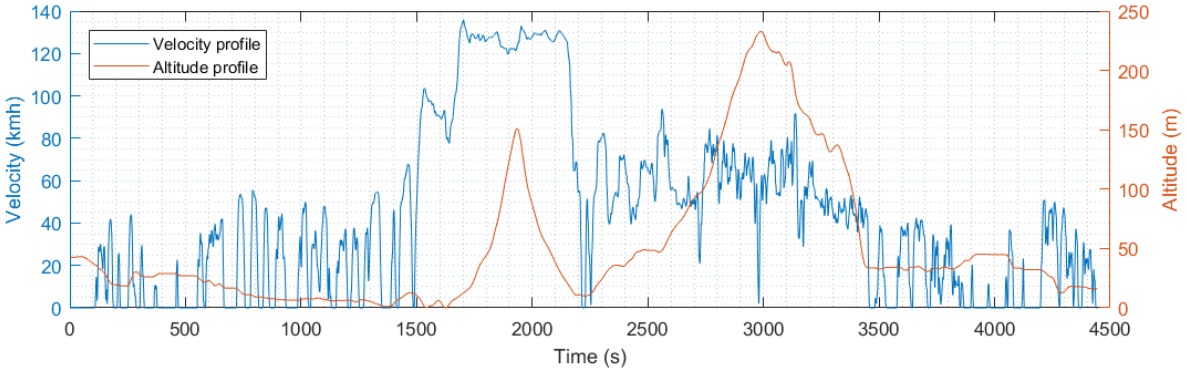

Figure 5.6: The altitude and velocity profile of the Graz drive cycle.

with and without the additional recuperation step are depicted. It can be seen that the LH strategy without the additional recuperation step clearly makes too much use of the ICE during the interval 0-500 seconds, and as a result, the upper SoC limit prevents further recuperation of electric energy between 500-1000 seconds.

Table 5.3: Comparison of the results for the 3F drive cycle from the dynamic programming solution and global estimation method with and without the additional recuperation step.

	Dynamic programming	LH estimation with recuperation step	LH estimation without recuperation step
Final SoC (%)	50.0389	50.0372	50.0026
Fuel consumption (gram)	476.14	478.61	686.32
Compensated fuel consumption (gram)	475.78	478.27	686.30
Optimality	-	99.48 %	69.33%

It can be concluded that the performance of the global estimation method is very high, because the solution is close (+0.07% and +0.52% fuel consumption for this simulation case) to the global optimal solution determined by DP. The computational requirements, however, are much lower: the global estimation solution for the 4447 second long Graz drive cycle was calculated in 6.7 seconds on average, where the computation of the DP solution took 490 seconds. Both results were determined on a PC with an Intel Core i5-7200U 2.5 GHz processor.

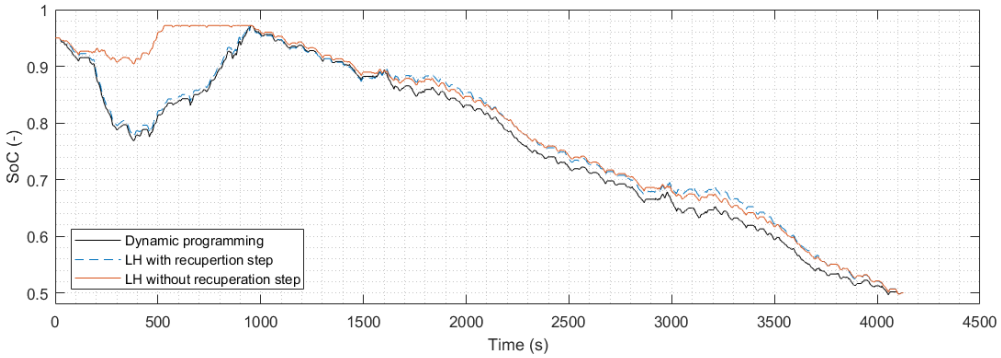

Figure 5.7: Battery SoC profile over time from the dynamic programming solution and the global estimation with and without the additional step to prevent loss of recuperation potential. Without the additional recuperation step, the control strategy is unable to capture the complete recuperation potential between 500-1000 seconds.

5.4 Evaluation SH control method

In this section, the performance of the local control method proposed in Section 4.6 is evaluated using the Graz drive cycle zoomed in at the SH interval from 2761 to 2820 seconds. The main goal is to assess the individual performance of the proposed adaptive heuristic control method over the local time scale in terms of fuel consumption. Also its ability to track the LH reference trajectory and the effect of including feasibility conditions are evaluated. All simulations are performed with the control-oriented simulation models only. For the LH reference the LH estimation method with complete preview of the future conditions is used. In this section the adaptive heuristic control method with and without the feasibility and drivability constraints are evaluated separately, which will be referred to as respectively the constrained and unconstrained case.

As the first step in determining the best calibration set for the upcoming short horizon interval, the bounds of the feasible domain are determined in an attempt to reduce the solution space following the proposed approach in Section 4.6.4. For this SH interval and the constrained simulation case, the feasible bounds of the P_{eDRV} calibration variable where found to be $[5.2, 47.2]$ kW. In Figure 4.12b and Figure 4.12a the contour plots of respectively the cost function and final SoC state for this problem (note that these are only available for offline analysis purposes) were already displayed. It can be seen that the most extreme values of the P_{eDRV} calibration variable that still satisfy the upper and lower bound of the LH reference are indeed respectively $[5.2, 47.2]$ kW. In the next step, the intelligent search method based on particle swarm optimization (PSO) is applied to obtain the optimal set of calibration variables (P_{eDRV} and T_{LPM}) that minimize the cost function. The algorithm converged to the point $[36.17\text{kW}, 95.75\text{Nm}]$ with a final cost value of 88.778, which indeed corresponds with the global minimum of the cost function in Figure 4.12b. A subsequent gradient-based optimization method was also applied a final step, which was only able to marginally improve the cost value to 88.7184.

In Figure 5.8a, three curves are depicted that represent the resulting battery SoC depletion profile of respectively:

- The DP solution for the SH interval of 60 seconds.
- The constrained heuristic control method with the previously found calibration variables.
- The unconstrained heuristic controller with a calibration set optimized towards the pure minimization of the equivalent cost, without taking any additional feasibility and drivability constraints or costs into account.

For all three curves, the instances where the ICE is active are marked by an asterisk and also the pure eDRV and maximal LPM curves are shown, which represent the most extreme feasible control policies. It can be seen that the DP solution and the unconstrained heuristic solution are very similar. The ICE is active at (roughly) the same instances and more thorough analysis of the data also demonstrates the power splits

have a high level of agreement. The optimal P_{eDRV} threshold was found at 25.4 kW for the unconstrained case, which aligns perfectly with every instance with relatively high power demands in Figure 5.8b. The instances with relatively low power demands are driven electrically due to the low operating efficiency of the ICE at these conditions. The constrained heuristic solution in Figure 5.8a on the other hand, differs strongly from the other two strategies and uses more distinctly separated phases of electric and ICE-based driving.

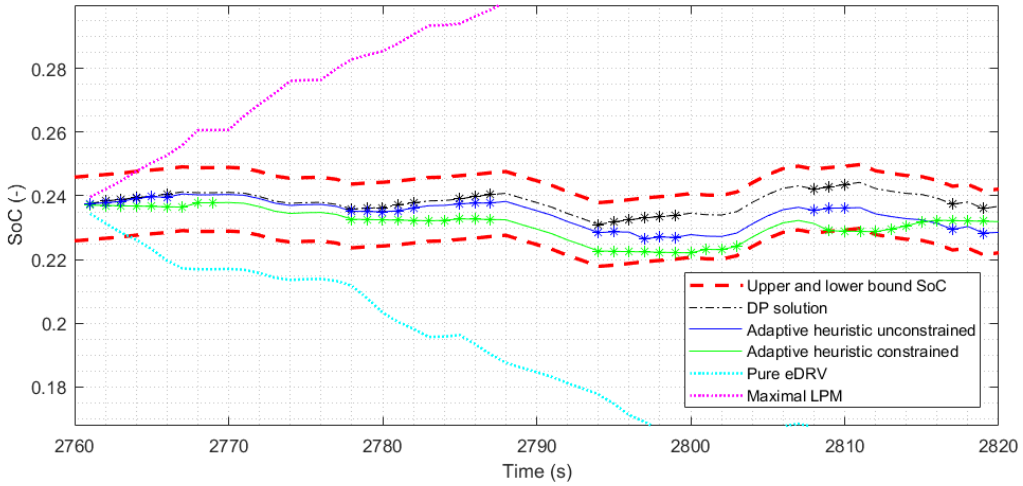

(a) SoC profile of different SH control methods. The instances where the ICE is active are marked by an asterisk. It is important to note that the hard constrained upper and lower SoC bound are only enforced at the end of the horizon.

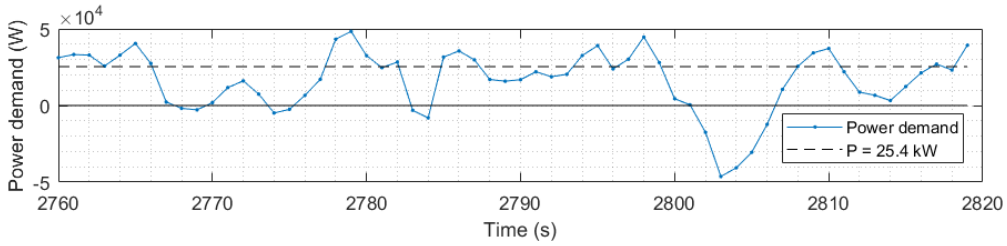

(b) The propulsion power demand over the SH interval. Also the P_{eDRV} power threshold is displayed for the unconstrained case.

Figure 5.8: Comparison of different SH control strategies over a SH interval.

In Table 5.4, the fuel economy of the three different control strategies are compared in terms of fuel consumption and depleted battery SoC. It was found that the heuristic control method with the unconstrained optimized calibration set has near optimal performance, with only 0.21 grams or 0.27% higher equivalent fuel consumption than the DP solution. This proves that a heuristic controller can indeed have near-optimal performance if its calibration is optimized towards known future driving conditions. However, both control strategies do not take into account conditions for feasibility and drivability, which results in respectively 7 and 8 short ICE on phases for the DP and unconstrained adaptive heuristic solution, with an average length of respectively 3.71 and 3.13 seconds. When also considering feasibility and drivability conditions, all ICE phases have a minimal length of 10 seconds and the total number of ICE phases is reduced to only 4 phases, as can be seen in Figure 5.8a. It can be seen in Figure 5.9 and Table 5.4 that the variations of the ICE torque resulting from the constrained calibration set are significantly reduced with respect to the unconstrained and DP solution (up to 40%). However, including the feasibility and drivability constraints in the optimization of the calibration set also leads to a higher equivalent fuel consumption of the HEV, which was increased by 2.20 grams or 2.84% over this interval in comparison to the unconstrained heuristic controller.

It can be concluded that the performance of the unconstrained adaptive heuristic control approach as a method is very high, because it close (+0.27% equivalent fuel consumption in this simulation case) to the global optimal solution determined by DP over the SH interval. In addition to that, the proposed control method is able to take additional feasibility and drivability conditions into account, by additional heuristic rules in its control logic. This has the potential to greatly improve the drivability and feasibility by reducing the number of ICE starts (-50% for this simulation case) and ICE torque variation (-36% for this simulation case), but comes at a cost of increased equivalent fuel consumption (+2.84% for this simulation case).

Table 5.4: Comparison of the fuel economy and drivability results of three different control strategies.

	Dynamic programming:	Adaptive heuristic unconstrained:	Adaptive heuristic constrained:
Final SoC (%)	23.67	22.85	23.17
Fuel consumption (gram)	77.31	70.19	75.10
Equivalent cost (-)	77.36	77.57	79.77
ICE phases	7	8	4
Avg. length (s)	3.71	3.13	10.25
Avg torque variation (Nm/s)	73.59	67.05	43.05

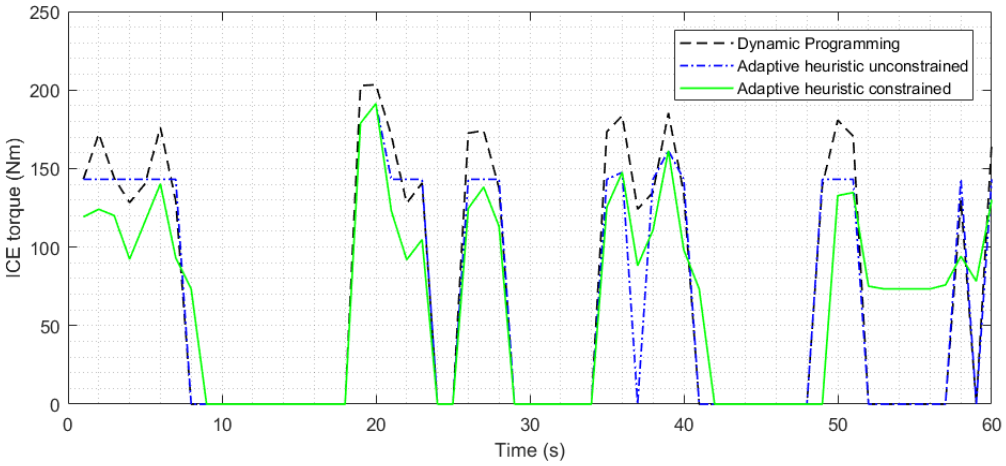

Figure 5.9: Requested torque from the ICE over the SH interval. The variations in the requested torque in the constrained adaptive heuristic control strategy are strongly reduced compared to the unconstrained strategies.

5.5 Evaluation combined control method

In this section, the performance of the combined control method as proposed in Section 4.7 is evaluated using the Graz drive cycle. The main goal is to assess the combined performance of the complete supervisory control system over the entire drive cycle in terms of fuel consumption and feasibility conditions with respect to other existing control method. Also the interaction between the two control stages is of interest, where the ability of the local control method to track the LH reference tracking is evaluated and a sensitivity study of local horizon length is performed. All simulations are performed with the control-oriented simulation modes only. Different LH reference profiles (complete, rough and distance-only preview of future conditions) are used to evaluate its impact on the performance of the combined control method.

To assess the performance of the proposed control method is compared with several other existing control methods (Full DP, LH estimation, MPC using a DP solver, A-ECMS, the proposed adaptive heuristic method in its constrained and unconstrained form and the conventional heuristic controller). For the adaptive heuristic and MPC-based control methods, a prediction horizon of 60 seconds is used with full preview

of the driving conditions during the next SH interval. In Figure 5.10a and Figure 5.10b, a comparison between the SoC trajectories and fuel consumption of these control methods is displayed using the fully detailed LH estimation reference trajectory. It can be seen that the conventional heuristic method clearly applies a CDCS strategy (first charge depletion, then charge sustaining), where the ICE is turned on for the first time once the SoC comes below 23% around 1780 seconds and the SoC remains relatively constant afterwards. The reference tracking local control methods (MPC, A-ECMS and adaptive heuristic (in both forms)) on the other hand, are able to track the LH reference trajectory very closely. To support these observations, the deviations from the LH reference SoC profile are listed in Table 5.5. It can be seen that the deviations are small, on average in the order of 0.7% SoC, which is negligible with respect to the 80% depletion over the complete route. This confirms that the tracking ability of all three control method is sufficient to follow a LH reference trajectory. Since the A-ECMS method is very sensitive to the initial value of the equivalence parameter [25, 40], this value was predetermined using an elaborate optimization process, which is not feasible for online applications. It is also important to note that conventional RB is unable to deplete battery completely for this simulation case. The reason for this is that it remains in its charge-sustaining mode around 17% SoC, even though the trip is nearly at its end. For the following results the remaining battery SoC is fully compensated , although this is not entirely a fair comparison, since the battery can usually be charged at the final destination for much lower costs.

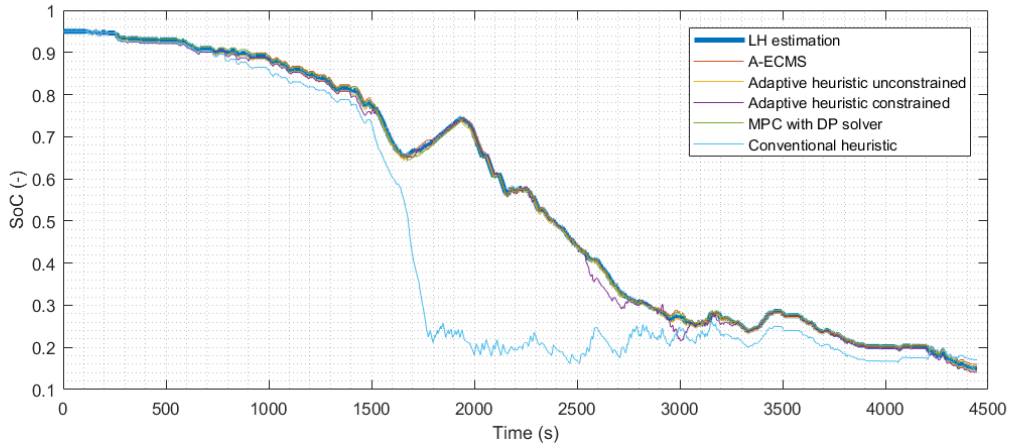

(a) Comparison of the battery depletion profile from different local control methods.

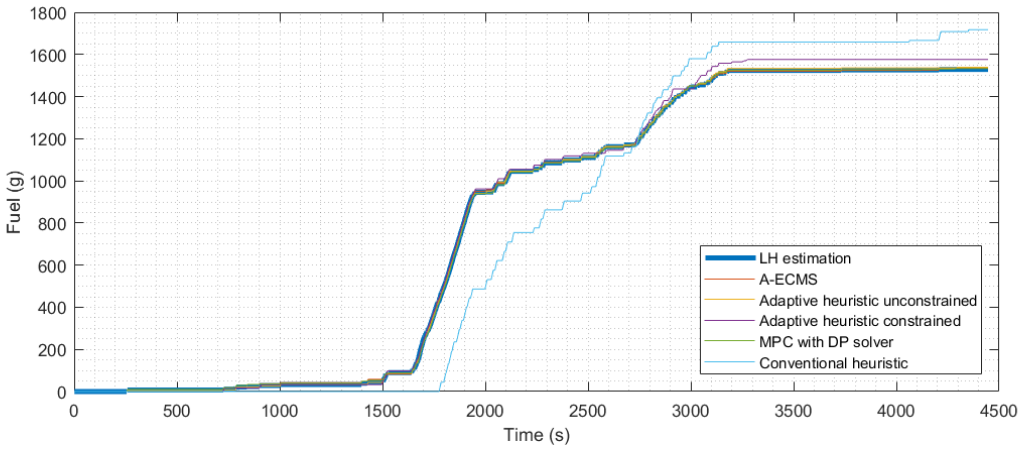

(b) Comparison of the cumulative fuel consumption over time form different local control methods.

Figure 5.10: Comparison of the control strategies from different local control methods. All reference tracking control methods remain in close proximity of the LH reference profile, while the conventional heuristic controller clearly applies a CDCS strategy.

Focusing on the unconstrained adaptive heuristic case for now, the three different control methods (A-ECMS, MPC and unconstrained adaptive heuristic) track the LH reference so closely, the differences in the

Table 5.5: Deviations between the reference trajectory and the actual SoC trajectories.

LH estimation vs	MPC	A-ECMS	Adaptive heuristic unconstrained	Adaptive heuristic constrained
Maximum deviation (% SoC)	1.45	1.44	1.43	5.39
Average deviation (% SoC)	0.39	0.39	0.47	0.69
Standard deviation (% SoC)	0.26	0.35	0.22	0.90

overall fuel economy are very small. In Table 5.6, the total fuel consumption is listed, compensated for the (small) differences in SoC . It can be seen that the final compensated fuel consumption of all three reference tracking methods is within 1.2% of the global optimal strategy. Compared to the conventional heuristic control method, a reduction in (compensated) fuel consumption of more than 9.0% is achieved by the introduction of predictive optimal control methods. This is however not a fair comparison, because these predictive control strategies do not take into account any feasibility or drivability considerations. Looking at constrained case of the adaptive heuristic method, it was found that 2.6% more (compensated) fuel was consumed than in the unconstrained case, but still a 6.7% reduction in (compensated) fuel consumption compared to conventional heuristic method was achieved. The feasibility and drivability of the control strategy is strongly improved though with respect to the MPC and ECMS methods, where the number of ICE starts was reduced by 45.4% and 46.6% less torque variation was achieved on average. The computation times vary strongly between the different control methods. The heuristic control method has been implemented in Simulink and can therefore be very efficiently computed in less than 1 ms per evaluation. The computation of the new calibration set by the recalibration process implemented in Matlab takes on average 2.2 seconds, which needs to be computed once every 60 seconds. The A-ECMS control method is implemented in matlab and can be computed relatively quickly, which takes on average 90 ms per evaluation. The MPC strategy on the other hand, using the DP solver needs 1.7 seconds per time step to compute its optimal trajectory over a 60 second prediction horizon (since it makes use of receding horizon control, this needs to be done every timestep).

Table 5.6: Comparison of the performance of the different SH control methods using the LH reference trajectory with full preview of the future conditions.

	Full DP	LH est.	MPC	A-ECMS	Adaptive heuristic Unconstrained	Adaptive heuristic Constrained	Conventional heuristic Constrained
Final SoC (%)	15.01	15.01	15.56	16.02	14.44	14.12	17.07
Fuel consumption (gram)	1525.93	1528.69	1532.84	1536.27	1539.01	1575.93	1717.57
Compensated FC (gram)	1525.87	1528.63	1527.65	1526.93	1544.20	1583.99	1698.50
ICE starts (-)	95	86	97	105	76	50	45
Avg time ICE on (s)	5.80	6.23	5.71	5.26	7.01	11.60	10.27
AVG torque variation (Nm/s)	47.94	47.75	48.31	51.12	40.64	25.66	51.19
Optimality (%)	100	99.82	99.88	99.93	98.81	96.33	89.84
Computational load per time step (ms)	-	-	1715	90	1 (+37)	1 (+37)	1

Since the LH reference solution is so close to the global optimal solution and is determined using the full preview of the exact future driving conditions, the SH control methods have to deal with only a very small amount of errors and perturbations in the LH reference solution. To investigate the performance of the SH control methods using a less perfect LH reference trajectory, the complete control method is also applied using a linear over distance depletion profile and the LH estimation solution based on rough velocity preview information as the LH reference trajectory. In Table 5.7 can be seen that fuel consumption is higher than the case where full knowledge on future conditions is available. The fuel savings are still considerable compared to the conventional heuristic case however, respectively (-5.9% and -5.5%) for the rough and linear LH reference trajectory. Unexpectedly, the MPC-based method performs significantly worse in the simulation case with the linear LH reference trajectory. Although the reason why this happened is not entirely clear, the MPC-based method followed a different local minimum SoC trajectory than the ECMS and adaptive heuristic method. This demonstrates that local control methods are not always able to correct suboptimal LH reference trajectories and the quality of the LH estimation is important for the

overall performance of the control method.

Table 5.7: Comparison of the performance of the different SH control methods using different LH reference trajectories. Displayed is the compensated fuel consumption and optimality with respect to the DP solution between brackets.

	Full DP	MPC	A-ECMS	Adaptive heuristic Unconstrained	Adaptive heuristic Constrained	Conventional heuristic Constrained
LH full preview	1525.87	1527.65 (99.88%)	1526.93 (99.93%)	1544.20 (98.81%)	1584.00 (96.33%)	1698.50 (89.84)
LH rough preview	1525.87	1535.10 (99.40%)	1543.52 (98.86%)	1555.21 (98.11%)	1597.93 (95.49%)	1698.50 (89.84)
LH linear	1525.93	1581.81 (95.95%)	1563.89 (98.41%)	1558.97 (97.57%)	1603.38 (95.10%)	1717.57 (89.84)

To investigate the influence of the length of the SH prediction horizon on the performance of the controller, a sensitivity study is performed and the results are displayed in Figure 5.11. It can be seen that a SH prediction length of 30 seconds achieves the lowest total fuel economy over the complete route. For typical predictive control strategies the optimality of the control strategy increases with longer prediction horizons, since the controller is better able to anticipate on future events. For the adaptive heuristic control method this is not the only consideration, since a longer SH interval means that the same calibration set is assigned for a longer time period. As a result, a more general calibration has to be adopted that performs well over the entire time interval, rather than multiple separate calibration sets that can be more closely optimized towards shorter SH intervals. It is believed that for this reason the performance of the control method increases with decreased short horizon lengths, however, for very short SH intervals the performance decreases again. The most probable reason for this behavior is that the reduced freedom to choose the starting point of the ICE-on phases and little anticipation to future events. The performance of the unconstrained adaptive heuristic control method was found to be relatively independent of the length of the SH interval. Since the ICE-on phases are much easier to distribute in the unconstrained case, the previous mentioned arguments are less important to this control method. In order to reduce the number of recalibration instances and distribute the computational loads of the recalibration process over a longer period of time, a prediction horizon of 60 seconds is used in this work.

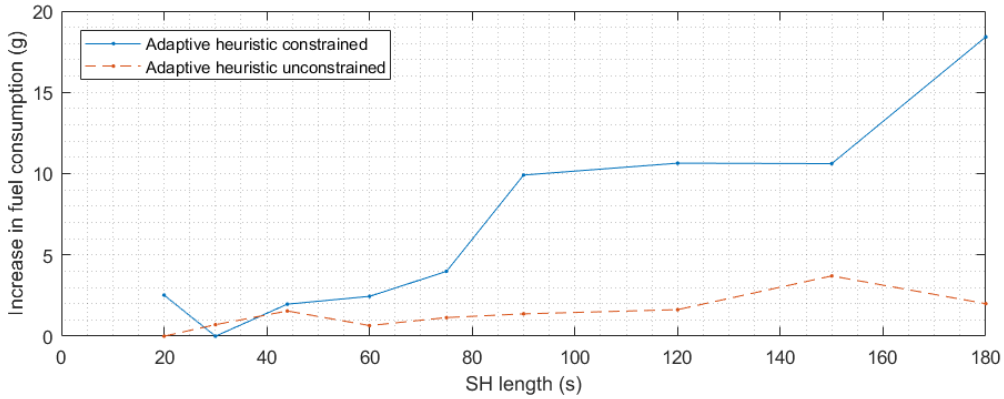

Figure 5.11: Sensitivity study for the SH length of the adaptive heuristic controller.

In order to gain a better perspective on the performance of the control method and the representativity of the results found in this work, the results are compared with results found in literature. In Appendix B different works are analyzed and the average performance of several control methods is obtained (summarized in Table 5.8). It should be noted that the variations in performance between different works are large, because the results are obtained for different simulation cases and different implementations. The validity of these average performance numbers is therefore debatable. When comparing the results from MPC, ECMS and unconstrained adaptive heuristic base on the rough LH reference trajectory (98.11-99.4%) with the average performance in literature (97.8%), it can be concluded that all three methods are able to obtain a high level of optimality. Also when using only a linear battery depletion trajectory, all three methods (95.95-98.41%) are able to obtain a high level of optimality compared to the average performance in literature (94.6%). The conventional heuristic controller (89.84%) performs slightly better than the average

heuristic controller in literature (88.4%).

Table 5.8: Overview of the average optimality of different control methods as found in literature.

Control method:	DP	SH+LH est.	SH+LH linear	ECMS fixed	Heuristic
Average optimality:	100%	97.8%	94.6%	96.5%	88.4%

5.6 Evaluation in high fidelity model

In this section, the performance of the combined control method is evaluated in the high fidelity model. The Graz drive cycle is used as the simulation case, but, due to difficulties with accurately implementing the altitude profile in the high fidelity model, the altitude profile is omitted and a flat road is used. The velocity profile in this simulation case is not prescribed to the vehicle, but tracked by a lower level control system in the CarMaker software environment that represents the behavior of a human driver model. As a result, the acceleration profile will differ (slightly) from the planned velocity profile, which introduces additional disturbances. The main goal is to assess the robustness of the combined method to prediction errors and its effectiveness when applied on a much more extensive and higher order simulation model, which is a close representation of an actual vehicle. All simulation cases are performed using the LH reference trajectory obtained with complete preview of the future conditions. Since the supervisory controller in the high fidelity model control tasks than just the instantaneous power split (e.g. controlling the clutches and rotational velocities during gearshifts and ICE startup schemes), the direct application of the A-ECMS and MPC control methods is not possible and only the adaptive heuristic control method is evaluated in the high fidelity simulation environment.

The recalibration process of the adaptive heuristic control method is solved at the start of each SH interval for the next 60 seconds using the actual vehicle states (i.e. SoC and vehicle velocity) at that point in time. Every SH interval, new values for the P_{eDRV} and T_{LPM} calibration parameters are written to the heuristic controller. A comparison of forward prediction and actual vehicle response is depicted in Figure 5.12-Figure 5.14. As described in Section 4.5.1, the first step in the heuristic control method is the selection of the driving mode, based on P_{eDRV} power threshold. For instances where the required electric power to drive electrically is higher than P_{eDRV} power threshold, the ICE is turned on. In Figure 5.12, the P_{eDRV} power threshold selected by the recalibration process is displayed, as well as a forward prediction of the required electric power and the actual required electric power from the high fidelity model. The instances where the ICE was started according to forward prediction and the actual ICE starts are also shown in figure. To improve the readability of the figure, only the interval between 1250-2250 seconds is displayed. It can be seen that for SH intervals where no use of the ICE is desired, a default value for P_{eDRV} of approximately 37 kW is chosen, or a margin of 5 kW is kept to prevent any undesired ICE starts (as introduced in Section 4.6.5). In other SH intervals where ICE-based driving is desired, the P_{eDRV} power threshold is lowered in order to trigger a start of the ICE (e.g. around 1500 sec), after which the ICE is constrained to remain on for at least 10 seconds. In the interval between 1900-2115 seconds, the P_{eDRV} threshold is lower than all power demands. As a result, the ICE is kept on during entire interval, which reduces the number of ICE starts in comparison to a strategy with a lot of short ICE-off phases. The ICE-on phases can be more easily recognized in Figure 5.13, which displays the planned and actual output torque of the EM and ICE.

Since forward predictions of the future driving conditions are not 100% correct, differences in predicted power demand and actual power demand are introduced, which can lead to the selection of an incorrect driving mode and false ICE starts. For the interval between 1250-2250 seconds, the predicted and actual ICE phases were very well aligned (except for some small delays), which demonstrates the robustness measures introduced in Section 4.6.5 were effective in preventing selections of the incorrect driving mode. An example where the ICE phases were not aligned happens during the SH interval 780-840 seconds, around time step 787 seconds. A close-up of this SH interval and the next SH interval is displayed in Figure 5.15-Figure 5.17. Here, the required electric power to drive electrically was slightly lower than the predicted electric power and therefore did not exceed the P_{eDRV} power threshold long enough (a period of

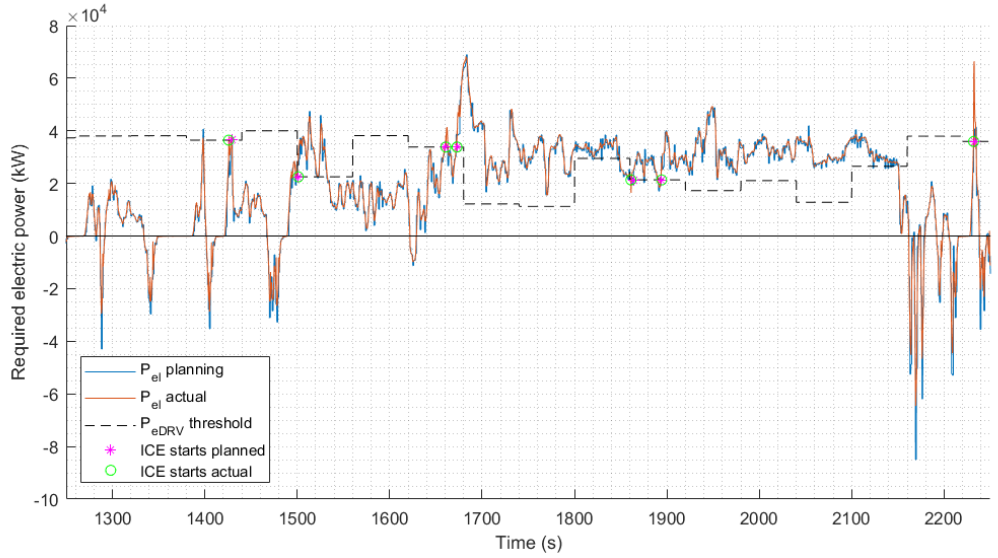

Figure 5.12: Comparison of the forward prediction of the required electric power for electric driving and the actual required electric power by the high fidelity model. Any instances above black P_{eDRV} threshold are driven with ICE on. The planned and actual ICE starts are also marked in this figure.

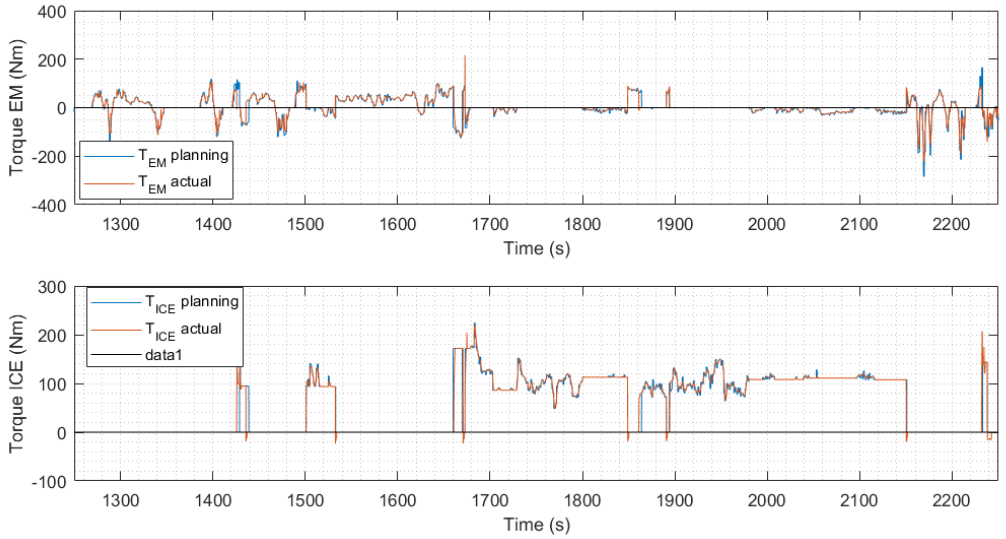

Figure 5.13: Comparison of the forward prediction of the requested EM and ICE torque and the actual torque requests by the high fidelity model.

at least 1 second is required) to trigger an ICE start, which can be seen in Figure 5.15. As a result, the ICE was not turned on (around time step 787 seconds) and the section was driven electrically instead, which can also be recognized in Figure 5.16. In the resulting SoC profile (Figure 5.17), it can be seen that in the interval 787-805 seconds, due to the missing ICE-on phase, significantly more battery SoC (approximately +1.3% SoC) was consumed than planned during the recalibration process. As a result, the final SoC at the end of the short horizon interval was outside the feasible bounds of LH strategy (the orange SoC trajectory (actual) is much lower than planned SoC trajectory (blue)). Due to receding horizon approach of the adaptive heuristic control method however, the SoC was corrected at the start of the new short horizon (at time step 840 seconds) to the actual SoC (86.8% SoC) and a new strategy was determined to converge back to the LH SoC reference profile. The original planned control policy is also displayed (in green) in Figure 5.16 and Figure 5.17 for the case where the ICE would have actually been triggered at time

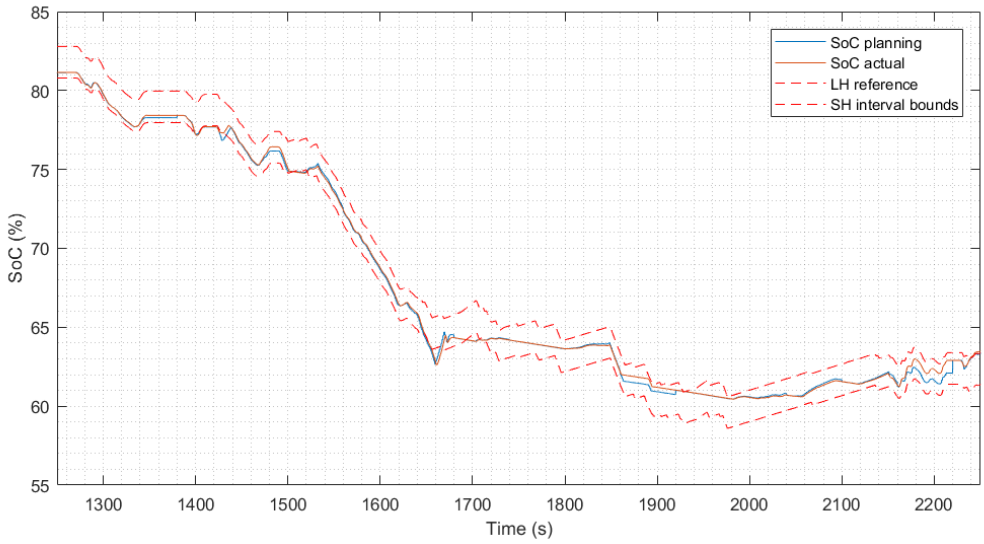

Figure 5.14: Comparison of the forward prediction of the battery SoC profile and the actual SoC profile over time from the high fidelity model.

step 787 seconds as planned. It can be seen that corrected control policies (both planned and actual), now have an additional ICE phase (between 840-850 seconds) compared to the original planned control policy, which would have used pure electric driving during this interval. Finally, Figure 5.17 demonstrates that the final SoC after this ICE phase and at the end of the second SH interval is approximately equal to the original planned control strategy. When comparing the fuel consumption over the time interval 760-920 seconds, it was found that the original and corrected trajectory consumed [13.49, 16.40] grams of fuel respectively. This illustrates that, although the trajectory was quickly back on its original trajectory, the relative costs for this mistake were quite significant (in the order of 0.2% of the total fuel consumption) and false drive mode selections should be prevented. In total, over the entire route, 3 cases occurred where an incorrect driving mode was selected.

The final results for this simulation cases are displayed in Table 5.9. Since the LH reference strategy was computed solely in the control-oriented model, the results are not directly comparable to those from the high fidelity simulation model. The performance of the adaptive heuristic control method on the other hand are directly comparable to the conventional heuristic controller. It can be seen that the adaptive heuristic control method is able to significantly reduce the fuel consumption of the vehicle by 7.3 % compared to a conventional heuristic controller, while taking all feasibility and drivability consideration of the conventional heuristic controller into account as well. Due to the better planning of the distribution of the energy in the battery, the number of ICE starts and torque variations of the ICE can be significantly reduced compared a conventional CDCS strategy. When calibrating the baseline heuristic rules of heuristic controller, one should strongly take into account the impact of the drivability constraints on the performance of the controller in terms of fuel economy. The results of an unconstrained adaptive heuristic control method indicate that additional fuel savings of over 2% are achievable for this simulation case.

Table 5.9: Results of the proposed adaptive heuristic control method compared with the conventional heuristic control method.

	LH reference	adaptive heuristic constrained	adaptive heuristic unconstrained	conventional heuristic
Final SoC (%)	15.15	15.57	14.63	17.96
Fuel consumption (gram)	1526.99	1552.93	1510.00	1697.25
Compensated FC (gram)	1525.60	1547.73	1513.39	1669.97
ICE starts (-)	97	25	74	48
Avg Time ICE on (s)	6.56	28.12	9.5	14.65
Avg torque variation (Nm/s)	40.00	18.68	32.96	58.65

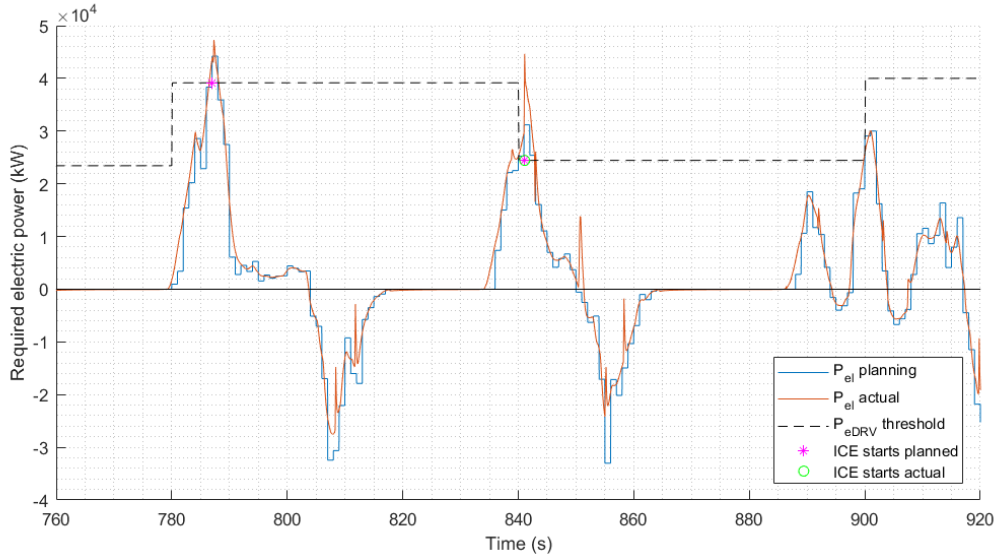

Figure 5.15: Closeup comparison of the forward prediction of the required electric power for electric driving and the actual required electric power by the high fidelity model. Due to the slightly lower power demand, the ICE is not started in the high fidelity model.

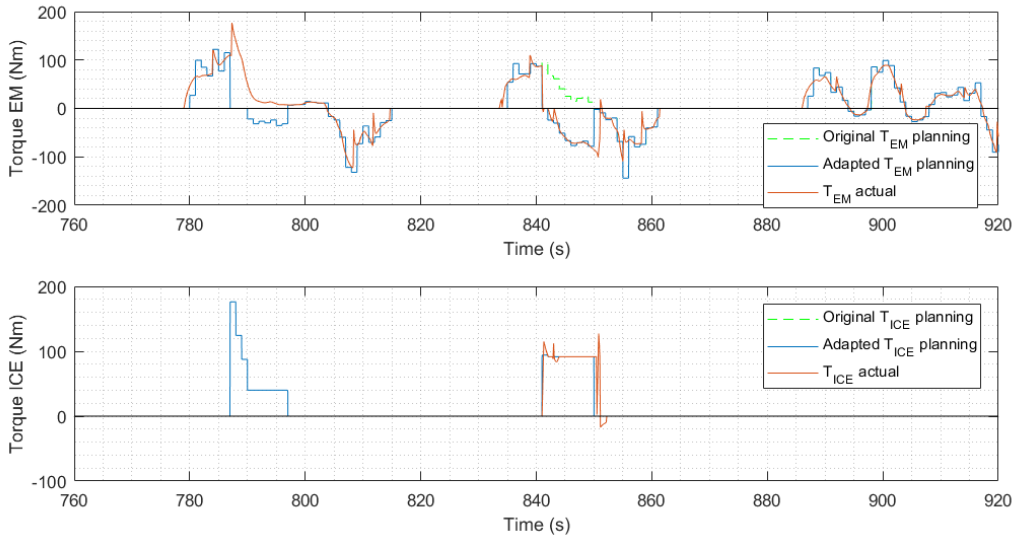

Figure 5.16: Closeup comparison of the forward prediction of the requested torque from the EM and ICE and the actual torque requests by the high fidelity model. Since the high fidelity model misses the ICE-phase around 790 seconds, it makes use of a substitutive ICE-phase around 850 seconds to correct its mistake.

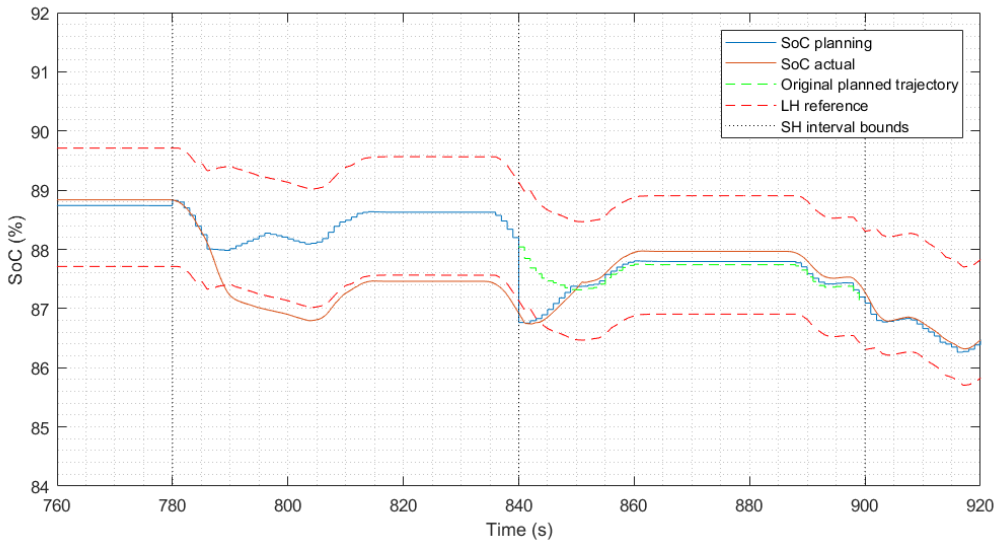

Figure 5.17: Closeup comparison of the forward prediction of the battery SoC profile and the actual SoC profile over time from the high fidelity model. Due to an incorrect drive mode selection in the 780-840 seconds SH interval, the strategy is corrected to converge back to the SoC reference in the succeeding SH interval.

6

Conclusion and recommendations

This chapter presents the conclusions drawn from this research and gives recommendations for future work. In Section 6.1 the proposed methods are described and the conclusions based on the simulation results are presented. In Section 6.3 recommendation for future work are discussed.

6.1 General conclusions

The growing worldwide fleet of vehicles and the resulting impact on the environment raises many concerns in today's society and automotive industry. PHEVs are believed to be a promising vehicle concept that can offer significant improvement of the overall vehicle efficiency compared to conventional combustion vehicles. However, the fuel consumption of a PHEV depends strongly on the supervisory control strategy that coordinates the hybrid powertrain and can be further improved by the use of predictive control methods with knowledge of future driving conditions.

The main aim of research into supervisory control systems for PHEVs is to improve the efficiency of an existing PHEV by developing more intelligent control strategies, rather than by the use of better powertrain components. Although predictive supervisory controllers have been relatively well established in literature, the necessary conditions for feasibility and implementation in real-life applications are often ignored or underestimated. The main aim of this work and its main contribution is to to develop and implement a predictive optimal control strategy for PHEVs that can minimize the fuel consumption, while taking into account necessary conditions for feasibility and implementation in real-life applications. More specifically, in this work the number of ICE starts, the variations in ICE torque and the update frequency the control method are considered.

In the proposed control method, the optimal control problem is simplified to an uni-directional problem, which allows the problem to be split into two main tasks that can be solved sequentially by dedicated solvers. This two-stage architecture that cooperatively controls the hybrid powertrain operates on two levels: The first level is the global energy management control, which determines the optimal battery depletion strategy over the complete route. To accomplish this, a power-based clustering method is applied, which is able to take into account all three levels of contribution. The second level is the local power management control, which determines the optimal driving mode and power split over the local range. For this objective, a novel adaptive heuristic based control method is proposed that is able to track a global reference trajectory and take into account all feasibility conditions. A conventional heuristic controller is the basis of this method for the direct control application, of which the calibration is adapted based on upcoming driving conditions over a short preview horizon. The proposed method offers close to optimal results, while having extremely low computational demands for its direct control logic that allows for high update frequencies of the control actions. Besides that, the control method makes it possible to include feasibility and drivability considerations in its control strategy.

The proposed control method was fine tuned on a P2 parallel PHEV model based on a VW Jetta HEV, and its effectiveness was evaluated in a high fidelity simulation environment on a representative drive cycle. Results indicate that the route-preview based control strategies can obtain substantial improvements in fuel economy of the PHEV of up to 7.3% relative to a non-predictive heuristic control strategy. The proposed control method can achieve a fuel economy within 1.19-2.43% of the global optimal solution, depending on the level of knowledge on the future driving conditions. The performance of the control method is slightly lower than that of a MPC-based and A-ECMS-based method.

Simulations also show that the direct application of optimization based control methods often lead to infeasible and undesirable control policies. The proposed control method offers the possibility to take feasibility constraints into account without additional computational loads. In its constrained form, the proposed control method is able to reduce the number of ICE starts and the level of ICE torque variation by respectively 45.4% and 46.6% compared to the MPC and ECMS control methods, but at the cost of 3.6% of increased fuel consumption. In addition, the proposed SH control method introduces closed loop control, which is able to track a LH reference trajectory. As a result, the method is better able to adapt to different drive cycles and conditions than control strategies that rely on a predetermine balance for the use of electric energy, like conventional heuristic control and ECMS control without preview. Also, since the method has the ability to deal with hard constraints, its robustness for local control is higher than error-based reference tracking, like A-ECMS.

Although the implementation of the proposed adaptive heuristic control method is specifically set up for a P2 parallel HEV topology, the principle of the proposed method is applicable to any type of HEV. In a broader sense, the principle of adaptive heuristic control could be applied to any system that applies heuristic control and has access to predictive information on future control requests.

6.2 Discussion

The adaptive heuristic control method proposed in this work is able to include feasibility and drivability considerations in its control strategy. In its unconstrained form, the other implemented control methods can be used to make an extensive evaluation of the performance of the developed method. Based on these results, it is assumed that the optimization process of the adaptive heuristic control method behaves in a similar way for the constrained optimization process and similar levels of performance can be obtained. For the constrained form of the control method however, there is little reference material to extensively evaluate the performance of the proposed method. To allow for a more thorough analysis, other methods should be investigated that can include drivability constraints in their control strategy. Next to that, it is not clear what the exact definition of an acceptable level of drivability is. Although drivability is a very subjective rating, the overall performance of the control method in terms of fuel economy strongly depends on the included level of drivability constraints and a good understanding of the acceptable limit required to obtain the highest fuel economy of the vehicle.

This work includes a number of measures to increase the robustness of the selected calibration set. Since the impact of incorrectly selected driving modes on the overall fuel economy of the vehicle is significant, these robustness measures should be investigated in more detail. In a more advance recalibration process, the system would have to make better assessments of the risks and consequences of incorrect control decisions and select a calibration set that is better in line with potential losses. For example, during a interval where no use of the ICE is planned, a more advanced system would still have to determine a suitable T_{LPM} value for the scenario incorrect control decisions are made.

In this work, it is assumed the supervisory control system has access to information on the future driving conditions determined by a predictive information system. The implementation of such a system is however a challenging task, especially since the performance of the supervisory control system can greatly benefit from more accurate predictions of the future power demand. Although the robustness of the control method to prediction uncertainties is included in this work, there are additional error sources (such as the vehicle parameters and large disturbances in the velocity profile) that need to be explored in further

detail in more demanding simulation cases.

6.3 Recommendations for future work

Some aspects of this work can be improved and new features can be added to extend the functionality of the proposed control method. In this section the most relevant points for future research are described.

6.3.1 More states and dependencies

In this work the only powertrain state that is considered is the battery SoC, however, more states that can benefit from LH state trajectory planning could be taken into account. States with relatively slow dynamics would be of most interest for this application and in particular states that could potentially limit the freedom of future control actions or significantly change their characteristics. The temperature of the electric powertrain components is a good example of these states, since they can potentially have large impacts on the future control strategies of the supervisory controller (e.g. an overheating EM can limit the control actions or a warm battery can reduce the efficiency of the component) [9, 22]. Planning the LH state trajectories to avoid any powertrain limitations can therefore have large benefits on the fuel consumption of the vehicle over the complete trip. The relevance to passenger vehicles, however, might be limited, since typically the cooling systems of these components prevent extreme operating conditions [24, 26]. Also warmed-up conditions for the operation of the ICE were assumed in this work. In practice however, the use of the ICE is significantly constrained under cold conditions, due to different emission characteristics and effectiveness of the catalyst [9]. When keeping the ICE warm-up phase in mind, it might be beneficial to favor ICE-based driving in the early stages of the trip in order to reach the warmed-up conditions earlier.

6.3.2 Integration with high level controller

In the most research and current vehicles, the high level planning of the velocity and trajectory of the vehicle and the control of the powertrain are two separated systems. The high level control only takes very simplified consideration of the powertrain control into account (e.g. reduced accelerations to save fuel) and the powertrain control takes the results of the high level controller as an input, rather than as a variable (e.g. the velocity trajectory). A more interactive operation of these two control systems can potentially significantly improve the overall performance of the vehicle on both levels. As an example, the powertrain controller could propose an adaptation of the deceleration trajectory from the high level controller in order to increase the amount of recuperated energy, or the acceleration trajectory could be modified such that an undesired ICE start is prevented.

6.3.3 Application in practice

The proposed predictive control method in this work strongly relies on the fact that (reasonable) accurate predictions of the future power demands can be made. In a software environment, these predictions can be made with relative ease, but the prediction making in practice is more difficult. First of all, as already mentioned in Section 4.2, the prediction of the future driving conditions is a difficult task and the predictions are strongly subjected to change and uncertainty. A supervisory control strategy for application in practice should be robust enough to deal with all these uncertainties and be able to rethink its strategy to recover from unexpected events. Even if the future driving conditions are well known, the future power demands are not directly available. For this step good vehicle models and accurate estimations of the vehicle parameters are required. Especially the parameter estimation can have a big impact on the quality of the predictions, since parameters can continuously change over trips due to e.g. road conditions, net mass of the car, vehicle maintenance, etc. Some works in literature therefore propose that online recursive parameter estimation is a good solution to obtain accurate estimations of the parameters [64].

6.3.4 Improvements of implementation

It was shown that the performance of the LH estimation method is already close to the global optimal DP strategy. There is still room for improvement in the clustering process however, since any performance losses of the LH estimation method are mainly the result of an incorrect cluster assigning process. First of all, it could be possible to implement more processes (like the checks that prevent the loss of recuperation potential, Section 4.4.5) that evaluate whether instances are actually assigned to the correct cluster, or whether it makes more sense to change the cluster based on certain criteria. Another problem with the implemented clustering process is that the linear cluster distribution leads to an unequal distribution of the number of instances over the clusters and, as a result, the influence factor of the instances on the overall strategy varies. More sophisticated clustering techniques, could be applied that could benefit the optimality of the final SoC reference.

Although the proposed intelligent search method for the recalibration process in the SH controller is capable of successfully solving the optimization problem with multiple local minima using the PSO optimization, the entire process might be overly complex for the problem that actually needs to be solved. It is believed that, with more a priori understanding of the optimization problem and the shape of the feasible domain, it should be possible to come up with a less complex solving technique that can handle this problem.

Increasing the complexity of the recalibration process has the potential to increase the performance of the control method. For example, adopting more complex versions of the current calibration maps (e.g. ramp functions or step functions) or implementing additional maps could potentially solve this problem and apply calibration sets that lead to control strategies closer to the global optimal strategy. Ther is also the opportunity to improve the level of drivability using the predictive information of future driving conditions and power demands. An example of this is that short ICE-off phases could be recognized and subsequently prevented by the supervisory controller to improve the drivability of the HEV. The heuristic controller would in this case require an additional heuristic rule that does not permit the ICE to be turned off based on the states of the vehicle (e.g. SoC or velocity), which also has to be present as one of the variables in the recalibration process.

Bibliography

[1] S. Onori, L. Serrao, and G. Rizzoni, *Hybrid electric vehicles: Energy management strategies* (Springer, 2016).

[2] A. A. Pesaran, *Choices and Requirements of Batteries for EVs, HEVs, PHEVs*, Tech. Rep. (National Renewable Energy Laboratory (NREL), Golden, CO., 2011).

[3] International Energy Agency (IEA), *Technology roadmap: Electric and plug-in hybrid electric vehicles,* International Energy Agency, Tech. Rep , 52 (2011).

[4] International Organization of Motor Vehicle Manufacturers, *World Vehicles in use*, Tech. Rep. (2017).

[5] J. T. Houghton, Y. Ding, D. J. Griggs, M. Noguer, P. J. van der Linden, X. Dai, K. Maskell, and C. A. Johnson, *Climate change 2001: the scientific basis* (The Press Syndicate of the University of Cambridge, 2001).

[6] European Commission, *EU Transport in figures - Statistical Pocketbook 2016* (European Commission, 2016) pp. 1–151.

[7] P. Mock, *EU CO2 standards for passenger cars and light-commercial vehicles,* International Council on Clean Transportation , 1 (2014).

[8] E. C. (EU), *Reducing CO2 emissions from passenger cars,* https://ec.europa.eu/clima/policies/transport/vehicles/cars_en (2018), [Accessed 2018-02-10].

[9] M. Ehsani, Y. Gao, and A. Emadi, *Modern electric, hybrid electric, and fuel cell vehicles: fundamentals, theory, and design* (CRC press, 2009).

[10] Greengear, *List of available PHEV models for German market,* https://www.greengear.de/vergleich-plug-in-hybrid-autos-phev/ (2017), [Accessed 2017-09-04].

[11] C. C. Chan, *The state of the art of electric, hybrid, and fuel cell vehicles,* Proceedings of the IEEE **95**, 704 (2007).

[12] C. Mi, M. A. Masrur, and D. W. Gao, *Hybrid electric vehicles: principles and applications with practical perspectives* (John Wiley & Sons, 2011).

[13] G. Pistoia, *Electric and hybrid vehicles: Power sources, models, sustainability, infrastructure and the market* (Elsevier, 2010).

[14] R. N. Neumann, J. Bavendiek, and L. Eckstein, *Strategic optimization of powertrain technology portfolios by means of market simulation,* Institute for Automotive Engineering, Aachen , 1 (2017).

[15] B. M. Al-Alawi and T. H. Bradley, *Review of hybrid, plug-in hybrid, and electric vehicle market modeling Studies,* (2013).

[16] C. Thiel, A. Perujo, and A. Mercier, *Cost and CO 2 aspects of future vehicle options in Europe under new energy policy scenarios,* Energy policy **38**, 7142 (2010).

[17] L. Guzzella and A. Sciarretta, *Vehicle Propulsion Systems - Introduction to Modeling and Optimization* (Springer, 2007) p. 350.

[18] A. Sciarretta and L. Guzzella, *Control of hybrid electric vehicles,* IEEE Control Systems **27**, 60 (2007).

[19] M. Vajedi, A. Taghavipour, N. L. Azad, and J. Mcphee, *A comparative analysis of route-based power management strategies for real-time application in plug-in hybrid electric vehicles,* in *American Control Conference (ACC)* (IEEE, 2014) pp. 2612–2617.

[20] C. Sun, S. J. Moura, X. Hu, J. K. Hedrick, and F. Sun, *Dynamic Traffic Feedback Data Enabled Energy Management in Plug-in Hybrid Electric Vehicles,* IEEE Transactions on Control Systems Technology **23**, 1075 (2015).

[21] A. Sciarretta, L. Serrao, P. C. Dewangan, P. Tona, E. N. Bergshoeff, C. Bordons, L. Charmpa, P. Elbert, L. Eriksson, T. Hofman, M. Hubacher, P. Isenegger, F. Lacandia, A. Laveau, H. Li, D. Marcos, T. Nüesch, S. Onori, P. Pisu, J. Rios, E. Silvas, M. Sivertsson, L. Tribioli, A. J. van der Hoeven, and M. Wu, *A control benchmark on the energy management of a plug-in hybrid electric vehicle,* Control Engineering Practice **29**, 287 (2014).

[22] C. M. Martinez, X. Hu, D. Cao, E. Velenis, B. Gao, and M. Wellers, *Energy Management in Plug-in Hybrid Electric Vehicles: Recent Progress and a Connected Vehicles Perspective,* IEEE Transactions on Vehicular Technology **66**, 4534 (2017).

[23] D. Shen, V. Bensch, and S. Müller, *Model predictive energy management for a range extender hybrid vehicle using map information,* IFAC-PapersOnLine **28**, 263 (2015).

[24] D. Ambuhl and L. Guzzella, *Predictive Reference Signal Generator for Hybrid Electric Vehicles,* IEEE Transactions on Vehicular Technology **58**, 4730 (2009).

[25] F. Tianheng, Y. Lin, G. Qing, H. Yanqing, Y. Ting, and Y. Bin, *A supervisory control strategy for plug-in hybrid electric vehicles based on energy demand prediction and route preview,* IEEE Transactions on Vehicular Technology **64**, 1691 (2015).

[26] G. Heppeler, M. Sonntag, U. Wohlhaupter, and O. Sawodny, *Predictive planning of optimal velocity and state of charge trajectories for hybrid electric vehicles,* Control Engineering Practice **61**, 229 (2017).

[27] D. Goerke, M. Bargende, U. Keller, N. Ruzicka, and S. Schmiedler, *Optimal Control based Calibration of Rule-Based Energy Management for Parallel Hybrid Electric Vehicles,* SAE International Journal of Alternative Powertrains **4**, 2015 (2015).

[28] K. Govindswamy, T. Wellmann, and G. Eisele, *Aspects of NVH Integration in Hybrid Vehicles (2009-01-2085),* SAE Paper , 1 (2009).

[29] B. Škugor, V. Ranogajec, and J. Deur, *On Smoothing HEV / EREV Supervisory Control Action Using an Extended ECMS Approach,* EVS27 International Battery, Hybrid and Fuel Cell Electric Vehicle Symposium (2013).

[30] A. Taghavipour, M. Vajedi, N. L. Azad, and J. McPhee, *Predictive Power Management Strategy for a PHEV Based on Different Levels of Trip Information,* IFAC Proceedings Volumes **45**, 326 (2012).

[31] Y. Huang, H. Wang, A. Khajepour, H. He, and J. Ji, *Model predictive control power management strategies for HEVs: A review,* (2017).

[32] C. Zhang, A. Vahidi, X. Li, and D. Essenmacher, *Role of Trip Information Preview in Fuel Economy of Plug-in Hybrid Vehicles,* Proceedings of the ASME 2009 Dynamic Systems and Control Conference , 1 (2009).

[33] T. van Keulen, B. de Jager, A. Serrarens, and M. Steinbuch, *Optimal Energy Management in Hybrid Electric Trucks Using Route Information,* Oil & Gas Science and Technology - Revue de l'Institut Français du Pétrole **65**, 103 (2010).

[34] G. Heppeler, M. Sonntag, and O. Sawodny, *Predictive planning of the battery state of charge trajectory for hybrid-electric passenger cars,* in *Internationales Stuttgarter Symposium* (2015) pp. 525–538.

[35] Q. Gong, Y. Li, and Z. Peng, *Trip-Based Optimal Power Management of Plug-in Hybrid Electric Vehicles,* IEEE TRANSACTIONS ON VEHICULAR TECHNOLOGY **57**, 3393 (2008).

[36] A. A. Malikopoulos, *Supervisory power management control algorithms for hybrid electric vehicles: A survey,* IEEE Transactions on Intelligent Transportation Systems **15**, 1869 (2014).

[37] H. Borhan, A. Vahidi, A. M. Phillips, M. L. Kuang, I. V. Kolmanovsky, and S. Di Cairano, *MPC-based energy management of a power-split hybrid electric vehicle,* IEEE Transactions on Control Systems Technology **20**, 593 (2012).

[38] D. P. Bertsekas, D. P. Bertsekas, D. P. Bertsekas, and D. P. Bertsekas, *Dynamic programming and optimal control*, Vol. 1 (Athena scientific Belmont, MA, 1995).

[39] A. Sciarretta, M. Back, and L. Guzzella, *Optimal control of parallel hybrid electric vehicles,* IEEE Transactions on Control Systems Technology **12**, 352 (2004).

[40] M. Vajedi, M. Chehrehsaz, and N. L. Azad, *Intelligent power management of plug-in hybrid electric vehicles, part II: real-time route based power management,* International Journal of Electric and Hybrid Vehicles **6**, 46 (2014).

[41] L. del Re, F. Allgöwer, L. Glielmo, C. Guardiola, and I. Kolmanovsky, *Automotive Model Predictive Control*, Vol. 402 (2010).

[42] E. F. Camacho and C. Bordons, *Model Predictive control* (Springer, 2007) p. 405.

[43] C. Kirches, *Saudi Med J*, Vol. 33 (2011) pp. 3–8.

[44] G. Pasaoglu, D. Fiorello, A. Martino, G. Scarcella, A. Alemanno, A. Zubaryeva, and C. Thiel, *Driving and parking patterns of European car drivers - a mobility survey* (2012) p. 112.

[45] P. Plötz, N. Jakobsson, and F. Sprei, *On the distribution of individual daily driving distances,* Transportation Research Part B: Methodological **101**, 213 (2017).

[46] C. Hou, H. Wang, and M. Ouyang, *IFAC Proceedings Volumes (IFAC-PapersOnline)*, Vol. 7 (IFAC, 2013) pp. 35–40.

[47] M. Vajedi, M. Chehrehsaz, and N. L. Azad, *Intelligent power management of plug-in hybrid electric vehicles, part I: real-time optimum SOC trajectory builder,* International Journal of Electric and Hybrid Vehicles **6**, 46 (2014).

[48] C. Zhang, A. Vahidi, P. Pisu, L. Xiaopeng, and K. Tennant, *Role of Terrain Preview in Energy Management of Hybrid Electric Vehicles,* Vehicular Technology, IEEE Transactions on **59**, 1139 (2010).

[49] J. Hedrick, *Vehicle Modeling and Control For Automated Highway Systems,* California PATH Research Report (1993).

[50] A. B. Nkoro and Y. A. Vershinin, *Current and future trends in applications of Intelligent Transport Systems on cars and infrastructure,* 2014 17th IEEE International Conference on Intelligent Transportation Systems, ITSC 2014 , 514 (2014).

[51] P. Stewart and P. J. Fleming, *Drive-by-wire control of automotive driveline oscillations by response surface methodology,* IEEE Transactions on Control Systems Technology **12**, 737 (2004).

[52] X. Wei, *Modeling and Control of a Hybrid Electric Drivetrain for Optimum Fuel Economy, Performance and Driveability*, Ph.D. thesis (2004).

[53] S. Jones, E. Armengaud, H. Böhm, C. Cheng, G. Griessnig, A. Huss, E. Kural, and M. Nica, *Safety Simulation in the Concept Phase: Advanced Co-simulation Toolchain for Conventional, Hybrid and Fully Electric Vehicles,* Lecture Notes in Mobility (2014).

[54] S. Jones, E. Kural, K. Knödler, J. Steinmann, S. Jones, Á. E. Kural, E. Kural, K. Knödler, Á. J. Steinmann, and J. Steinmann, *Optimal Energy Efficiency, Vehicle Stability and Safety on the OpEneR EV with Electrified Front and Rear Axles,* Lecture Notes in Mobility (2013).

[55] SAE, *Stepwise Coastdown Methodology for Measuring Tire Rolling Resistance*, Tech. Rep. (1999).

[56] O. Sundstrom and L. Guzzella, *A generic dynamic programming Matlab function,* in *2009 IEEE International Conference on Control Applications* (IEEE, 2009) pp. 1625–1630.

[57] Mathworks, *fmincon documentation,* https://nl.mathworks.com/help/optim/ug/fmincon.html (2018), [Accessed 2018-02-02].

[58] M. Clerc, *Particle swarm optimization*, Vol. 93 (John Wiley & Sons, 2010).

[59] P. J. Angeline, *Evolutionary optimization versus particle swarm optimization: Philosophy and performance differences,* Lecture Notes in Computer Science: Evolutionary Programming VII **1447**, 601 (1998).

[60] Z. Chen, R. Xiong, and J. Cao, *Particle swarm optimization-based optimal power management of plug-in hybrid electric vehicles considering uncertain driving conditions,* (2016), 10.1016/j.energy.2015.12.071.

[61] Mathworks, *Particle swarm documentation,* https://nl.mathworks.com/help/gads/particle-swarm.html (2018), [Accessed 2018-02-02].

[62] K. McAleer, *Rde - development process & tools*, Tech. Rep. (AVL, 2015).

[63] Wikipedia, *Ftp-75 drive cycle,* https://en.wikipedia.org/wiki/FTP-75, year = 2018, note = [Accessed 2018-02-11], urldate = 2018-02-11,.

[64] A. Vahidi, A. Stefanopoulou, and H. Peng, *Recursive least squares with forgetting for online estimation of vehicle mass and road grade: theory and experiments,* Vehicle System Dynamics **43**, 31 (2005).

[65] E. D. Tate, M. O. Harpster, and P. J. Savagian, *The Electrification of the Automobile: From Conventional Hybrid, to Plug-in Hybrids, to Extended-Range Electric Vehicles,* SAE Int. J. Passeng. Cars - Electron. Electr. Syst. **1**, 156 (2008).

[66] Wikipedia, *BMW i3,* https://en.wikipedia.org/wiki/BMW_i3 (2017), [Accessed 2017-09-05].

[67] M. F. M. Sabri, K. A. Danapalasingam, and M. F. Rahmat, *A review on hybrid electric vehicles architecture and energy management strategies,* Renewable and Sustainable Energy Reviews **53**, 1433 (2016).

[68] S. S. Williamson, *Energy Management Strategies for Electric and Plug-in Hybrid Electric Vehicles* (Springer, 2013).

[69] M. Ehsani, G. Yimin, and J. M. Miller, *Hybrid Electric Vehicles: Architecture and Motor Drives,* Proceedings of the IEEE **95**, 719 (2007).

[70] C. Zhang and A. Vahidi, *Route preview in energy management of plug-in hybrid vehicles,* IEEE Transactions on Control Systems Technology **20**, 546 (2012).

A

Appendix

A HEV is a vehicle that uses a combination of an electric and IC powertrain to propel the vehicle. It is important the reader is aware of the key characteristics of these individual powertrains, discussed in Appendix A.1, and how these two powertrains can be combined to form a more superior hybrid powertrain. The combination of these two powertrains can offer very promising advantages over a conventional combustion powertrain, which are described in Appendix A.2. HEVs exist in different forms, topologies and levels of hybridization, which will be introduced in Appendix A.3 and Appendix A.4). Finally, in Appendix A.5, a generalization towards a control strategy of a P2 parallel HEV is described.

A.1 Key characteristics individual powertrains

The electric powertrain consists of a high voltage battery for energy storage and makes use of an electric motor as the power source to convert the electric energy from the battery into mechanical power. Technically the direct current (DC) output of the battery is first transformed by an inverter to an alternating current (AC), but often in simulation purposes the inverter and electric motor are combined in a single system called the electric machine (EM) that has the combined characteristics (in terms of dynamics, losses, etc) of the two subcomponents. Since electricity is the energy source in this powertrain, the powertrain is completely emission free during operation. The electric powertrain is characterized by its relatively high efficiency over a broad speed range (typically 80-90%), as well as its ability to deliver its maximum torque from zero speed (see Figure A.1a where the efficiency map of the EM used in this work is displayed). Also the electric powertrain allows a bidirectional power flow, which makes it possible to (re)generate electric energy by applying negative torque with the electric motor. The downside of the electric powertrain is the relatively low energy density of the energy storage and therefore, due to practical constraints, the amount of electric energy that is available in the vehicle is limited (and thus the all-electric range of the HEV) [11–13]. Also the continuous charging power is relatively low, which means the empty-full charge time is long compared to the refueling of conventional vehicles (typically in the order of hours) [11, 12].

The IC powertrain in HEVs uses hydrocarbon fuels (mostly petroleum-derived fuels like diesel or gasoline) as the energy carrier and consists of a internal combustion engine (ICE) to convert the chemical energy from the fuel into mechanical power. The IC powertrain has conventionally been used as the only power source in nearly all vehicle applications because of its high energy density of the fuel and the high power to weight ratio of the ICE. The IC powertrain is however characterized by a relatively low average efficiency (typically 20-35%), which also varies strongly over load and operating speed (see Figure A.1b where the efficiency map of the ICE used in this work is displayed). The operating points at each operating speed where the ICE efficiency is the highest can be distinguish and is referred to as the optimal operating line (the red line in Figure A.1b). Since the ICE is not able to generate torque under its idle speed and its efficiency is especially poor under low load conditions, the IC powertrain is in almost all vehicle applications supported by a multi-ratio transmission system and a clutch. It is also worth noticing that the IC powertrain still consumes fuel when it is temporarily not used but not completely shut off (running idle) and startup times take a significant amount of time. Also, the combustion of fuel under high temperatures and

pressures emits harmful exhaust emissions (such as CO_2, but also byproducts like nitrogen oxides, sulfur oxides and particular matter) during operation [9]. Finally, the dynamics of the IC powertrain are relatively slow (in particular turbocharged engines), which leads to the fact that in practice the response time to setpoint changes has to be taken into account [17].

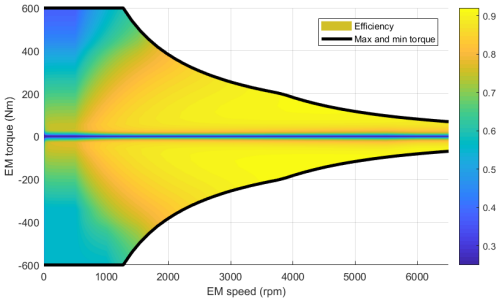

(a) Efficiency of the EM over torque and speed. The black curves indicate the maximal output torque of the EM.

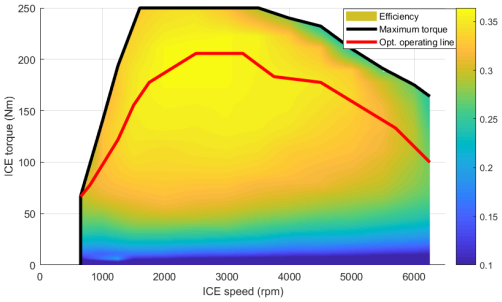

(b) Efficiency of the ICE over torque and speed. The black curve indicates the maximal output torque of the ICE. The red curve indicates the maximal efficiency of the ICE at each operating speed.

Figure A.1: Efficiency maps of the EM and ICE.

A.2 Main advantages

The hybrid powertrain of HEVs offers a couple of advantages over conventional combustion vehicles that can significantly increase the overall efficiency of the vehicle and reduce the amount of harmful emissions [1, 17, 18].

First of all, the electric powertrain provides the possibility to operate the vehicle in pure electric mode. This offers a higher operating efficiency under most conditions than conventional ICE powertrains and especially under low load conditions. Also the pure electric driving mode offers zero emission operation that completely prevents harmful emissions during its use, which is particularly beneficial in urban areas. Since urban areas are also characterized by stop and go traffic and frequent low load operation of the vehicles, the pure electric driving mode is particularly well suited for urban driving [1, 17, 18].

The second main advantage of the hybrid powertrain is that the electric powertrain has the possibility to operate electric motor(s) as generator(s), which makes it possible to regenerate braking energy that was otherwise dissipated in mechanical brakes. The recuperation of energy increases the available electric energy stored in the battery and since this amount was initially limited, recuperation of energy can increase the all-electric range of a HEV significantly [1, 17, 18].

Thirdly, another main advantage of the hybrid powertrain lies in the fact that the combination of both powertrains enables more efficient operation of the IC powertrain than a conventional pure ICE system. Traditionally the ICE power output is sized towards its maximum power demand under acceleration. This demand is however higher than the steady-state power demand typically found during cruising, which means the ICE has to operate under relatively low loads during cruising and therefore only moderate efficiencies can be achieved. A hybrid powertrain with two power sources makes it possible to reduce the power output requirement of the ICE, and therefore enables the use of a smaller (less powerful) ICE. Since the operating conditions of the ICE during cruising are now closer to the optimal operating line, the overall efficiency of the ICE under cruising is increased with a hybrid powertrain [1, 17, 18]. In the case of a parallel topology (more on this in Appendix A.4 on hybrid topologies), the reduction of the ICE size is possible because the electric powertrain can be used to support the IC powertrain (eBoost) during phases of high power demand and cover part of the total power demand. In the case of a series topology, this

is the case because the IC powertrain is only used as a generator for electric energy, but not to directly propel the vehicle. This allows the IC powertrain to be sized more towards the average power demand found during cruising rather than the peak power demand found under acceleration.

Finally, fourth main advantage of the hybrid powertrain can be found in the possibility to apply LPM strategies [1, 12, 18]. Under this term control strategies are grouped where the torque and/or speed operating conditions of the ICE are modified in order to move the operating point to a different area of the torque map than the original operating area. In these cases the EM is operated such that it compensates the change in torque and/or speed of the ICE. In most cases, the intent of these LPM strategies is to operate the ICE in a more efficient area than the original conditions. These LPM strategies can benefit the overall efficiency of the complete powertrain if the efficiency gained in the ICE outweigh the losses in the energy conversion process from electrical to mechanical power and vice versa. Alternatively, rather than focusing mainly on increasing the operation efficiency of the ICE, the main intent of the load point moving strategies can also be to either charge or discharge the battery to a certain desired level that is more beneficial for the remaining of the trip (e.g. to make sure enough electric energy is available for all-electric driving later in the trip). In these cases there exists a power difference between the supplied power by the ICE and the actual demanded power by the vehicle, which is subsequently used by the electric powertrain to either charge or discharge the battery.

A.3 Different types of hybrid vehicles

Automotive manufacturers have developed many different types of hybrid electric vehicles over the years. HEVs can be classified in different categories based on level of hybrid functionality and their maximum electric power output. The following classes are defined, where the typical specifications are gathered from the sources [1, 9, 11, 13, 65]:

- **Micro Hybrid Electric Vehicle:** The lowest form of the HEV, the electric motor typically operates at 12 Volt with a low power output of 2.5 kW. The only hybrid functionality the micro hybrid adds is the closer integration of the starter motor of the ICE in the powertrain, which enables the electric motor to be used as a generator to regenerate energy and restore the energy in the low voltage battery. This type of HEV does not have any hybrid propulsion modes however and the main increase in fuel economy results from the ICE being turned off more often. An example of a micro HEV is the VW Polo Bluemotion.
- **Mild Hybrid Electric Vehicle:** In this form, the electric motor typically has a power output of 10-20 kW. The topology is similar to the micro hybrid and also features recuperation of braking energy, but in the mild hybrid the electric motor is, in contrast to the micro hybrid, also able to provide electric propulsion power during acceleration to support the ICE (often referred to as eBoost). The full electric driving mode is however not possible in this type of HEV. An example of a mild HEV is the Suzuki Baleno SHVS.
- **Full Hybrid Electric Vehicle:** In this form, the electric motor typically has a power output of 20-40 kW and a battery capacity of 1-2 kWh. This type of HEV operates using a high voltage system of 200-600 Volt. The full hybrid can make use of all the driving modes a hybrid powertrain has to offer, including pure electric driving. The size of the battery and maximum power output of the electric motor are limited however, which leads to a short all-electric driving range (typically 2 km of city driving) and limited conditions under which the electric driving mode is possible (i.e. only city driving). Since conventional fuel is the only energy source in this type of HEV, in the end all electric energy also comes from the fuel, either through direct generation or indirectly via recuperation of braking energy. An example of a full HEV is the Lexus RX450H.
- **Plug-in Hybrid Electric Vehicle (PHEV):** The most common form of the HEV currently on the market, the electric motor typically has a power output of at least 50 kW and a battery capacity of 7-12 kWh. This type of HEV has the possibility to recharge the battery from the power grid which means the vehicle is truly emission-free during electric operation and potentially CO_2 neutral if renewable energy sources are used to charge the battery. The PHEV has a large all-electric range (typically over 40 km) and is able to drive electrically in most conditions (e.g. city and highway driving). The plug-in

hybrid powertrain can truly benefit from all the advantages of a hybrid powertrain. An example of a PHEV is the Mitsubishi Outlander PHEV.

- **Range Extender Electric Vehicle (range extender electric vehicle (REEV)):** The REEV concept is actually a pure Battery Electric Vehicle (BEV) with an additional small auxiliary power unit to extent the range. This concept is a very different concept from the other HEV types, because its ICE cannot directly propel the vehicle. In principle, the auxiliary power unit does not necessarily have to be a ICE, but could also be a different kind of power source, like a hydrogen fuel cell. Currently (mid 2017), only one REEV is available on the market, which is the BMW i3 Range Extender [66]. The BMW i3 Range Extender has very different specifications from the typical PHEV models with an electric power output of 125 kW, an ICE with a power output of only 28 kW and a battery capacity of 33 kWh, which provides an all-electric driving range of 200-300 km.

- **Battery Electric Vehicle (BEV):** For the completeness of this overview, also the BEV vehicle concept is included. A BEV has only the battery as its energy storage and also only the electric motor(s) as its power source. The driving range of BEVs can be over 500 km, but varies strongly per brand and model. An example of a BEV is the Tesla Model S.

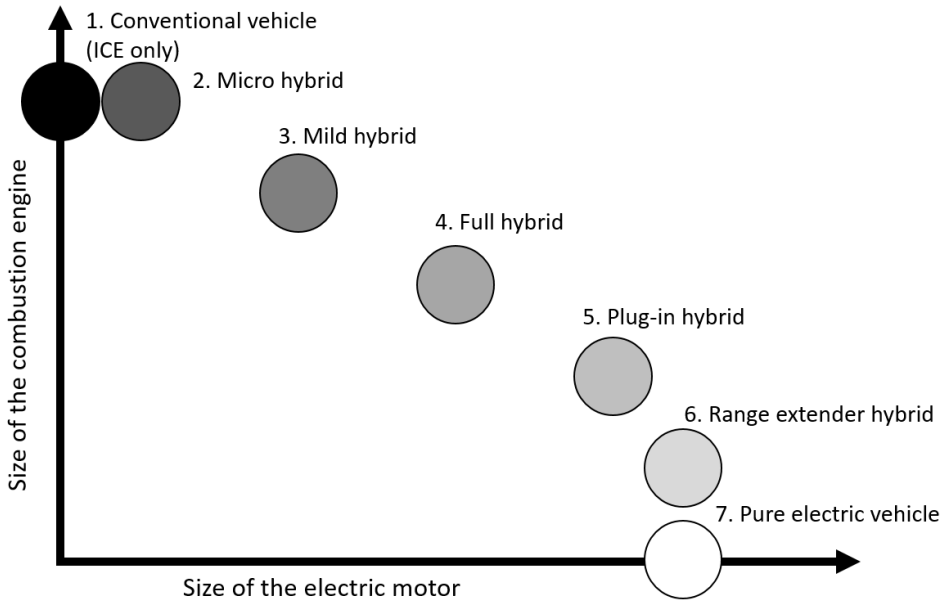

Figure A.2: A graphical representation of the different types of hybrid vehicles [1],[2]

A.4 Different hybrid topologies

Next to the classification based on the level of hybridization and electric power output, HEVs can be classified in different categories based on the configuration of the powertrain components, called the hybrid topology. Within HEVs three main topologies exist: the series, parallel and power-split or series-parallel architecture. A schematic diagram of these topologies is displayed in Figure A.3). The dissimilarities of these topologies lie in the power flow from the energy sources (i.e. the battery energy and conventional fuel in the tank) to the wheels. Although the electric power flow from battery to the wheels is similar between the concepts, large differences can be found in the combustion power flow from the ICE to the wheels. There are many works in literature that describe the different hybrid topologies and their advantages: [11], [9], [67], [17], [68], [1], [12], [69], [13], [36]

A.4.1 Series HEV

In the series topology the power flow from the ICE is cascaded over a single path down to the wheels. Rather than mechanically driving the wheels, in this topology the ICE in combination with an electric generator functions as an auxiliary power unit (APU) that is used to supplies electric energy to the battery. This means there are two electrical power sources that collectively or individually feed one electric drive unit, which is the sole power source that propels the vehicle. The combination of the ICE and generator is a unidirectional power source, where the battery is a bidirectional power source that can also store energy during regenerative braking or in cases where the ICE power output is greater than that required to propel the vehicle. Since the ICE is mechanically fully decoupled from the wheels, its operation is not related to the velocity nor the power requirements of the vehicle. For this reason it can be independently operated at any point of the torque map, which provides the opportunity to be operated in its overall most efficient operating area under all conditions (if controlled by a sophisticated enough control system). Since the only power source is an electric motor, which can efficiently deliver high torques over a broad speed range (see Appendix A.1), it is possible to completely remove the clutch and drastically simplify the multi-ratio transmission system to a single ratio system [17, 36, 69]. Also, due to the absence of a mechanical connection and the multi-ratio transmission system, the packaging freedom of the series topology is greatly increased which can offer new possibilities for drivetrain concepts like (in the case multiple electric motors are used)the removal of the differential, individual wheel control or in-wheel drive systems. The series topology however bears also some disadvantages. The main disadvantage is the that the series topology requires two energy conversion (first from mechanical power from the ICE to electrical in the generator and later from electrical to mechanical in the drive motor). The losses introduced in these conversion steps can outweigh the gains in efficiency achieved by the shifting of the operating point in certain cases, especially when the power demand is close to the optimal torque line of the ICE (e.g. highway driving). Due to these cases, passenger vehicles with series hybrid have an average efficiency of 24% according to Williamson [68], which is on par or a lower than some modern conventional ICE vehicles [1, 17]. Other disadvantages of the series topology are the need for an additional EM as the generator and the fact that the drive motor is the sole power source (there is no power split with another component), which means it has to be sized to fully support the power requirements of the vehicle on its own.

A.4.2 Parallel HEV

In the parallel topology, the ICE is mechanically coupled to the wheels via the transmission. The power from the two energy sources is supplied over two parallel paths to the transmission: an electrical and a mechanical path. Within the parallel topology, two architectures can be recognized based on the connection of the EM: pre-transmission (P2) or post-transmission (P3) [9, 36]. The P2 architecture is the most common architecture, because it offers the easiest integration in the powertrain and eliminates the need for an separate starter motor. The power of the engine and electric drive motor are combined together by a mechanical coupling (this can be seen in Figure A.3b). This type of configuration offers the freedom to choose any combination of traction sources or to operate just one separately to fulfill the power requirements of the vehicle. The ICE is a unidirectional power source, where the battery in combination with the drive motor is a bidirectional power source that can also store energy during regenerative braking or in cases where the ICE power output is greater than that required to propel the vehicle. The mechanical coupling between the wheels and the ICE solves the main problem of the series concept's conversion losses, since both the ICE and the electric motor directly supply torques to the driven wheels and no additional energy conversions occur. The parallel architecture has only two propulsion devices, which saves the need for an additional generator compared to the series topology. In principle, an additional advantage of the parallel topology is that by combining the two different traction sources neither of the two have to be sized to fulfill the full power requirement of the vehicle on their own, which allows for the use of both a smaller ICE and a smaller EM. However, this decision would lead to reduced electric driving and regenerative braking capabilities (and therefore a reduction in overall efficiency), so the electric powertrain is often still scaled to be sufficient for most driving conditions, especially the PHEV types. The main disadvantage of the parallel topology is the result of the mechanical connection to the transmission, which means the operating conditions cannot be determined as freely as in a series hybrid architecture, because the ICE and MOT speed is mechanically related to the vehicle velocity in a fixed ratio. The torque distribution between the two power sources is not prescribed however and therefore, any output torque at the given

operating speed can be chosen, which provides the opportunity to operate the ICE closer to or at the optimal operating line. Since the operating speed of the ICE can however not freely be chosen, efficient operation of the ICE can not always be ensured under all conditions. More specifically, during frequent stop and go traffic and when the vehicle is stationary [67]. In contrast to the series HEV, the mechanical connection of the ICE to the wheels does require a multi-ratio transmission with clutch system and has less packaging freedom compared to the series topology. The absence of losses caused by the additional energy conversion processes typically lead to higher overall system efficiencies than conventional IC powertrains [17, 68]. Williamson [68] describes how parallel HEV can easily achieve efficiency ranges between 40-50%.

A.4.3 Series-parallel HEV

The third HEV topology is the series-parallel architecture, which is a combination of the previous two categories put together in single architecture. In this architecture both the electrical and mechanical link to the ICE are present, as well as the distinctive generator and drive electric motors. Compared to the series hybrid, the architecture consists of an additional mechanical link and relative to the parallel hybrid, an additional generator is attached to the ICE. The presence of a power split device (usually a planetary gear set) makes sure the output power of the ICE and drive motor are merged and allows for the decoupling of the speed of the ICE from the wheel speed. The main advantage of the series-parallel topology is that it can be operated as both a series or parallel HEV. This combined configuration enables the advantages of both topologies, while it solves most of the problems associated to the individual topologies. For example, the high efficiency losses during highway operation due to additional energy-form conversions of the series topology can be avoided by mainly operating the HEV in the parallel topology. On the other hand, the HEV can be operated in the series topology in stop and go traffic to allow the ICE to be continuously operated under efficient operating conditions. Although the series-parallel topology is able to combine some of the advantages of both series and parallel configurations, it also combines some of the drawbacks of these two configurations. The main disadvantage of the series-parallel HEV is that the number of powertrain components has even further increases, since both the generator and multi-ratio transmission with clutch system are present in this architecture and an additional power split device is added to the system. This high number of components makes the series-parallel architecture relatively complex and costly and also decreases the packaging freedom. In terms of the control strategy, this powertrain concept also leads to bigger challenges and complexity since the number of degree of freedom (DOF)s is increased from 1 to 2 [39].

A.4.4 Trade off hybrid topologies

It can be concluded that the series HEV is best suited for urban driving because of the electric-intensive structure [68] and the possibility to freely operate the ICE in the efficient operation area, even under frequent stop and go traffic and when the vehicle is stationary [36, 67]. However, due to the high efficiency losses during highway driving, it mainly finds applications in heavy, low speed applications such as urban buses [36, 69].

The fact that the ICE can directly propel the vehicle and does not require additional energy conversion steps significantly increases the efficiency of the HEV during driving compared to the series topology [1, 69, 69]. The topology also offers a relative compact design and low number of components, especially in comparison to the series-parallel topology [11, 69, 69]. However, since the topology has less freedom in choosing the operation point of the ICE [1, 69, 69], efficient operation of the ICE cannot always be ensured, in particular during urban stop and go traffic [36, 67, 68].

The series-parallel HEV topology combines the advantages of both the series and parallel topology, leading to the highest overall vehicle efficiency. [11, 12, 36, 67–69]. However, the topology requires more powertrain components and is less compact and more complex that the other topologies [1, 11, 12, 69]. This in turn increases the cost of the system and requires more complex control strategies [11, 12, 68].

Although the efficiency of series-parallel topology is higher, the cost effective, compact and conventional powertrain layout and light and low volume parallel topology is a popular solution. In production passenger vehicles, both the parallel and series-parallel topologies are applied to PHEVs [11, 12, 69].

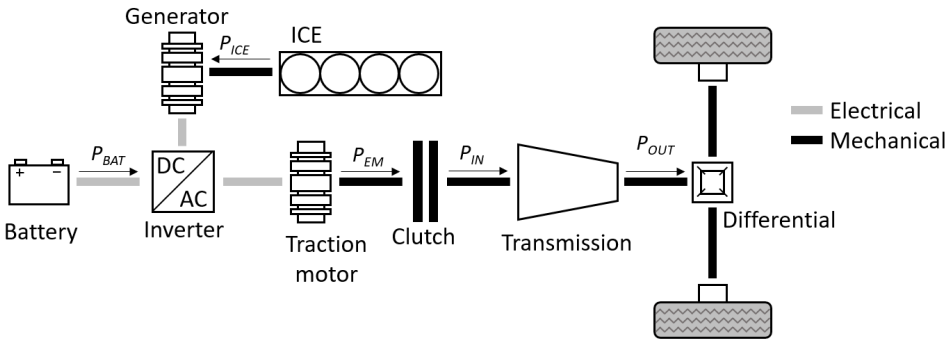

(a) Schematic overview of the main components of a series HEV topology.

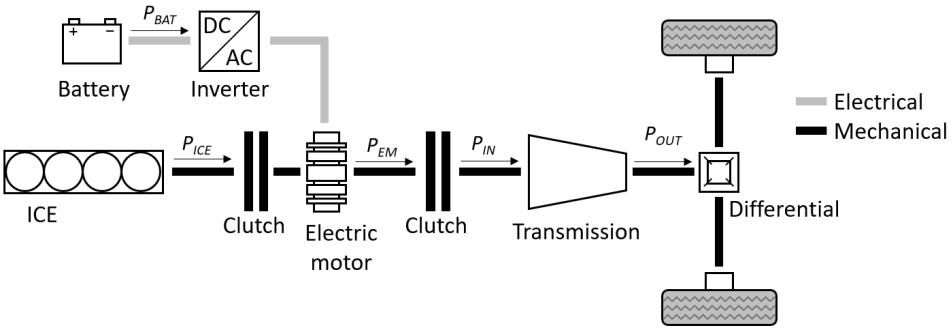

(b) Schematic overview of the main components of a parallel HEV topology.

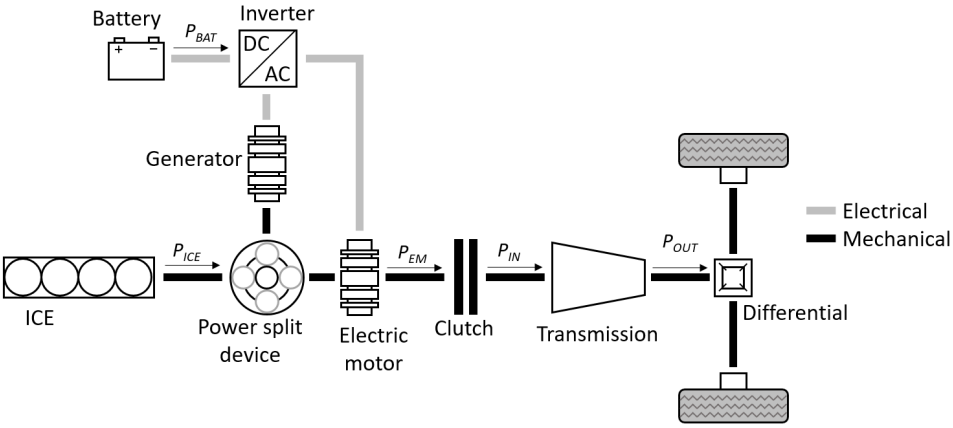

(c) Schematic overview of the main components of a series-parallel HEV topology.

Figure A.3: Schematic overview of the different hybrid topologies.

A.4.5 Different driving modes

HEVs have different driving modes that use the hybrid powertrain characteristic ways [11, 12]. The HEV with a P2 parallel topology used in this work can make use of 5 different characteristic driving modes :

1. **Motor-alone mode (eDRV)**
   The ICE is turned off in this driving mode and the vehicle is solely propelled by the EM.
2. **Engine-alone mode**

The ICE is turned on in this driving mode and the vehicle is solely propelled by the ICE.

3. **Combined power mode (eBoost)**
   Both the ICE and EM are turned on in this driving mode and jointly supply the desired power to propel the vehicle. This driving mode is typically only used at very high power demands.
4. **Power-split mode**
   The power of the ICE is divided in a portion to propel the vehicle and a portion is converted into electric energy by the EM.
5. **Regenerative braking mode**
   During braking the EM can be operated as a generator to recuperate the kinetic energy of the vehicle.

A.5 Generalization towards control strategy

The previous paragraphs show that the key characteristics of these individual powertrains often contradict each other. These strengths in different areas make the combination of the electric and internal combustion powertrain so promising, because one powertrain can compensate the aspects where the other has its weaknesses. This idea is generally speaking the basis of most hybrid powertrain supervisory controllers and allows for the highest overall efficiency of the complete powertrain [12]. For P2 parallel hybrids, the basic principle is to operate the electric powertrain in areas where the IC powertrain efficiency is relatively low and use the ICE as the power source in conditions where the efficiency of the ICE is relatively high [21]. Alternatively, if both standalone solutions are infeasible or suboptimal, the supervisory controller can opt to apply LPM strategies by making use of both power sources in parallel. During LPM strategies, the operating point of the ICE is actively shifted to a different torque level (for a parallel HEV) to achieve a higher overall efficiency. LPM can be applied in both directions: electric energy can be generated by requesting more torque from the ICE that the torque demand of the vehicle, or electric energy can be used by supporting the ICE torque with additional torque from the EM (eBoost).

B

Appendix

In order to gain a better perspective on the performance of the developed control method, the method was compared to well-known methods proposed in literature: heuristic control method, an ECMS-based control method, a MPC-based control method and a DP solution over the complete route. To further improve the comparability of the results and to get an idea of the typical performance of the well-known methods, a study is made that combines the results of 8 different works in literature.

The results found in these works are normalized towards global optimal solution (often obtained by DP), which represents a fuel economy 100%. Most works include multiple simulation scenarios, which are each given a simulation case number. In works where no global optimal solution is given as a reference, the results are normalized based on the average relative fuel economy of the other works in literature (e.g. heuristic control is used as a reference based on the average performance of heuristic controllers). The different methods applied in each works are listed in Table B.1.

The performance of these methods is graphically displayed in Figure B.1. Since the results are based on different vehicles, different drive cycles, different qualities of preview information and different implementation of the control strategies, the variation of the data samples is very high. There is however a clear trend visible, where the global optimal strategy gives the highest fuel economy, followed by the LH estimation method + SH method, followed by the linear LH reference + SH method and conventional heuristic control methods with the lowest performance in terms of fuel economy. ECMS methods with a fixed equivalence parameter can obtain a relatively high performance or even outperform more advanced control methods. As has been noted before, however, the equivalence parameter is in these cases predetermined by an extensive optimization problem to obtain the lowest fuel consumption. Since the ECMS method is highly sensitive to the value of the equivalence parameter, these performance levels are unrealistic for online applications.

Table B.1: Overview of the different methods applied in several works in literature.

Simulation case:	DP	SH+LH est.	SH+LH linear	ECMS fixed	Heuristic	Reference:
1-3	Yes	Yes	Yes	No	No	[24]
4-13	Yes	No	No	No	Yes	[32]
13-19	Yes	Yes	Yes	No	Yes	[70]
20-23	Yes	Yes	No	Yes	Yes	[25]
24-25	Yes	Yes	Yes	No	Yes	[19]
26	Yes	Yes	No	Yes	No	[34]
27	No	Yes	No	Yes	No	[26]
28	No	No	Yes	No	Yes	[30]
Average:	100%	97.8%	94.6%	96.5%	88.4%	

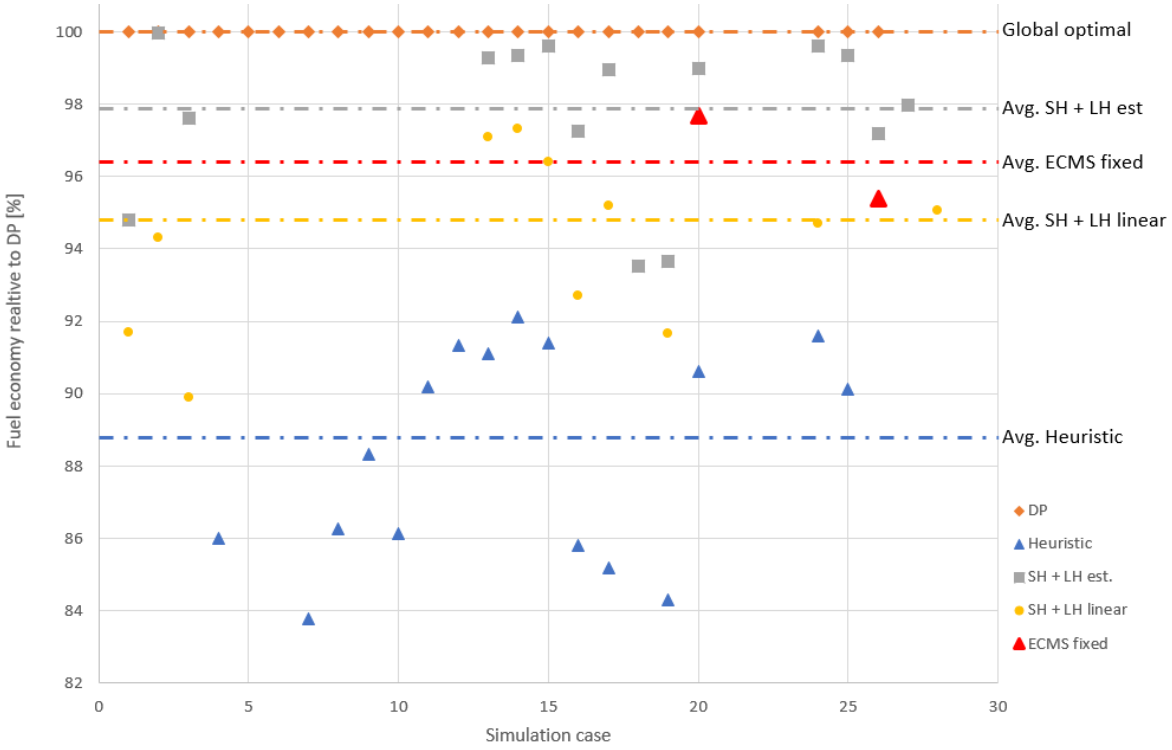

Figure B.1: Graphical representation of the performance of different control methods based on simulation results found in literature.